

# Protocols for Measuring Dairy Lagoon Seepage Using the Water Balance Method

## Technical Field Guide

March 2012





Protocols for Measuring Dairy Lagoon Seepage Using the Water Balance Method  
Technical Field Guide

March 31, 2012

This document can be downloaded at <http://www.westernuniteddairymen.com/environmental-mainmenu-34>

**Prepared by:**

Till E. Angermann, P.G., C.Hg., Luhdorff and Scalmanini, Consulting Engineers

**Prepared for:**

Western United Dairymen  
1315 K Street  
Modesto, CA 95354

**Project partners:**

California Department of Food and Agriculture  
Dairy CARES  
East Stanislaus Resource Conservation District  
Luhdorff and Scalmanini, Consulting Engineers  
University of California at Davis  
Western United Dairymen

**Project review team:**

Casey Walsh Cady, Staff Environmental Scientist, Division of Marketing Services, California Department of Food and Agriculture  
J.P. Cativiela, Program Coordinator, Dairy CARES  
Andrea Bowling, Administrative Manager, East Stanislaus Resource Conservation District  
Deanne Meyer, Ph.D., Livestock Waste Management Specialist University of California at Davis  
Michael L. H. Marsh, CPA, Chief Executive Officer, Western United Dairymen  
Paul E. Martin, Director of Environmental Services, Western United Dairymen  
Paul Sousa, Environmental Specialist, Western United Dairymen

This demonstration project was made possible by Conservation Innovation Grant funding from USDA NRCS, through industry funds administered by the California Department of Food and Agriculture, and through the collaborative efforts of the project partners named above.

This material is based upon work supported by the Natural Resources Conservation Service, U.S. Department of Agriculture.

**Disclaimer**

This document was prepared as the result of work sponsored by the Natural Resources Conservation Service, U.S. Department of Agriculture (NRCS USDA). Any opinions, findings, conclusions, or recommendations expressed in this document are those of the author(s) and do not necessarily reflect the views of the NRCS USDA. The NRCS USDA, the State of California, its employees, contractors and subcontractors make no warrant, express or implied, and assume no legal liability for the information in this document; nor does any party represent that the uses of this information will not infringe upon privately owned rights. This document has not been approved or disapproved by the NRCS USDA nor has the NRCS USDA passed upon the accuracy or adequacy of the information in this document.

---

# Table of Contents

<b>Executive Summary</b> .....	<b>iii</b>
<b>1 Preface</b> .....	<b>1</b>
1.1 Purpose and Introduction.....	1
1.2 Motivation .....	2
1.3 Introduction to the Water Balance Method.....	3
1.4 Background of the Water Balance Method.....	3
1.5 Limitations of the Water Balance Method.....	4
1.6 Normalization of Seepage Estimates.....	4
1.7 Estimation of Labor Effort.....	5
<b>2 Water Balance Approach</b> .....	<b>6</b>
2.1 Depth Measurements .....	7
2.2 Evaporation Model.....	7
<b>3 Application of Water Balance Method</b> .....	<b>12</b>
3.1 Case 1 – Testing under Favorable Conditions .....	12
3.2 Case 2 – Testing under Adverse Conditions .....	19
<b>4 Uncertainty Analysis</b> .....	<b>25</b>
4.1 Concepts and Nomenclature .....	25
4.1.1 Random Error.....	26
4.1.2 Systematic Error.....	30
4.1.3 Overall Uncertainty of a Measured Variable .....	30
4.2 Uncertainty Analysis Applied to the Water Balance Test .....	32
4.2.1 Uncertainty Surrounding Depth Calculations .....	33
4.2.2 Uncertainty Surrounding Evaporation .....	34
4.2.2.1 Monte Carlo Method.....	35
4.2.2.2 Taylor Series Method.....	36
4.2.3 Other Sources of Uncertainty.....	38
4.2.3.1 Sky Radiant Energy .....	38
4.2.3.2 Lagoon Water Density .....	39
<b>5 Practical Guidance</b> .....	<b>41</b>
5.1 Instrumentation and Deployment .....	41
5.1.1 Meteorological Measurements .....	41
5.1.2 Depth Measurements .....	43
5.2 Site Selection .....	44
5.3 Hydraulic Isolation.....	45
5.4 Communication with Facility Operator .....	45
5.5 Weather Conditions.....	46
5.6 Test Duration .....	46
5.7 Data Processing and Computations.....	47
5.8 Summary.....	47
<b>6 References</b> .....	<b>49</b>

---

## Tables and Figures

Table 1	Manufacturers' Instrumentation Technical Specifications .....	33
Table 2	Estimates of Systematic Standard Uncertainties .....	33
Figure 1	Air and water surface temperature; Dairy A, Case 1 .....	13
Figure 2	Air temperature, relative humidity, wind speed, and wind direction; Dairy A, Case 1 ....	14
Figure 3	Scaled cumulative and night time evaporation; Dairy A, Case 1 .....	15
Figure 4	Scaled water level elevation changes; Dairy A, Case 1 .....	16
Figure 5	Scaled cumulative and night time change in depth and evaporation; Dairy A, Case 1 ....	17
Figure 6	Normalized seepage rates computed from overnight and cumulative water balance testing; Dairy A, Case 1 .....	18
Figure 7	Air and water surface temperature; Dairy A, Case 2 .....	19
Figure 8	Air temperature, relative humidity, and wind speed; Dairy A, Case 2 .....	20
Figure 9	Scaled cumulative and night time evaporation; Dairy A, Case 2 .....	21
Figure 10	Scaled water level elevation changes; Dairy A, Case 2 .....	22
Figure 11	Scaled cumulative and night time change in depth and evaporation; Dairy A, Case 2 ....	23
Figure 12	Normalized seepage rates computed from overnight and cumulative water balance testing; Dairy A, Case 2 .....	24
Figure 13	Example of lagoon layout and instrumentation deployment with respect to predominant wind direction .....	42
Figure 14	Meteorological station .....	43

## Appendix

A1	Instrumentation Specifications
A2	Water Balance Testing – Plastic Lined Lagoon
A3	Water Balance Testing – Examples with Confounding Results

---

## EXECUTIVE SUMMARY

In May 2007, the California Central Valley Regional Water Quality Control Board (CVRWQCB) adopted Waste Discharge Requirements General Order No. R5-2007-0035 for Existing Milk Cow Dairies (General Order). The General Order imposes significantly more stringent requirements than were previously mandated. This includes the performance evaluation of existing lagoons<sup>1</sup> based on groundwater monitoring results. While it is recognized that lagoons contribute to subsurface loading of nutrients and salts via seepage, lagoon-specific seepage and its contribution to the overall subsurface loading relative to other sources on a given dairy farm in California (e.g., livestock housing areas such as corrals and exercise areas, and irrigated, manure-fertigated agriculture) are unknown. Furthermore, groundwater monitoring data are not suitable to quantify seepage.

This Technical Field Guide provides guidance to carry out field measurements and computations to support a water balance used to estimate the actual seepage rate of operational lagoons. For this purpose, pertinent information of over 10 years of research was compiled in this document and complemented with knowledge and experience gained during water balance testing carried out specifically for the development of this Technical Field Guide.

Field measurements of ambient air temperature, relative humidity, and wind speed; water surface temperature; and the relative water level elevation change are obtained with widely available instrumentation. Best results are obtained when inflows to and outflows from the lagoon can be halted for several days. The seepage rate estimate can be augmented with an uncertainty interval: a range around the seepage rate estimate is specified within which the true seepage rate is expected to reside with 95% confidence. If uninterrupted multi-day testing is not possible, repeated overnight testing provides a viable alternative. For the latter testing protocol, confidence in results is not gained via formal uncertainty analysis. Rather, confidence can be gained, although less quantitatively, by carrying out the water balance during several successive or near successive nights.

This Technical Field Guide documents the water balance testing that was performed on five dairy lagoons located on five commercial dairy farms in the Central Valley of California, including one plastic-lined lagoon. Testing was performed in winter/spring 2011. The testing was conducted under both favorable and adverse environmental conditions and, consequently, the quality of results differs. Two particularly informative cases provide an appreciation of potential difficulties one may encounter. Three of the five tested lagoons exhibited difficult-to-interpret signals in the water level measurements. In these cases, signals in the water level measurements cast doubt on the hydraulic isolation of the tested lagoon. The experience of these water balance tests underscores the importance of hydraulic isolation of the tested lagoons (and certainty that hydraulic isolation in fact exists), review and evaluation of raw data, and an overall comprehensive analysis including assessment of the local hydrologic conditions.

Overall, the work conducted for the development of this Technical Field Guide shows that the water balance method is a viable, practical, and cost effective tool to estimate lagoon seepage of lagoons that are not intersected by the groundwater table and can be hydraulically isolated from operational inflows and outflows for a sufficient amount of time.

---

<sup>1</sup> In the General Order, lagoons subjected to regulatory oversight are basins that receive a “waste discharge” (i.e., wash water used to remove manure from animal housing areas and other discharges identified as wastes in the General Order). The term ‘lagoon’ is used herein without differentiation and/or implication of a particular utility of the basin (i.e., storage and/or treatment).



---

# 1 PREFACE

## 1.1 Purpose and Introduction

This Technical Field Guide provides guidance to carry out field measurements and computations to support a water balance used to estimate the seepage rate of operational lagoons<sup>2</sup>. This document does not suggest regulatory guidelines or a standard protocol for regulatory compliance monitoring.

The water balance approach discussed herein has been thoroughly researched since 1999 and has experienced substantial improvements since. This document aims to make the methodology accessible to a larger, non-academic audience by compiling the pertinent information of over 10 years of research into one document and complementing this information with knowledge and experience gained during seepage testing carried out specifically for this Technical Field Guide, including guidance on practical aspects of the testing not discussed in the referenced literature.

Field measurements of ambient air temperature, relative humidity, and wind speed; water surface temperature; and the relative water level elevation change are obtained with widely available instrumentation. Using research-grade instrumentation and under favorable environmental conditions, a lagoon's seepage rate can be estimated on a sub-millimeter scale. Best results are obtained when inflows to and outflows from the lagoon can be halted for several days. The seepage rate estimate can be augmented with an uncertainty interval: a range around the seepage rate estimate is specified within which the true seepage rate is expected to reside with 95% confidence. The uncertainty analysis accounts for uncertainty in the measured variables and random error introduced by environmental conditions.

If uninterrupted multi-day testing is not possible, shorter-term testing provides a viable alternative. Best results are obtained when measurements are limited to the night. Overnight testing benefits from generally more favorable meteorological conditions resulting in reduced evaporative losses. However, the short duration significantly increases the uncertainty in the results because both the absolute and relative uncertainty contribution from depth measurements increases. As a result, uncertainty analysis loses its utility in conjunction with overnight testing. Confidence in results can be gained, although less quantitatively, by carrying out the water balance during several successive or near successive nights.

This Technical Field Guide documents the water balance testing that was performed on five dairy lagoons located on five commercial dairy farms in the Central Valley of California, including one plastic-lined lagoon. Testing was performed in winter/spring 2011. The testing was conducted under both favorable and adverse environmental conditions and, consequently, the quality of results differs. Two particularly informative cases provide an appreciation of potential difficulties one may encounter. Three of the five tested lagoons exhibited difficult-to-interpret signals in the water level measurements. In these cases, signals in the water level measurements cast doubt on the hydraulic isolation of the tested lagoon. The experience of these water balance tests underscores the importance of hydraulic isolation of the tested lagoons (and certainty that hydraulic isolation in fact exists), review and evaluation of raw data, and an overall comprehensive analysis including assessment of the local hydrologic conditions.

---

<sup>2</sup> See footnote in the *Executive Summary*.

---

Overall, the work conducted for the development of this Technical Field Guide shows that the water balance method is a viable, practical, and cost effective tool to estimate lagoon seepage.

*Section 2* discusses the mathematical foundation of the water balance method and develops the equations needed to process instrumentation output and solve for the seepage rate. *Section 3* discusses the results from two particularly informative water balance tests carried out on the same lagoon at two different times of the year. Case 1 represents testing under favorable conditions and Case 2 represents testing under adverse conditions. *Section 4* discusses the theoretical background for the uncertainty analysis, explains its relative importance, and provides step-by-step instructions to carry out the analysis. *Section 5* summarizes itemized practical guidance and *Section 6* lists pertinent references. Detailed specifications of instrumentation used in this work effort are provided in *Appendix 1*. The results of the testing performed on a plastic-lined lagoon are presented in *Appendix 2*, and the results from three additional water balance tests with difficult-to-interpret signals in the water level measurements are discussed in *Appendix 3*.

## 1.2 Motivation

In May 2007, the California Central Valley Regional Water Quality Control Board (CVRWQCB) adopted Waste Discharge Requirements General Order No. R5-2007-0035 for Existing Milk Cow Dairies (General Order). The General Order regulates waste discharges to land for approximately 1,400 dairies in California's Central Valley, and imposes significantly more stringent requirements than were previously mandated. Under the General Order, dairies may be required to provide an engineering evaluation of an existing lagoon and propose and implement approved remedial measures when groundwater monitoring demonstrates that an existing lagoon may have adversely impacted groundwater quality. Dairies may be required to design and construct new lagoons and reconstruct existing lagoons to comply with the groundwater limitations of the General Order.

Almost all lagoons on existing dairy farms in California's Central Valley were constructed as earthen pits without plastic liners or leachate collection systems. Most of the lagoons were constructed without engineered clay liners in locally existing earthen materials according to the regulatory mandates of California Code of Regulations, Title 27<sup>3</sup>. Documentation of construction specifications, quality assurance protocols, and quality control measures were not required and are, therefore, typically not available.

While it is recognized that lagoons contribute to subsurface loading of nutrients and salts via seepage, the magnitude of seepage and its contribution to the overall subsurface loading relative to other sources on dairy farms in California (e.g., livestock housing areas such as corrals and exercise areas, and irrigated, manure-fertilized agriculture) is unknown.

Unless lagoon seepage is actually measured, the General Order has the potential to obligate the California dairy industry with very costly lagoon retirements, retrofits, and/or construction of new lagoons based on inadequate evidence derived from groundwater monitoring programs.

---

<sup>3</sup> Under this state law, retention basins receiving waste from confined animal facilities have to be lined with or underlain by soils that contain at least 10% clay and not more than 10% gravel.

---

### 1.3 Introduction to the Water Balance Method

The seepage out of a lagoon can be calculated using a water balance approach. The water balance accounts for inflow to and outflow from the lagoon and accounts for changes in storage over a given period of time. Inflows may be wash water carrying manure from the flush lanes of freestall barns where livestock are housed, discharge from other lagoons or settling basins, irrigation tail water from adjacent crop fields, wash water from the milk barn and other facilities, direct precipitation, and precipitation runoff from the lagoon's banks, facility roofs and roadways, and any other surfaces at the facility from where storm water is routed to the lagoon. Outflows may be intentional removal (typically with submersible pumps deployed on floats) to irrigate crop fields or to flush freestall barns (recycling of lagoon water), transfer to other lagoons operated in series, evaporation (or sublimation from frozen lagoon surface), and seepage.

By avoiding times of precipitation, discharge to the lagoon, and the removal of water (all of which introduce uncertainties to the water balance that can far exceed the magnitude of the lagoon's seepage rate), the seepage rate can be computed as a residual by measuring the decline of the water level and subtracting evaporative losses from the water surface<sup>4</sup>.

### 1.4 Background of the Water Balance Method

This Technical Field Guide follows the methodology first introduced by Ham and DeSutter (1999) and further developed by Ham (1999). Some instrumentation used in their research efforts had already been tested and compared to other sensor types in the context of soil surface temperature measurements (Ham and Senock, 1992). In previous studies, the water balance methodology was applied over a 4-year period to 20 anaerobic lagoons (Ham, 2002a) and was substantially improved with the addition of a statistical method to quantify the uncertainty surrounding the seepage rate estimates (Ham, 2002b). Research results prompted recommendations for a framework of site specific design standards of anaerobic lagoons (Ham and DeSutter, 2000) and standards for seepage measurements (Ham and DeSutter, 2003). The methodology was further reviewed and tested, resulting in major improvements (Ham, 2007; Ham and Baum, 2009). While the basic water balance approach has not changed since its introduction in 1999, the methodology has experienced repeated review and testing, leading to substantial refinement over the years. Most importantly:

- ❑ The performance of a wide range of sensors has been systematically tested under various environmental conditions. Testing has included the comparison of measurements obtained near the center of the lagoons to those obtained near the bank and on the bank of the lagoons.
- ❑ A bulk aerodynamic transfer model (BT model) outperformed several other evaporation models over a wide range of ambient conditions (i.e., air temperature, wind speed, and relative humidity) including those developed by Bowen (1926), Penman (1948), Priestley and Taylor (1972), and DeBruin (1978).

---

<sup>4</sup> The seepage rate is expressed in millimeters per day ( $\text{mm d}^{-1}$ ). One  $\text{mm d}^{-1}$  is equal to approximately 37 centimeters per year ( $\text{cm y}^{-1}$ ). For comparison, a seepage rate of  $10^{-6} \text{ cm s}^{-1}$  (these units are commonly used when designing clay liners for lagoons) is equal to approximately 32  $\text{cm y}^{-1}$ .

- 
- ❑ The accuracy of the BT model and the overall water balance approach were demonstrated using systematic testing on a plastic-lined lagoon (i.e., seepage approaching zero) (Ham, 1999). Similar testing was conducted herein and results are presented in *Appendix 2*.
  - ❑ Most recently, the consistent performance and accuracy of the BT model and water balance approach was demonstrated by comparison to evaporation estimates determined via eddy covariance (Ham and Baum, 2009), a technique estimating evaporation rates by measuring and calculating vertical turbulent flows within atmospheric boundary layers.

Key improvements to the to the early (i.e., 1999) methodology include the

- ❑ elimination of instrumentation that did not produce reliable measurements or was cumbersome to use (e.g., thin-film heat flux transducers and heat flux plates),
- ❑ elimination of the need for floating evaporation pans filled with lagoon water and partially submerged in the lagoon,
- ❑ elimination of the need for custom-made floating meteorological rafts or instrumentation deployment via ring buoys in the center of the lagoon,
- ❑ ability to obtain all needed measurements, with the exception of water depth measurements, on the banks of the lagoons,
- ❑ reduction of the testing duration from more than one week to an overnight water balance test.

These improvements have substantially increased the overall confidence in the method's results, decreased its cost, and increased its user-friendliness.

## 1.5 Limitations of the Water Balance Method

Use of the water balance method requires hydraulic isolation of the lagoon (i.e., separation of the lagoon bottom from underlying groundwater by an unsaturated zone). The seepage rate of lagoons that are in direct subsurface hydraulic communication with shallow groundwater (i.e., the groundwater table intersects the lagoon) cannot be reliably computed with the water balance method. Under such conditions, the seepage rate would be a function of ambient groundwater levels (other variables constant) and subject to potentially large temporal changes. In addition, subsurface inflows and outflows could occur simultaneously in different portions of the lagoon, thereby making results unreliable.

## 1.6 Normalization of Seepage Estimates

The focus is on the description and demonstration of the methodology used to estimate seepage rates. Knowledge of the computed magnitudes of individual seepage rates is not needed in this context. To emphasize the focus on methodology, results were normalized to yield uniform seepage rates of 1.0 mm d<sup>-1</sup>. Normalization was achieved by scaling (i.e., linearly transforming) the results of the BT model and the water depth changes such that the proportional contribution of evaporative and seepage losses to the overall water level changes remained unchanged. The proportional variability of overnight testing results was preserved with the normalization scheme.

---

## 1.7 Estimation of Labor Effort

An experienced person can set up the instrumentation in less than three hours under favorable conditions (e.g., direct vehicular access, good weather, and good ground conditions). Approximately the same amount of time is needed to remove the instrumentation. In a best-case scenario, no additional site visits will be needed. Prior to instrumentation set-up, lagoon infrastructure and operational realities can be discussed without necessitating a reconnaissance site visit, although such a visit can help avert later surprises. Prior to instrumentation take-down, data should be downloaded and reviewed to determine that testing can be terminated.

A significant variable affecting the labor effort is the level of effort to ensure hydraulic isolation. Capping a large number of inflow pipes extending over the water surface can be challenging and time consuming, especially if it needs to be repeated for overnight testing.

For safety reasons, deployment of two staff should be contemplated, particularly for capping pipes extending over the water surface, deploying of pressure transducers, and installing infrared radiation transducers. Steep earthen banks can be difficult to negotiate and plastic liners are extremely slippery when wet. Also, staff should be aware of vehicle traffic in the vicinity of the lagoon.

Precipitation can force the need to repeat or extend testing. Similarly, if valves are found to leak, or if other incidental in- or outflows are noticed, testing needs to be repeated. Such circumstances may require additional site visits. Telemetry for data downloads can save travel time. However, in many situations, the physical presence of the analyst at the site helps in the identification of problems.

Data compilation and plotting can be somewhat automated by setting up a template spreadsheet. However, test-specific modifications will need to be made depending on test duration, time of year, number of test interruptions, etc. Lastly, the level of effort required for reporting purposes may vary widely and will, thus, have a significant effect on the overall cost.

In summary, for the preparation and execution of a water balance test, an average labor effort of 3 to 5 workdays should be anticipated. For the analysis and reporting, an average labor effort of 3 to 7 workdays should be expected. This estimate assumes negligible travel time. It does not account for direct costs associated with travel and instrumentation purchase/rental. Testing of several lagoons in conjunction with consolidated reporting has the potential to reduce costs.

---

## 2 WATER BALANCE APPROACH

The seepage rate from a working lagoon is estimated using a water balance that accounts for inflows to and outflows from the lagoon. The most general formulation of a water balance expresses the change in storage as a function of the sum of all inflows and the sum of all outflows

eq. 2-1

$$\text{Change in Storage} = \sum \text{Inflows} - \sum \text{Outflows}$$

Inflows may be the wash water discharges from the flush lanes and precipitation. Outflows may be via pumps, evaporation, and seepage. When inflows and outflows are measured as positive values, a decline in storage will be indicated by a negative sign. The change in storage is determined by measuring the decline of the water level in the lagoon over a given period of time. By avoiding times of managed inflows and outflows, eq. 2-1 becomes

eq. 2-2

$$\Delta D = \sum P - \sum E - \sum S$$

where

$\Delta D$  = change in water depth [mm]

$\sum P$  = cumulative precipitation depth [mm]

$\sum E$  = cumulative evaporation depth [mm]

$\sum S$  = cumulative seepage [mm]

Solving eq. 2-2 for the seepage rate ( $S$ , mm d<sup>-1</sup>) over the duration of the test ( $\Delta t$ , d), yields

eq. 2-3

$$S = \frac{\sum P - \Delta D - \sum E}{\Delta t}$$

The seepage rate can then be calculated using the operational form of eq. 2-3

eq. 2-4

$$S = \frac{\sum_{t_0}^{t_f} P - (D_{t_f} - D_{t_0}) - \sum_{t_0}^{t_f} E}{t_f - t_0}$$

$t_0$  = clock time at the beginning of the test (initial time)

$t_f$  = clock time at the end of the test (final time)

$t_f - t_0$  = duration of the test [d]

$\sum_{t_0}^{t_f} P$  = cumulative precipitation depth over the test period [mm]

$D_{t_0}$  = relative water depth at the beginning of the test [mm]

$D_{t_f}$  = relative water depth at the end of the test [mm]

---

$\sum_{t_0}^{t_f} E$  = cumulative evaporation depth over the test period [mm]

Depth measurements need not represent the actual liquid depth of the lagoon. Rather, depth measurements are in reference to the position of the deployed instrumentation (e.g., 20 cm below the water surface at the beginning of the test).

In practice, testing is preferably done during times of no precipitation as even small precipitation events (i.e., on the order of a few millimeters or less) may dominate the overnight water balance and introduce significant uncertainty in the result. Therefore, when no precipitation occurs, eq. 2-4 reduces to

eq. 2-5

$$S = \frac{(D_{t_0} - D_{t_f}) - \sum_{t_0}^{t_f} E}{t_f - t_0}$$

Evaporative losses from the lagoon surface into the atmosphere are entered as positive values into eq. 2-5 to yield a positive seepage rate indicating a net flux of liquid into the subsurface.

## 2.1 Depth Measurements

Eq. 2-5 indicates that only two depth measurements are needed to estimate the change in storage. While additional depth measurements over the course of the testing are not required, it will be shown in the discussion of specific water balance results that they are very useful to evaluate the progress of the testing (*Section 3*). Furthermore, this places particular importance on the accuracy of the beginning and ending depth measurements as discussed in the context of uncertainty analysis in *Section 4.2* and further discussed in *Section 5.1.2*.

The liquid depth of the lagoon is insignificant in the context of the water balance. All depth measurements are relative to the deployment depth of the transducer and all depth measurements are relative to the initial depth measurement at the beginning of the test. The difference between the initial and final depth readings is used in the water balance calculation.

## 2.2 Evaporation Model

The evaporation rate,  $E$ , is estimated using the bulk aerodynamic transfer model (BT model):

eq. 2-6a

$$E = \rho(q_s - q_a)WC_e$$

$\rho$  = air density [ $\text{kg m}^{-3}$ ]

$q_s$  = saturated specific humidity at water surface temperature [ $\text{kg kg}^{-1}$ ]

$q_a$  = specific humidity of the air [ $\text{kg kg}^{-1}$ ]

$W$  = mean wind speed at some reference height [ $\text{m s}^{-1}$ ]

$C_e$  = bulk transfer coefficient [dimensionless]

The operational form of eq. 2-6a is

---

**eq. 2-6b**

$$E = \frac{0.622}{R_d(T_s + 273.15)} [e_s(T_s) - RH e_s(T_a)] W C_e$$

$E$  = evaporation rate [ $\text{m s}^{-1}$ ]

$R_d$  = gas constant [ $287.04 \text{ J kg}^{-1} \text{ K}^{-1}$ ]

$T_s$  = temperature of water surface [ $^{\circ}\text{C}$ ]

$T_a$  = air temperature [ $^{\circ}\text{C}$ ]

$e_s(T_s)$  = saturation vapor pressure at the temperature of the water surface [kPa]

$e_s(T_a)$  = saturation vapor pressure at the temperature of the air [kPa]

$RH$  = relative humidity of the air as a fraction  $0 \leq RH \leq 1$  [dimensionless]

0.622 = ratio of molecular weights of water and dry air [dimensionless]

273.15 = constant to convert temperature measurements in  $^{\circ}\text{C}$  to Kelvin, K

The units of  $E$  are simplified such that

**eq. 2-7**

$$E = \left[ \frac{1}{\frac{\text{J}}{\text{kg K}} \text{K}} (\text{kPa} - \text{kPa}) \frac{\text{m}}{\text{s}} \right] = \left[ \frac{1}{\frac{\text{N m}}{\text{kg K}} \text{K}} \left( 1000 \frac{\text{N}}{\text{m}^2} \right) \frac{\text{m}}{\text{s}} \right] = \left[ \frac{1000 \text{ kg}}{\text{m}^2 \text{ s}} \right]$$

Where Joule,  $\text{J} = \text{Nm}$  and kilo Pascal,  $\text{kPa} = 1000 \text{N m}^{-2}$ . Since 1000 kg of water occupy a volume of  $1 \text{ m}^3$ , the units of  $E$  are equal to a change-of-depth rate expressed as  $\text{m s}^{-1}$ . The use of a ratio of molecular weights of water and dry air of 622 (instead of 0.622) automatically converts the output of the BT model to  $\text{mm s}^{-1}$ .

Inspection of eq. 2-6 shows that the calculation of  $E$  requires measurement of  $T_s$ ,  $T_a$ ,  $RH$ , and  $W$ , estimation of  $C_e$ , and computation of the saturation vapor pressures,  $e_s(T_s)$  and  $e_s(T_a)$ <sup>5</sup>. Meteorological measurements of  $T_a$  and  $RH$  are directly input in the evaporation model; measurements of  $W$  should be reduced by 25% to approximate conditions near the water surface (Ham and Baum, 2009). Based on extensive research and testing, a bulk transfer coefficient,  $C_e$ , applicable to evaporation from lagoons in agricultural settings of  $2.5 \times 10^{-3}$  was proposed by Ham and Baum (2009). The saturation vapor pressures are computed using the formula of Murray (1967).

**eq. 2-8**

$$e_s(T_x) = 0.61078 \exp\left(\frac{17.2693882 T_x}{237.3 + T_x}\right)$$

Where  $T_x$  [ $^{\circ}\text{C}$ ] represents  $T_s$  or  $T_a$ .

The temperature of water surface,  $T_s$ , is measured with infrared radiation transducers (IRT). The radiation detected with IRTs includes two components (i) the radiation directly emitted by the target surface and (ii) reflected radiation from background (in the case of this application the background radiation is

---

<sup>5</sup> While wind direction is not a variable needed for the BT model, its quantification can be useful to address potential discrepancies between water level measurements (retrieved with two or more independent instruments) during times of high winds.

incoming long wave radiation from the universe, also referred to as sky radiation). IRTs are calibrated against an approximated blackbody standard with emissivity  $\epsilon=1$ . A blackbody is an idealized object that absorbs all light that falls on it and emits light in a wavelength spectrum determined solely by its temperature. In practice, objects have an emissivity smaller than 1. Therefore, IRT measurements in the field need to be corrected for the effects of the emissivity of the target surface with emissivity,  $\epsilon<1$ . As stated above, the IRT also senses background radiant energy reflecting off the target surface. The ratio of the two components in the radiation detected by the IRT is weighted according to the emissivity of the target surface

**eq. 2-9**

$$R_{IRT} = \epsilon_{target}R_{target} + (1 - \epsilon_{target})R_{background}$$

$R_{IRT}$  = radiant energy detected by the IRT [ $W\ m^2$ ], where Watts,  $W = J\ s^{-1}$

$R_{target}$  = radiant energy emitted by the target [ $W\ m^2$ ]

$R_{background}$  = background radiant energy incident to the target surface [ $W\ m^2$ ]

$\epsilon_{target}$  = emissivity of the target [dimensionless]

The target surface in this application is the water surface and background radiant energy is supplied by the atmosphere, i.e., the sky. Inspection of eq. 2-9 shows that for the quantification of  $R_{target}$ , three quantities are needed (i) a sensor measurement, (ii) an estimate of the target's emissivity, and (iii) an estimate of background radiant energy emitted by the sky.

To express the energy terms in eq. 2-9 as temperatures, the Stefan-Boltzmann law is invoked, which states that the total energy radiated per unit surface area of a black body per unit time is directly proportional to the fourth power of its thermodynamic or absolute temperature (i.e., temperature expressed in Kelvin, K).

**eq. 2-10**

$$R = \sigma T^4$$

$\sigma$  = Stefan-Boltzmann constant [ $5.670400 \pm 0.000040 \times 10^{-8}\ W\ m^{-2}\ K^{-4}$ ]

For any object in nature (i.e., not the idealized black body but a so-called gray body with  $\epsilon < 1$ ), the radiation emitted is

**eq. 2-11**

$$R = \epsilon\sigma T^4$$

Writing eq. 2-9 in terms of temperature by application of the Stefan-Boltzmann law and using notation applicable to the lagoon measurements yields

**eq. 2-12**

$$\sigma T_{IRT}^4 = \epsilon_{pond\ surface}\sigma T_{pond\ surface}^4 + (1 - \epsilon_{pond\ surface})\sigma T_{sky}^4$$

$T_{IRT}$  = temperature sensed by the IRT [K]

$T_{pond\ surface}$  = true surface temperature of the lagoon surface [K]

---

$T_{sky}$  = sky temperature [K]

$\epsilon_{pond\ surface}$  = emissivity of the lagoon surface, i.e., 0.96 [dimensionless]<sup>6</sup>

$T_{sky}$  relates to the incoming long wave radiation from the universe and is very small. Also,  $T_{sky}$  has no relation to the ambient air temperature. Typically, measurements of  $T_{sky}$  are not available, and the effects of long wave clear sky radiation is represented by a single variable,  $B$ .  $B$  can be approximated using the Stefan-Boltzmann law

**eq. 2-13**

$$B = \epsilon_{clear\ sky} \sigma (T_a + 273.15)^4$$

$B$  = background clear sky radiant energy incident to the target surface [W m<sup>2</sup>]

$\epsilon_{clear\ sky}$  = emissivity of the clear sky [dimensionless]

The emissivity of clear sky is then approximated based on near-ground (i.e., at 2 m above ground) meteorological measurements of air temperature,  $T_a$ , and relative humidity,  $RH$ , and the ambient vapor pressure at  $T_a$  (Brutsaert, 1975):

**eq. 2-14**

$$\epsilon_{clear\ sky} = 1.72 \left( \frac{RH e_s(T_a)}{T_a + 273.15} \right)^{\frac{1}{7}}$$

Therefore, solving eq. 2-12 for the target temperature yields its operational form to compute the surface temperature of the lagoon water under clear sky conditions.

**eq. 2-15**

$$T_{pond\ surface} = \sqrt[4]{\frac{\sigma T_{IRT}^4 - (1 - \epsilon_{pond\ surface})B}{\epsilon_{pond\ surface} \sigma}}$$

Night time radiant energy from the sky can also be measured directly by pointing an IRT into night sky such that

**eq. 2-16a**

$$R_{IRT} = \epsilon_{sky} R_{sky}$$

**eq. 2-16b**

$$R_{sky} = \frac{R_{IRT}}{\epsilon_{sky}}$$

and by analogy to eqs. 2-11 and 2-12

---

<sup>6</sup>Ham (2002)

---

**eq. 2-16c**

$$T_{sky} = \sqrt[4]{\frac{T_{IRT}^4}{\epsilon_{sky}}}$$

$T_{sky}$  can then be directly calculated and used in eq. 2-12, and the computation of the true lagoon surface temperature simplifies.

**eq. 2-17**

$$T_{pond\ surface} = \sqrt[4]{\frac{T_{IRT}^4 - (1 - \epsilon_{pond\ surface})T_{sky}^4}{\epsilon_{pond\ surface}}}$$

---

## 3 APPLICATION OF WATER BALANCE METHOD

In this section, results from two water balance tests are discussed. The tests were conducted on the same lagoon but under different ambient conditions. The first test (Dairy A, Case 1) was conducted in February 2011, when air temperatures were comparatively low. As a result, evaporative losses from the lagoon surface were small and contributed only a small portion to the measured water level decline. Overnight testing occurred between 18:00 to 07:00 h (6:00 PM to 7:00 AM). The second test (Dairy A, Case 2) was conducted in June 2011 when ambient air temperatures were much higher and evaporative losses accounted for nearly the entire measured water level decline. Also, due to longer days, night time testing durations were shorter. *Case 1* illustrates testing under favorable ambient conditions whereas *Case 2* illustrates testing under adverse ambient conditions.

The Dairy A lagoon was constructed in the mid 2000s, when applicable state law (California Code of Regulations, Title 27) required that retention basins receiving waste from confined animal facilities be lined with or underlain by soils that contain at least 10% clay and not more than 10% gravel. The lagoon's earthen depth is 7.3 m. In February 2011, the liquid depth was approximately 6 m. In June 2011, the liquid depth was approximately 5.5 m. The lagoon's water surface area in February 2011 was 0.4 ha (and essentially the same in June 2011).

### 3.1 Case 1 – Testing under Favorable Conditions

In February 2011, diurnal fluctuations of air temperature,  $T_a$ , were distinct with daily minima and maxima ranging from slightly below 0 to 5 °C and 15 to 20 °C, respectively (**Figure 1**). IRT measurements indicated diurnal fluctuations of water surface temperature of similar magnitude. IRT measurements also indicated spatial variability of the water surface's temperature. During the night, the water surface temperature sensed by the IRT deployed on the eastern side of the lagoon,  $T_s(E)$ , was typically 1 to 2 degrees Celsius greater than that sensed by the IRT in the southwestern location,  $T_s(SW)$ . In the early to late afternoon (i.e., during the time of greatest air and water surface temperatures) spatial water surface temperature differences tended to be more pronounced (typically about 5 °C). At night time, the air was typically cooler than the water surface. This relationship was maintained during day time on day of year (DOY) 40 and 41, whereas on DOY 37 and 38, day time air temperatures were more similar to the water surface temperatures. DOY 39 presents an exception, when day time water surface temperatures remained virtually unchanged from night time temperatures but the air temperature rose 5 to 7 °C above that of the water surface. This phenomenon is explained by high winds causing higher evaporation rates and higher associated thermal cooling of the water surface (**Figure 2B**). Specifically, wind speed was typically less than 2 m s<sup>-1</sup> during the test and considerably less at night. However, wind speed increased after 19:00 h on DOY 38 from 0.2 to 7 m s<sup>-1</sup> on the following day with gusts up to 11 m s<sup>-1</sup> (not shown) during mid day. During most of the testing, northwestern to northeastern winds prevailed. While the wind direction is displayed in **Figure 2B**, it was found to be of no consequence to the seepage calculations at any of the dairies. Diurnal fluctuations of relative humidity, RH, were inverse to air temperature, with day time minima of 40 to 55% and night time maxima exceeding 89% (**Figure 2A**).

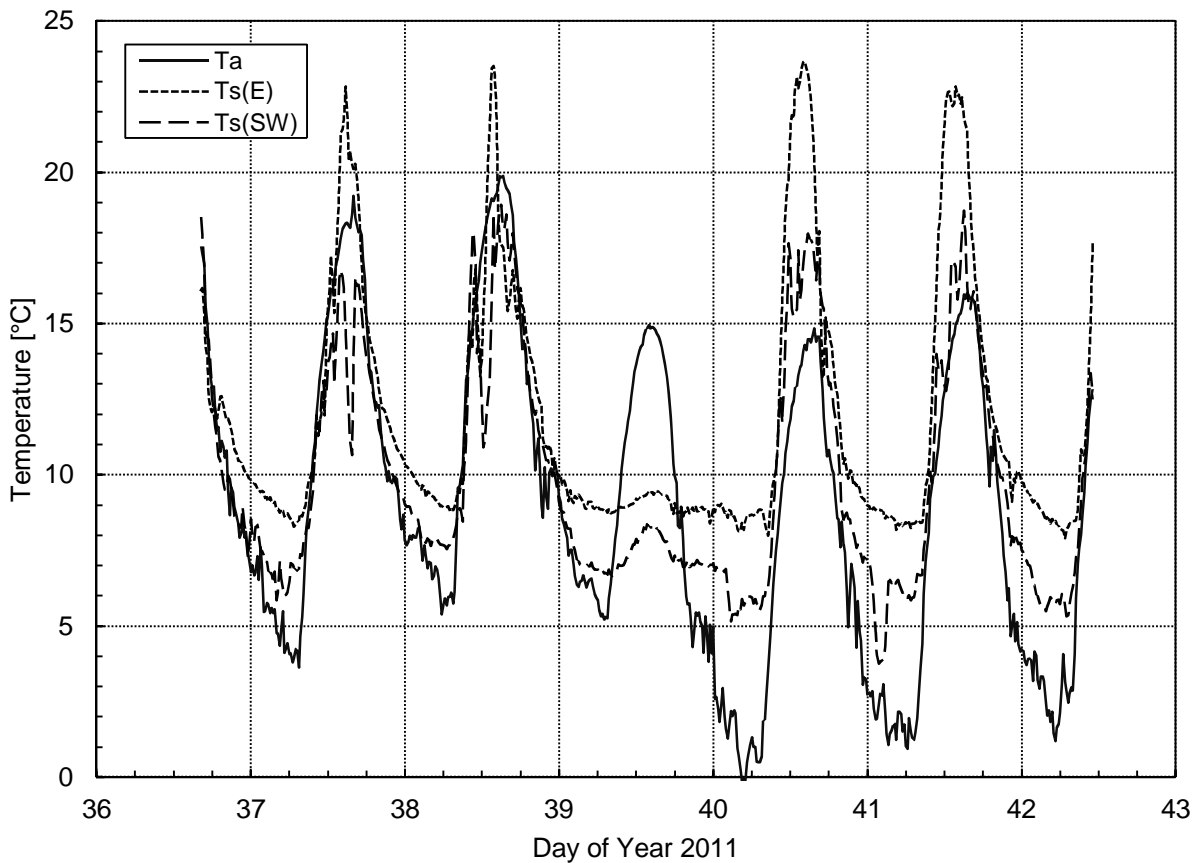


**Figure 1:** Temperature measurements at Dairy A, Case 1. Air temperature,  $T_a$ ; water surface temperature sensed in the eastern,  $T_s(E)$ , and southwestern  $T_s(SW)$  portions of the lagoon.

The scaled mean cumulative evaporation over the testing period of 5 d 18.5 h was 2.1 mm (**Figure 3A**). Day time evaporation rates were significantly greater than night time rates as affected by greater air and water surface temperatures, higher winds, and lower relative humidity. Nearly half of the evaporation occurred during the period of high winds lasting from the evening of DOY 38 to the early afternoon of DOY 39. The results, separately computed and presented with input from the two IRT's, show the effect of spatially variable water surface temperatures on evaporation rates, and highlight the importance to obtain water surface temperature readings at more than one location of the lagoon. Mean scaled night time evaporation (i.e., between shortly after sunset until shortly before sun rise; in this case from 18:00 h to 07:00 h; i.e., 13 h testing period) ranged from approximately 0.1 mm during most night to slightly over 0.3 mm during the night from DOY 38 to DOY 39 (**Figure 3B**).

Excellent agreement was observed between the two pressure transducers measuring water level elevation changes (**Figure 4**). Integrated over the duration of the test, measurements indicate a scaled linear mean water level elevation drop of 7.8 mm. At the end of the test, the two instruments, deployed at opposite ends of the lagoon, were in very good agreement indicating relative scaled water elevation changes of 8.1 mm (northern deployment) and 7.6 mm (southern deployment). **Figure 4** also shows that day time water level readings are more unsteady than during the night. This phenomenon is explained by higher wind speeds and other factors contributing to greater day time evaporation rates.

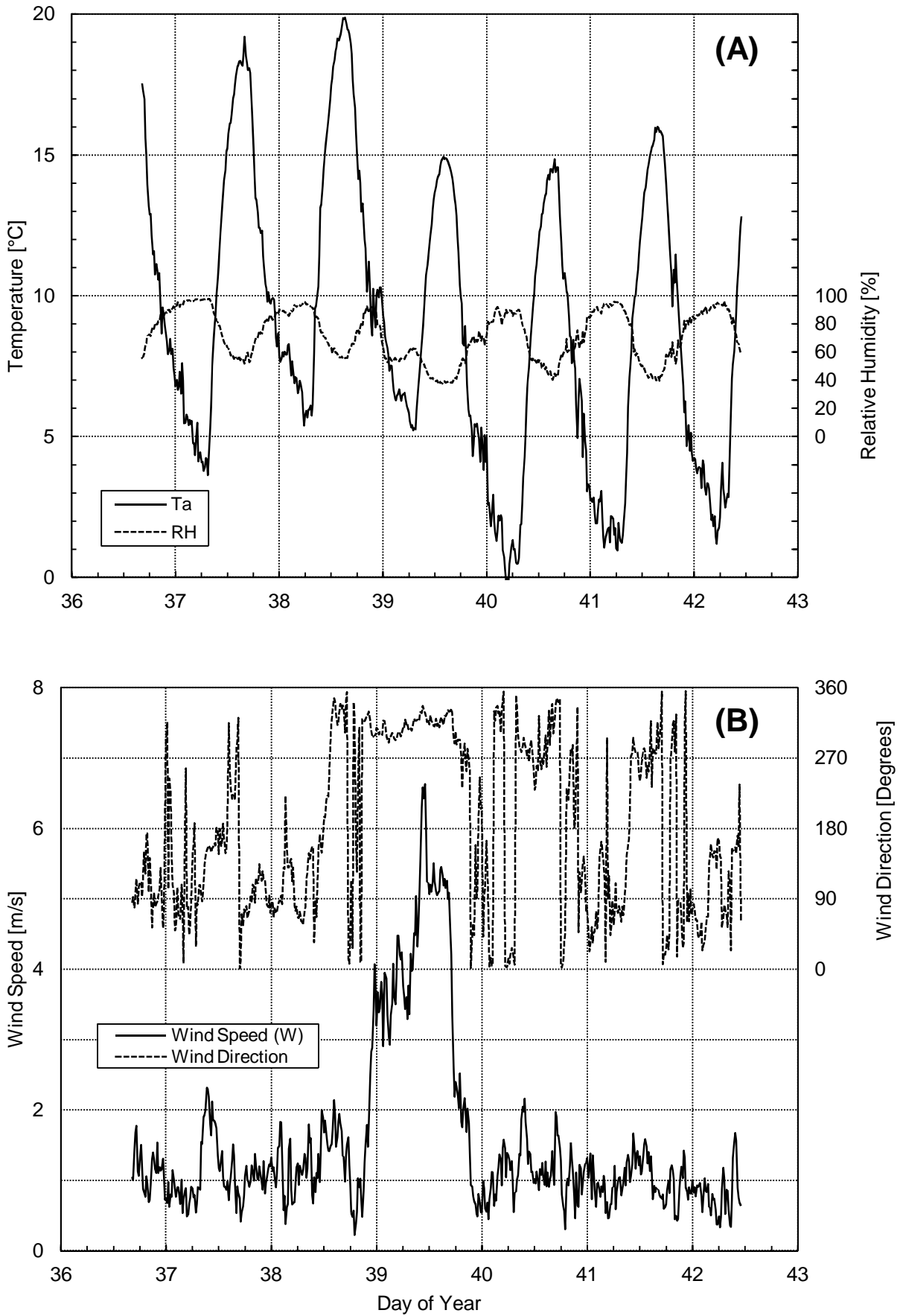


**Figure 2:** (A) Air temperature, Ta, and relative humidity, RH (B) Wind speed, W, and direction; Dairy A, Case 1.

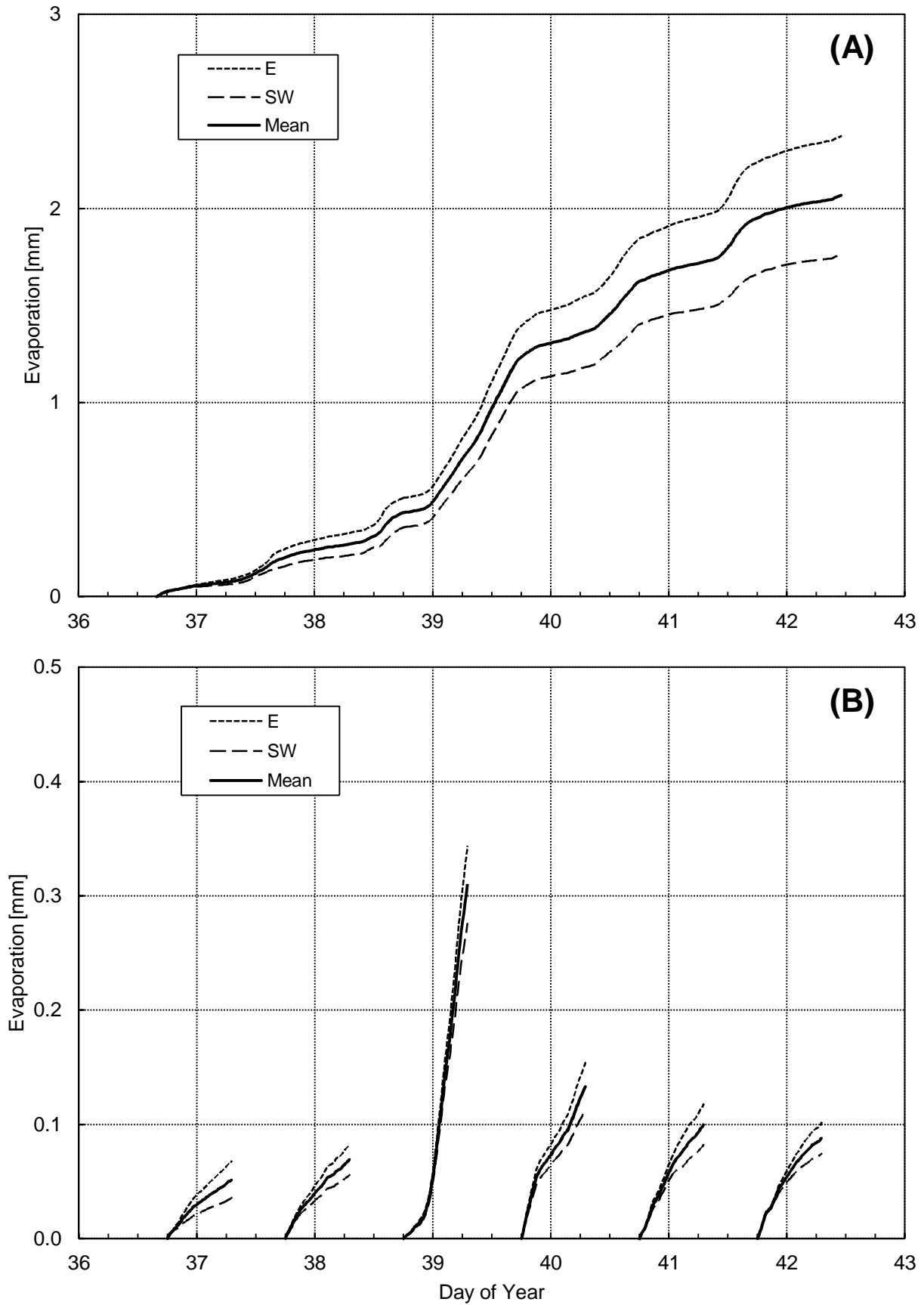


**Figure 3:** Scaled cumulative (A) and night time (B) evaporation, eastern (E) and southwestern (SW) lagoon areas; Dairy A, Case 1.

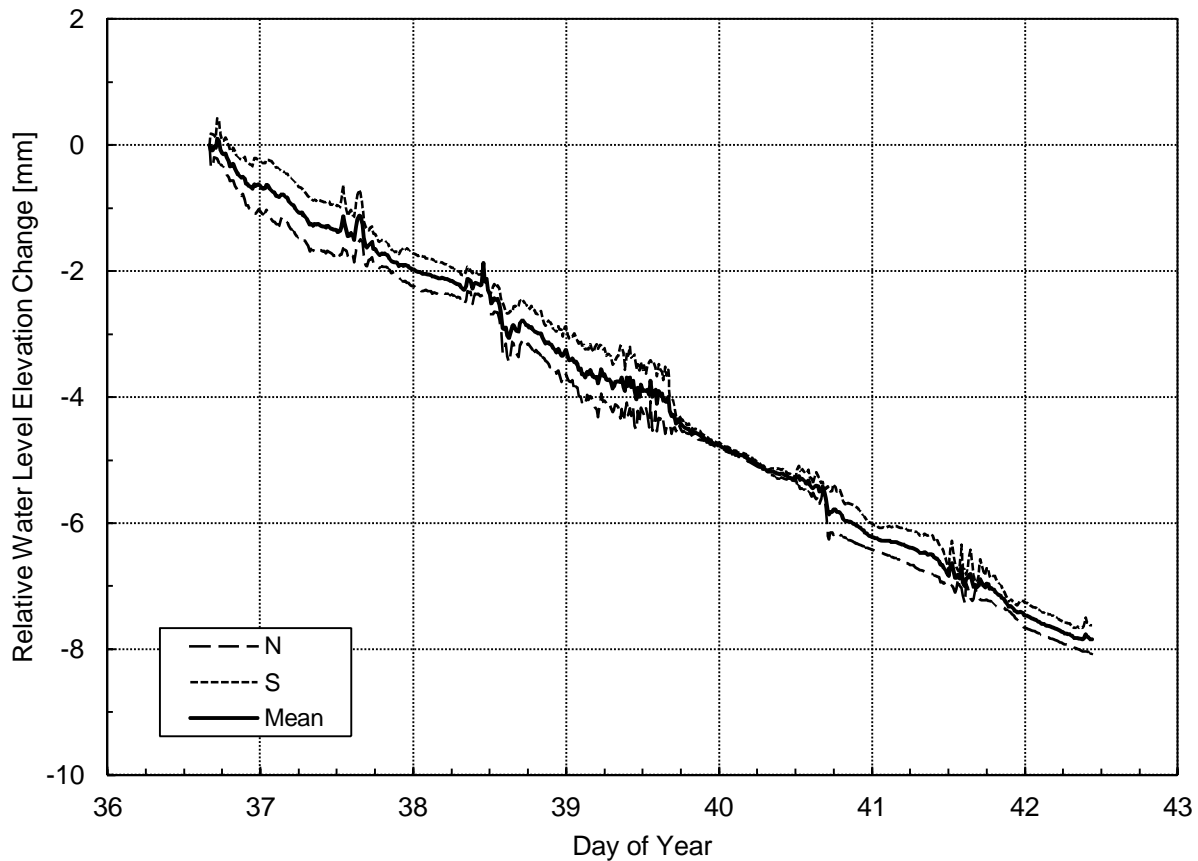


**Figure 4:** Scaled water level elevation changes as measured in the northern (N) and southern (S) lagoon areas; Dairy A, Case 1.

Expressing a reduction in storage as a positive quantity (and conversely, a storage increase as a negative quantity) provides for a direct, visual comparison of the change in storage, evaporative losses, and their difference, i.e., the seepage (**Figure 5**). A clear divergence between the storage change and evaporation was visible a few hours after the test started, and this trend continued throughout the duration of the test (**Figure 5A**). At the conclusion of the test, evaporative losses accounted for 26% of the measured depth change. During five of the six consecutive overnight tests, evaporative losses accounted for only 5 to 19% (**Figure 5B**). During the night from DOY 38 to DOY 39, when exceptionally high winds occurred, evaporative losses accounted for 35%.

Seepage rates were computed from 6 consecutive overnight water balance tests and from the cumulative duration of the test during which operational inflows to and outflows from the lagoon were stopped (**Figure 6**). The results show that extending the duration of the water balance test reduced the effects of random error. For example, at the beginning of the overnight tests, the variance in the computations was high, and became more stable over time. The same phenomenon is exhibited by the cumulative test results. This pattern was not caused by changes in the actual seepage rate. Rather, it shows how the effect of random errors in the input variables was moderated with continued sampling. Results at any given time represent seepage rates that would have been calculated if the experiment had been stopped at that moment. The elapsed time at that moment is  $t_f$  in eq. 2-5.

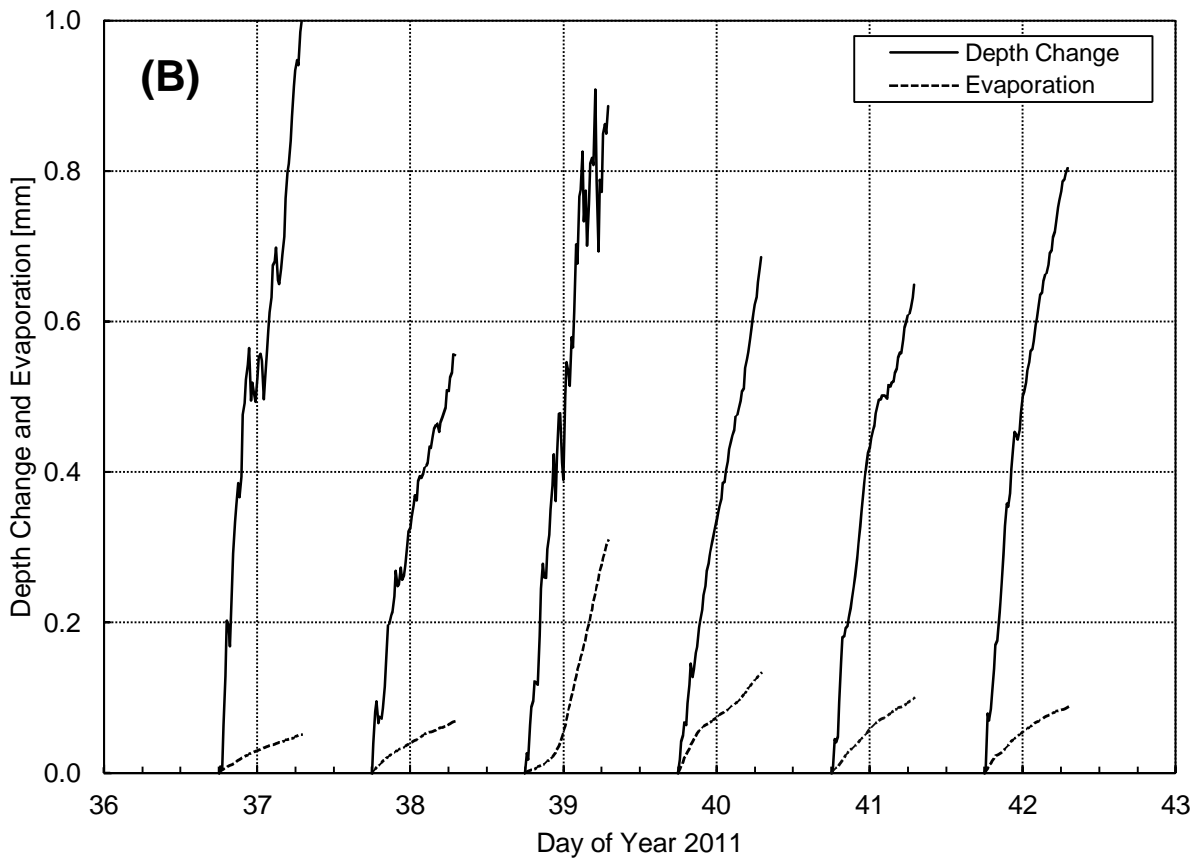
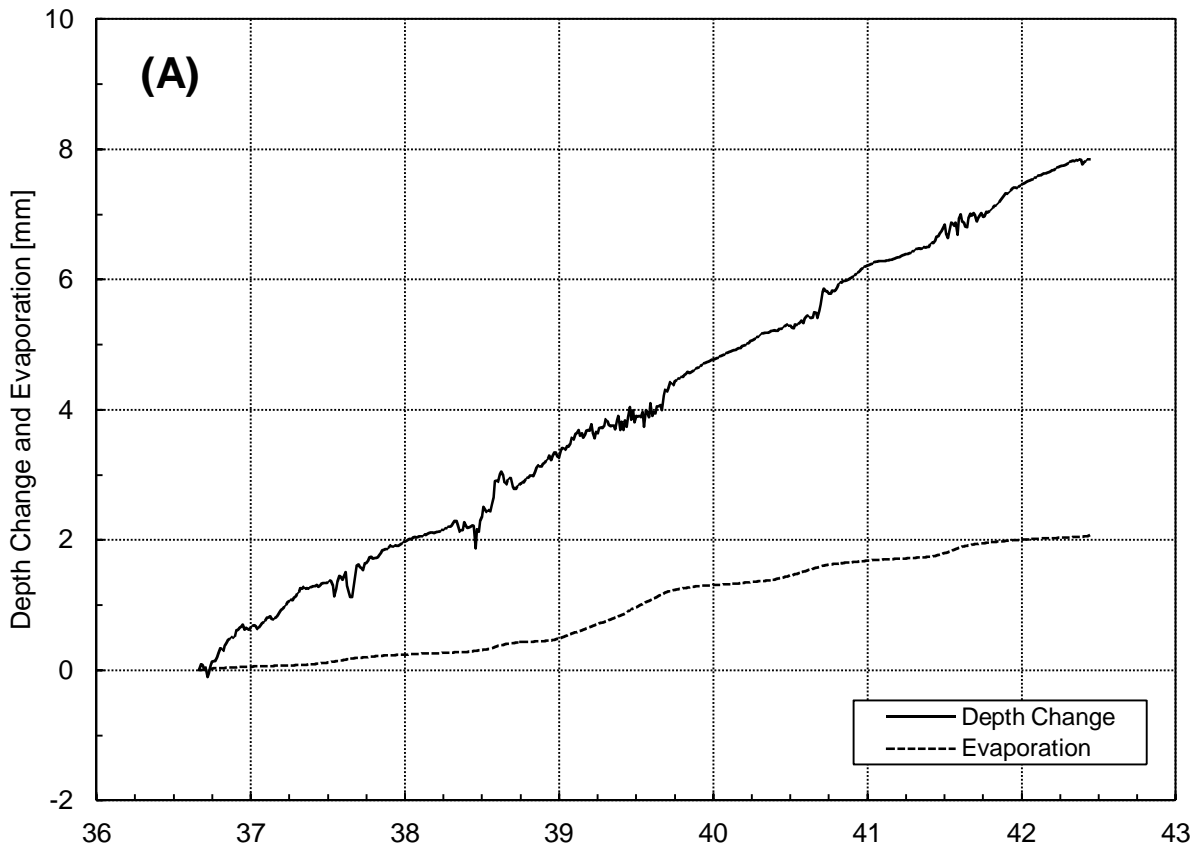


**Figure 5:** Scaled cumulative (A) and night time (18:00 h – 07:00 h) (B) change in depth and evaporation; Dairy A, Case 1.

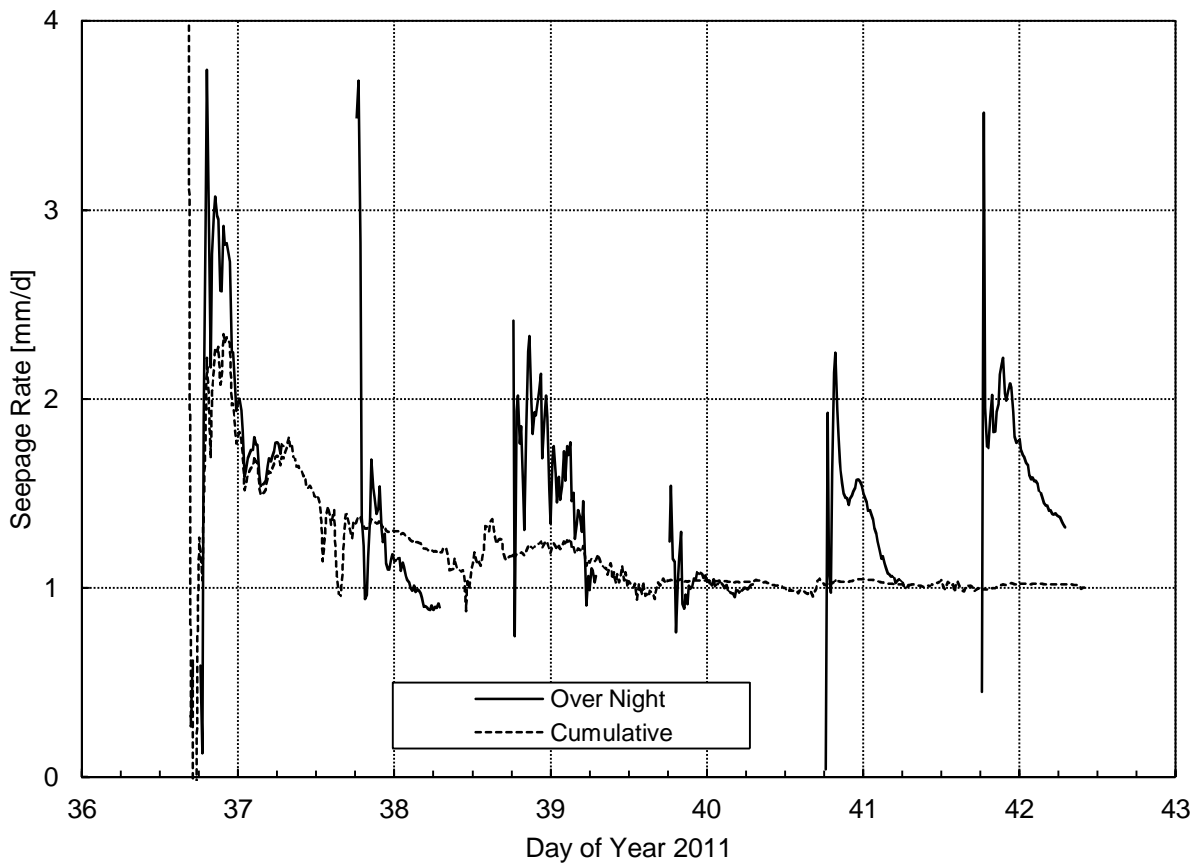


**Figure 6:** Normalized seepage rates as computed from the overnight water balance and the entire (cumulative) test duration; Dairy A, Case 1.

The normalized seepage rate computed from the cumulative test duration stabilized on DOY 39 and remained virtually invariable throughout the remaining test, resulting in a seepage rate of  $1.0 \pm 0.2 \text{ mm d}^{-1}$  (i.e., the true seepage rate is expected to fall within the given range with 95% confidence).

The results from the overnight testing show quick convergence to a normalized seepage rate of  $0.9 \text{ mm d}^{-1}$  during Night 2 and stabilization between  $1.1 \text{ mm d}^{-1}$  during Night 3 and  $1.0 \text{ mm d}^{-1}$  during Nights 4 and 5. During the first and last nights, it appears that environmental conditions were such that the test duration was not sufficient to allow the apparent computed seepage rate to stabilize. Despite generally more favorable environmental conditions at night, **Figure 6** suggests that the short duration of the night time testing may not always suffice for random error to fully attenuate. In addition, the shorter a water balance test the more the uncertainty surrounding depth measurements is amplified (*Section 4.2.1*). For example, during Nights 3, 4, and 5, normalized seepage rates were estimated at  $1.1 \pm 1.1 \text{ mm d}^{-1}$ ,  $1.0 \pm 0.9 \text{ mm d}^{-1}$ , and  $1.0 \pm 0.5 \text{ mm d}^{-1}$ , respectively. Clearly, the result of one individual overnight test would not be very useful due to the width of the uncertainty interval. In other words, a formal uncertainty analysis is less useful in conjunction with short-term testing. Confidence in the results from overnight testing is gained when similar seepage rates are computed from consecutive or near-consecutive nights.

### 3.2 Case 2 – Testing under Adverse Conditions

Lagoon performance at Dairy A was evaluated for a second time in early summer (June) when meteorological conditions were considerably different (**Figures 7 and 8**). Specifically, higher air temperatures and wind speeds, and lower relative humidity caused substantially higher evaporative losses (**Figure 9**). The mean scaled cumulative evaporation during the testing period of 9 d 6 h was 44.6 mm, and diurnally varying evaporation rates are observed. The scaled mean night time evaporation (computed between 23:30 h and 05:30 h) ranged from 0.6 to 0.9 mm.

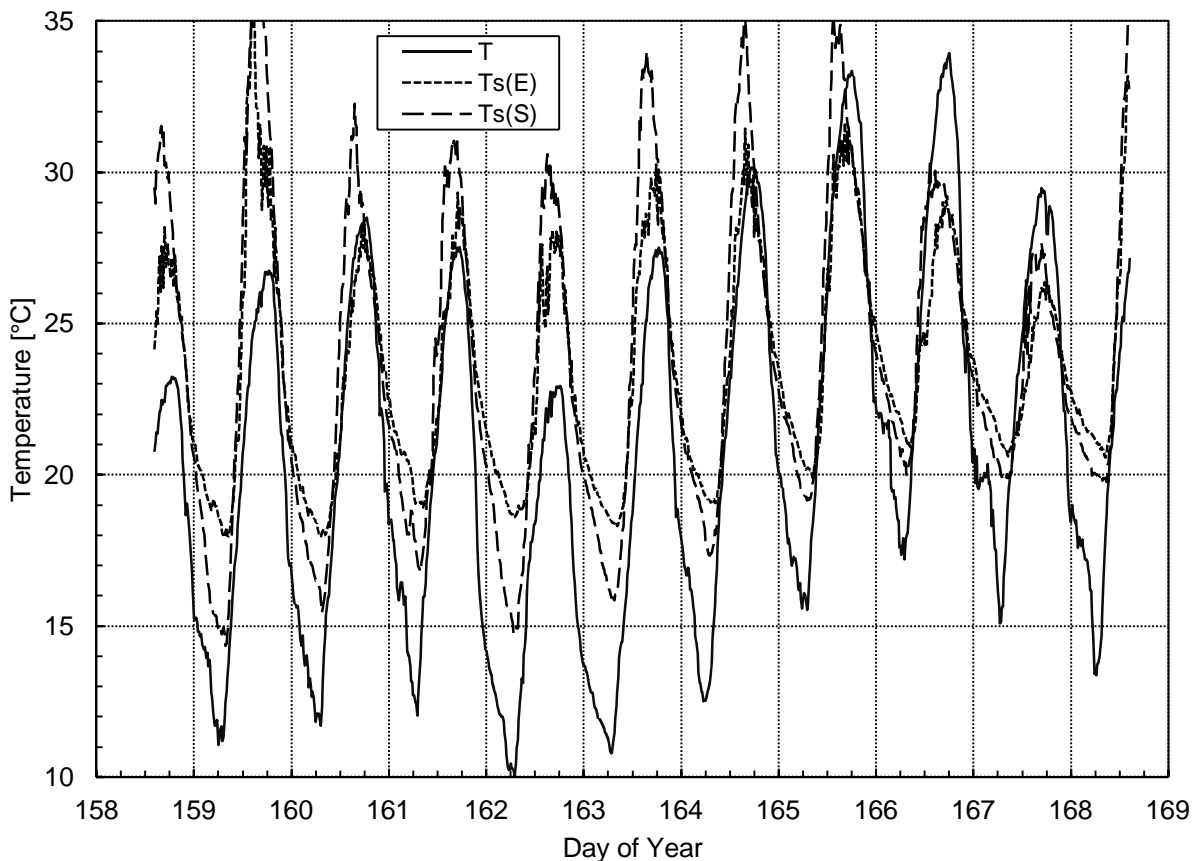


**Figure 7:** Temperature measurements at Dairy A, Case 2. Air temperature,  $T_a$ ; water surface temperature sensed in the eastern,  $T_s(E)$ , and southern  $T_s(S)$  portions of the lagoon.

The scaled mean water level elevation decline was 54.2 mm (**Figure 10**). Water level measurements were in good agreement with the pressure transducer deployed at the north and south ends of the lagoon indicating a scaled elevation change of 52.8 and 55.6 mm, respectively. Although the overall water level decline was linear, transducer data (especially at the south end location) clearly indicated a pattern of intermittently rising water elevations during the mid-day. It was determined that this phenomenon did not reflect actually rising water levels but was caused by solar heating of the transducers' stainless steel housing. The transducers had been deployed with the upper portion of the housing above the water surface. The effect of solar heating on transducer readings (indicated by non-linearity) was apparent until well after sunset. Therefore, night time seepage computations could only be carried out during a 6 h window (i.e., between 23:30 h and 05:30 h). The scaled cumulative water level elevation decline of 54.2 mm does not appear to have been affected by solar heating and is considered valid.

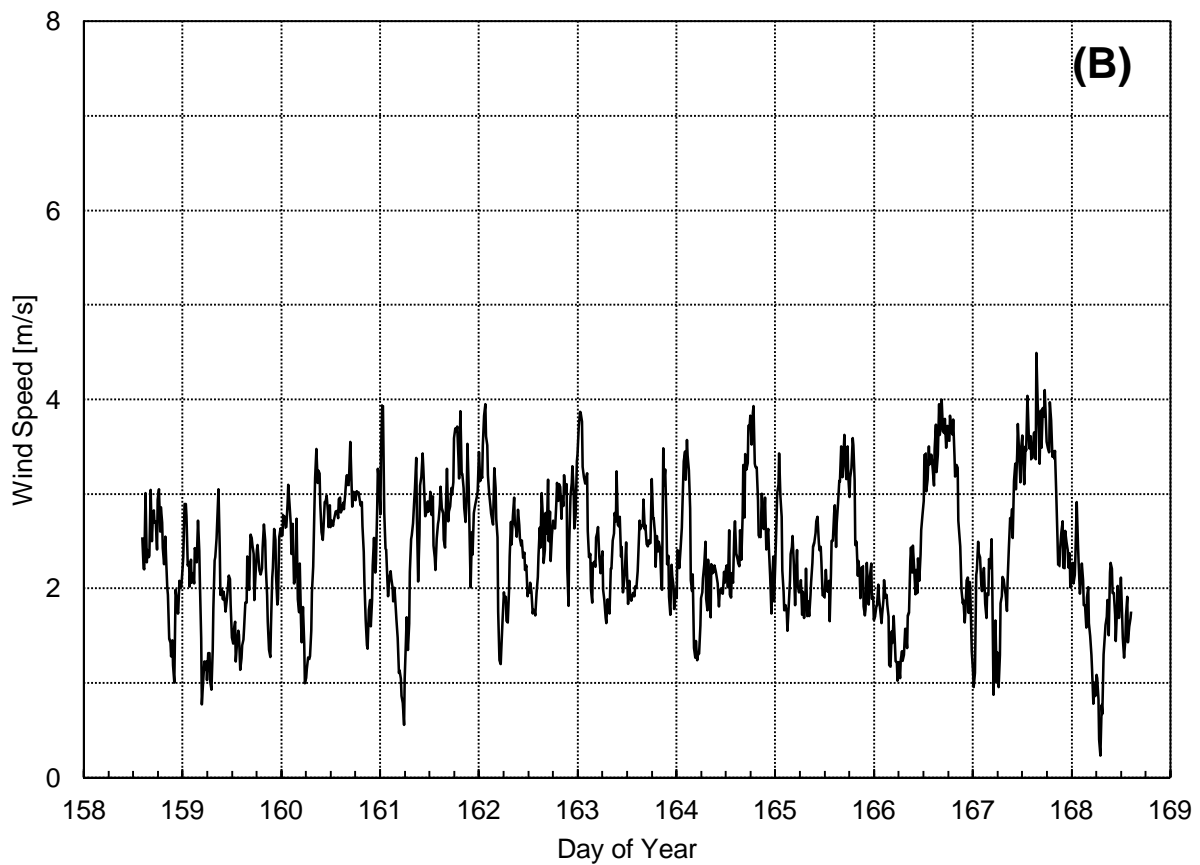
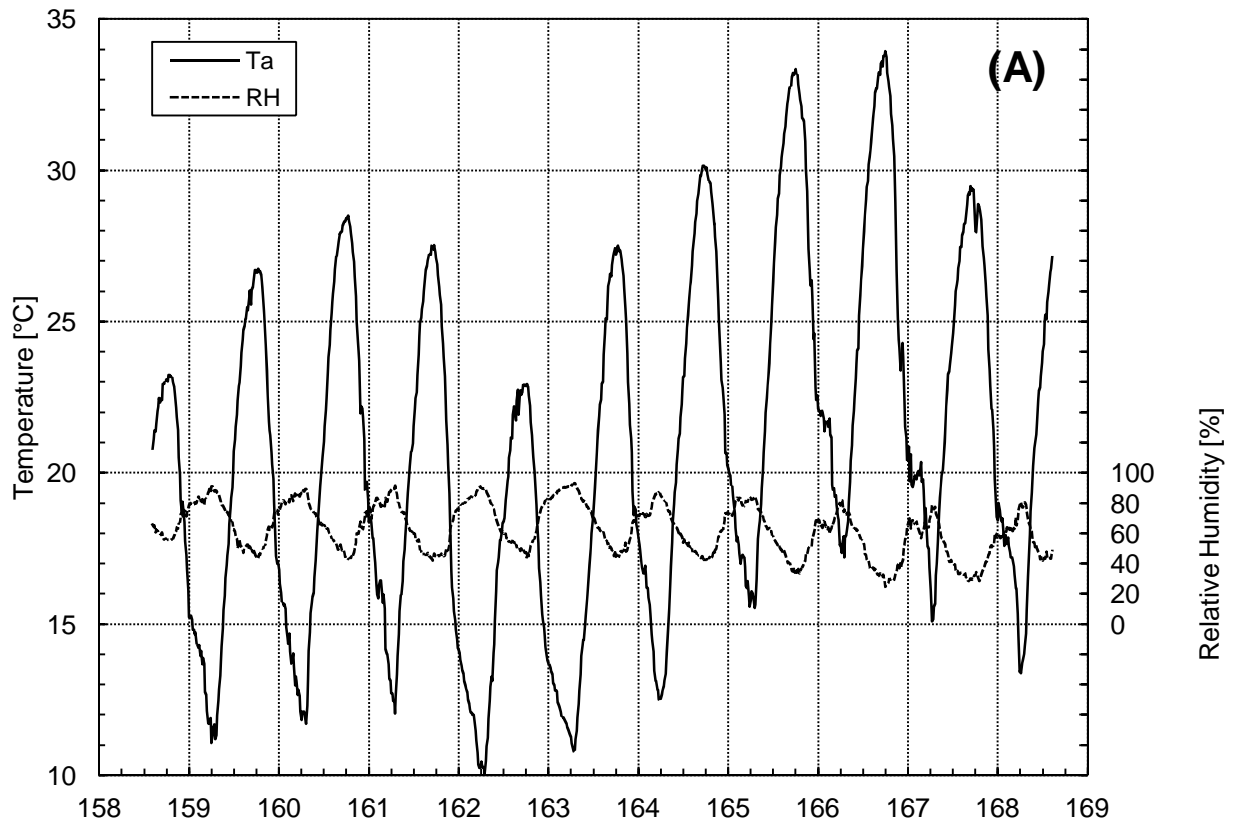


**Figure 8:** (A) Air temperature, Ta, and relative humidity, RH (B) Wind speed; Dairy A, Case 2.

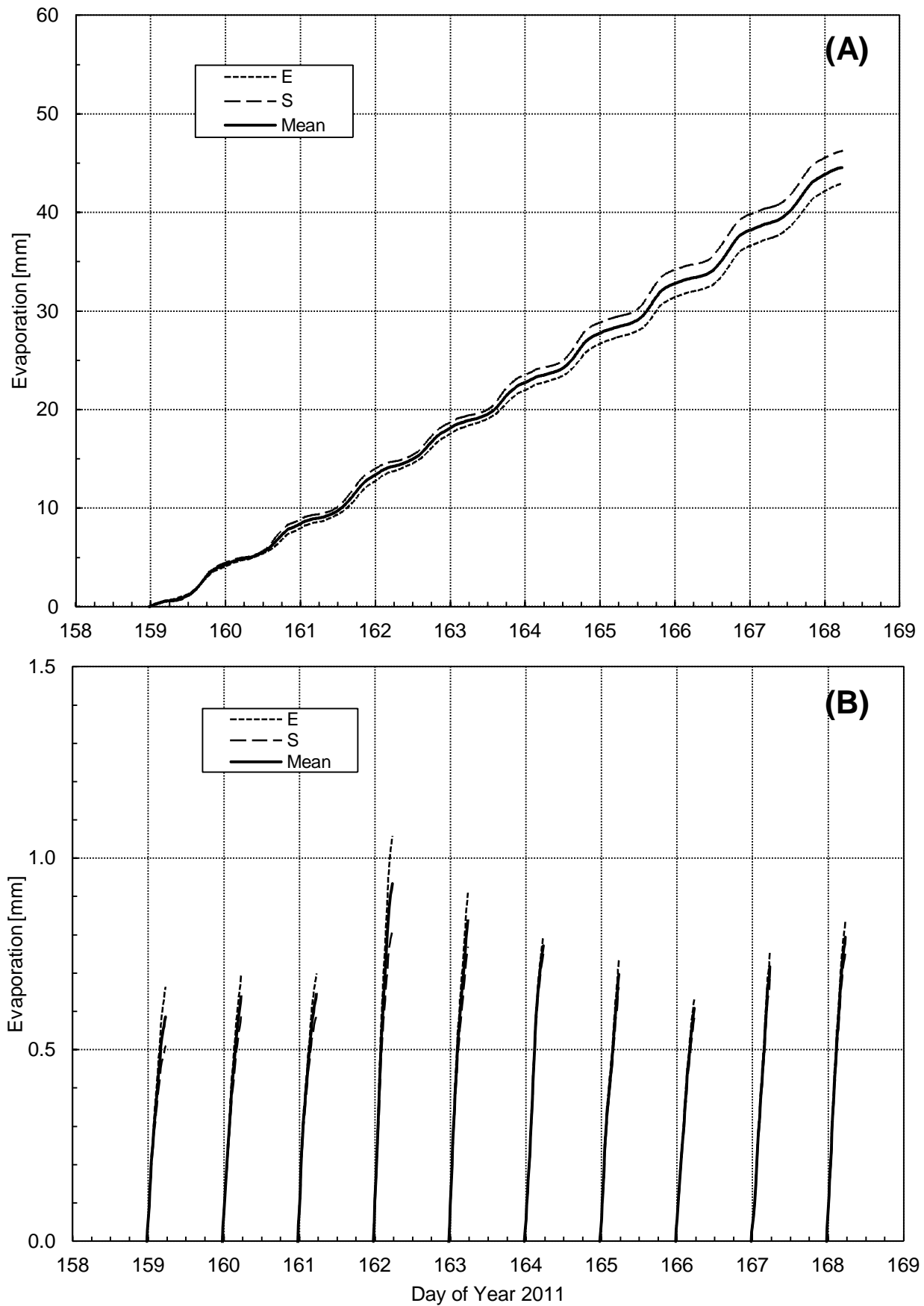


**Figure 9:** Scaled cumulative (A) and night time (B) evaporation, eastern (E) and southern (S) lagoon areas; Dairy A, Case 2.

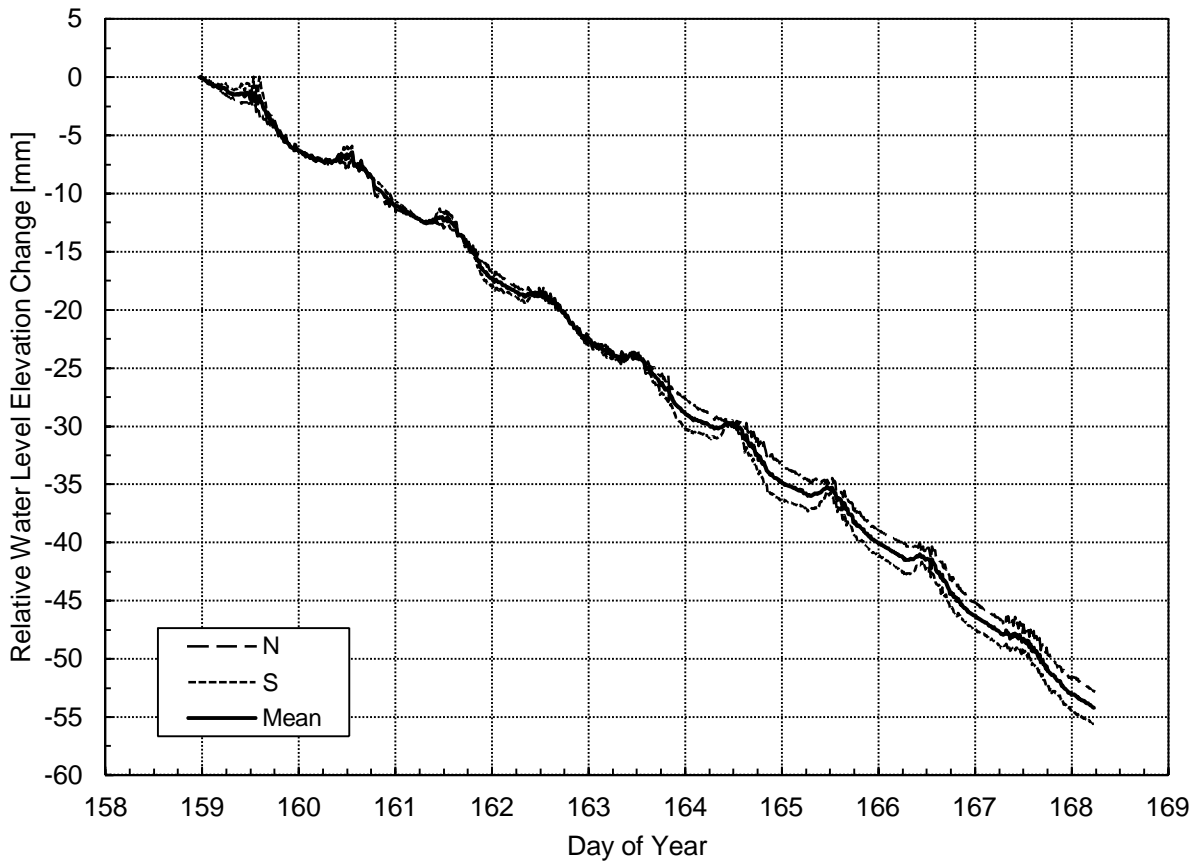


**Figure 10:** Scaled water level elevation changes as measured in the northern (N) and southern (S) lagoon areas; Dairy A, Case 2.

Comparison of cumulative water level elevation change and evaporation shows that approximately 82% of the water level elevation change is due to evaporative losses (**Figure 11**). This is in stark contrast to the results of the earlier lagoon performance testing in February 2011 (Case 1) and highlights the fact that seepage estimates from the June 2011 performance test are dominated by the evaporation estimates. The normalized seepage rate computed from the cumulative test duration (9 d 6 h) is  $1.0 \pm 2.3 \text{ mm d}^{-1}$  (**Figure 12**). More than 90% of the uncertainty surrounding the seepage estimate is due to the high evaporation rates during this water balance test. This demonstrates the advantage of completing the water balance during times of low evaporative demand.

Normalized seepage rates computed from 10 consecutive overnight water balance tests averaged  $1.8 \text{ mm d}^{-1}$ , ranged from  $0.8$  to  $2.8 \text{ mm d}^{-1}$ , and did not converge to a steady value. Apparently, the night time test duration of 6 hrs in combination with the site-specific ambient conditions was not sufficient for random error to achieve full attenuation.

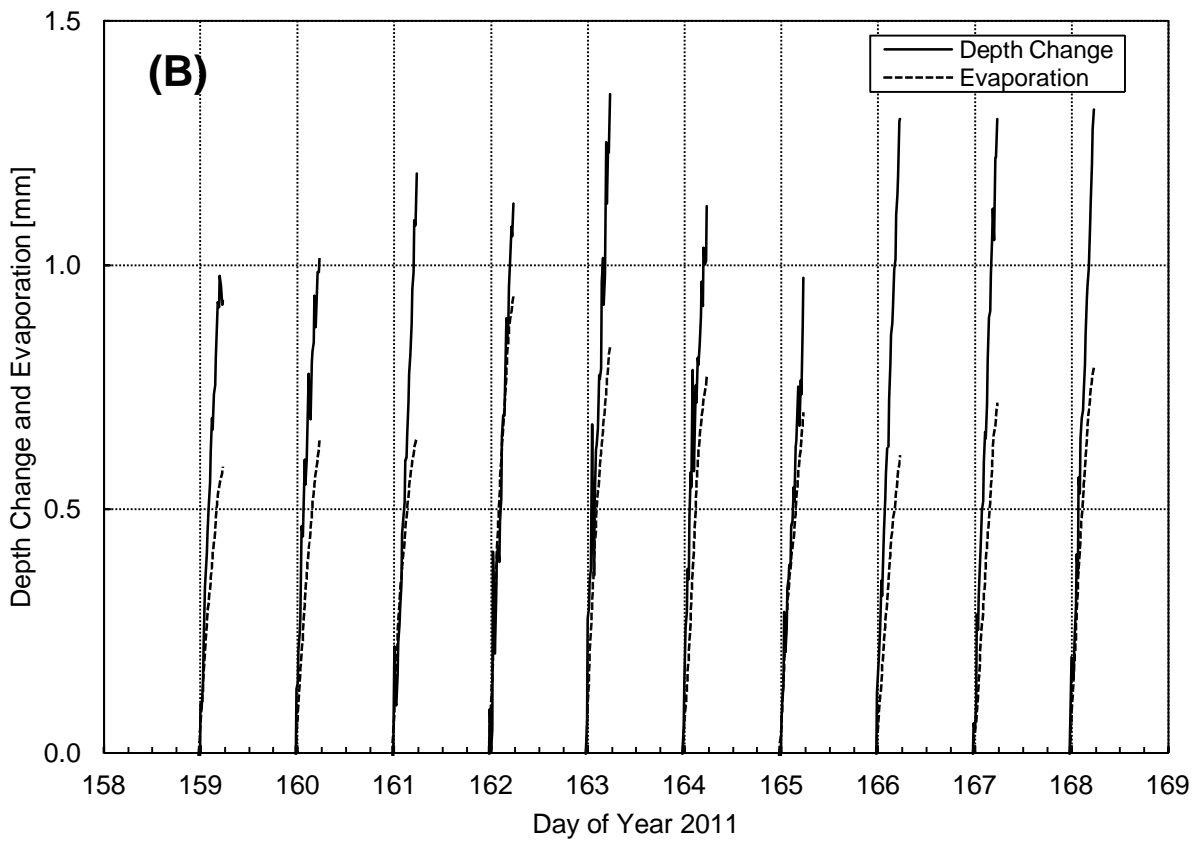
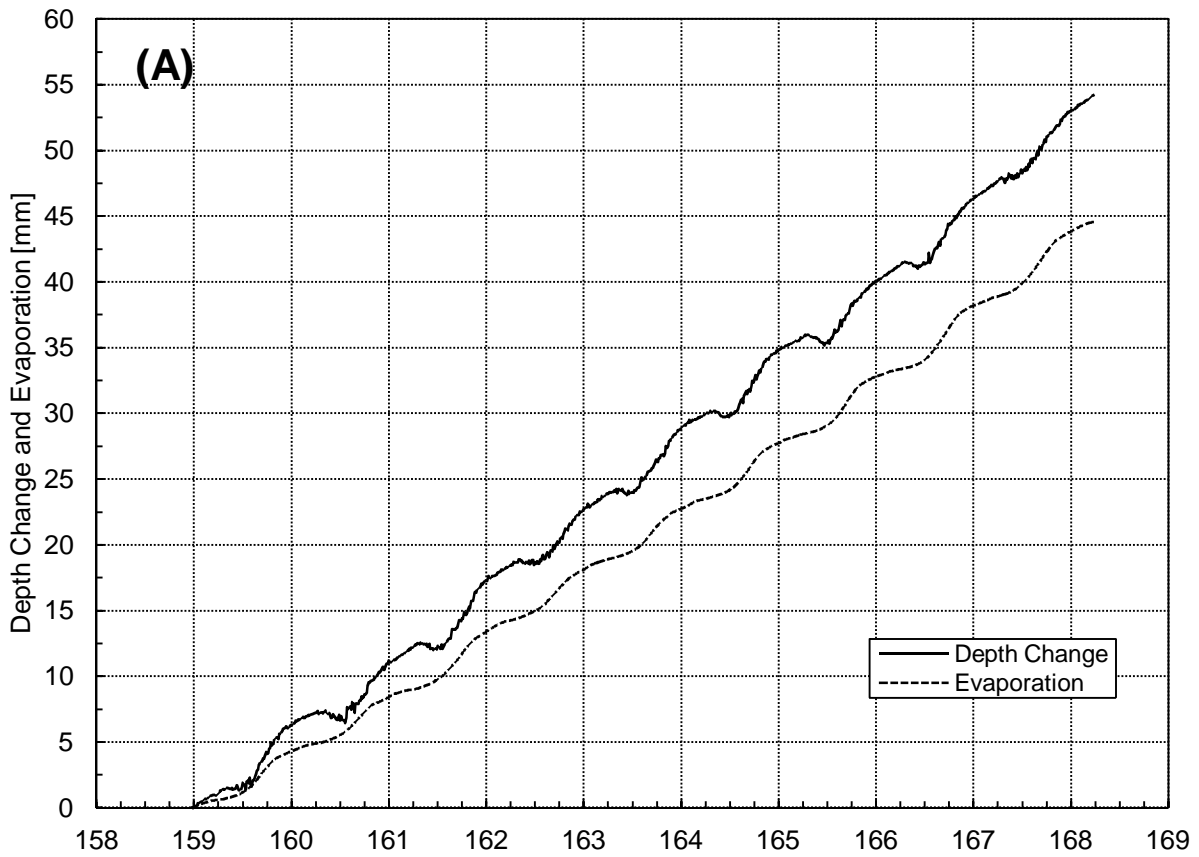


**Figure 11:** Scaled cumulative (A) and night time (23:30 h – 05:30 h) (B) change in depth and evaporation; Dairy A, Case 2.

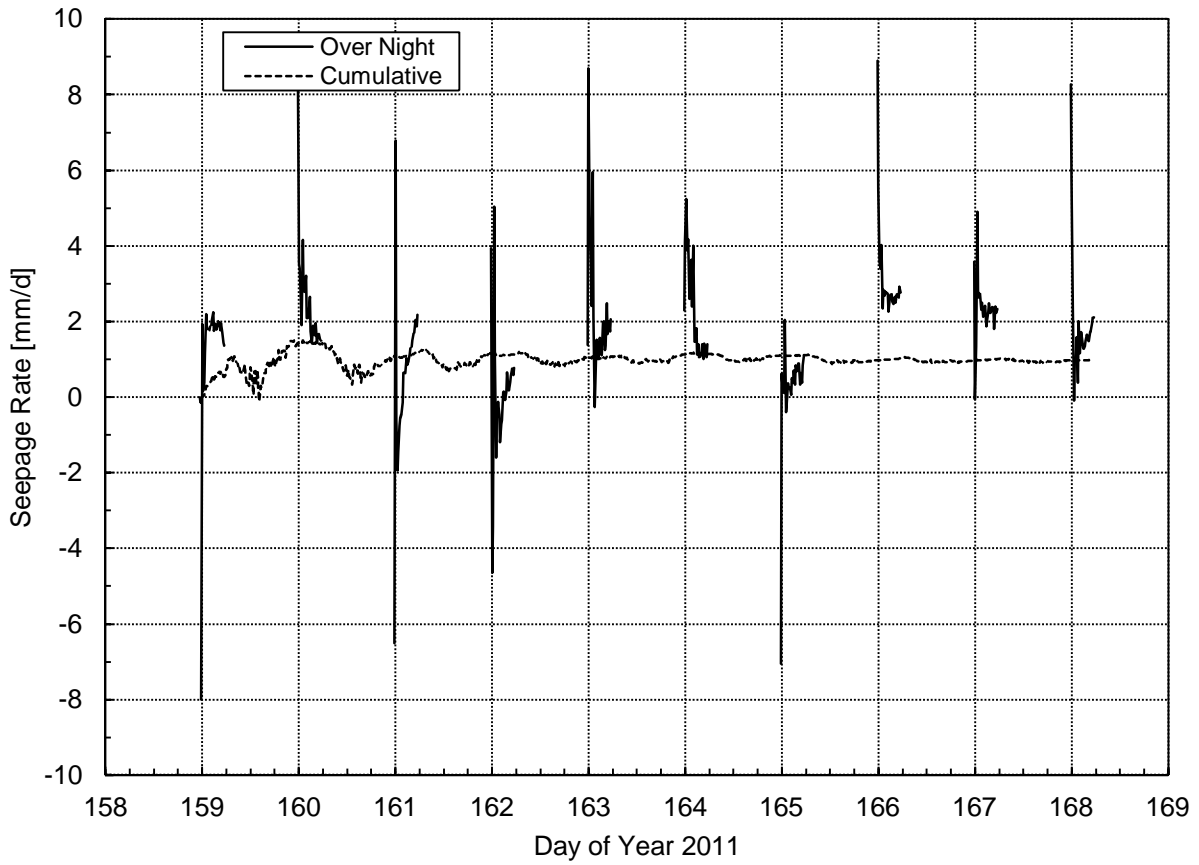


**Figure 12:** Normalized seepage rates as computed from the overnight water balance and the entire (cumulative) test duration; Dairy A, Case 2.

---

## 4 UNCERTAINTY ANALYSIS

In general, the concept of uncertainty is used to describe the degree of goodness of a measurement, experimental result, or analytical/numerical simulation result (Coleman and Steele, 2009). In particular, the uncertainty analysis discussed herein considers measurement error (i.e., relating to the quality of instrumentation) and environmental conditions during testing. Therefore, uncertainty is unique for each water balance test. In this document, uncertainty is expressed as a 95% confidence interval on the computed seepage rate<sup>7</sup>. For example, a seepage rate of  $1.0 \pm 0.1$  mm d<sup>-1</sup> suggests that, with 95% confidence, the true seepage rate resides within 0.9 and 1.1 mm d<sup>-1</sup> (where the uncertainty is  $\pm 0.1$  mm d<sup>-1</sup>).

In *Section 3*, it is shown that uncertainty analysis is most useful in conjunction with uninterrupted multi-day testing. If such testing is not possible, shorter-term testing provides a viable alternative. However, the shorter duration significantly increases the uncertainty in the results because both the absolute and relative uncertainty contributions from depth measurements increase. As a result, uncertainty analysis loses its utility in conjunction with overnight testing. Confidence in results can be gained, although less quantitatively, by running the water balance during several successive or near successive nights. While uncertainty analysis provides a very useful tool, the analyst's experience and judgment, involvement in the data collection and compilation effort, and visual inspection of site conditions and interpretation of the results are equally important. Also, uncertainty analysis provides a lower bound on the total uncertainty as it does not consider all potential sources of error (*Section 4.2.3*).

### 4.1 Concepts and Nomenclature

This section introduces basic concepts and statistical equations that make up the foundation for uncertainty analysis.

An error  $\delta$  is a quantity with a particular sign and magnitude. A specific error  $\delta_i$  is the difference caused by error source  $i$  between a quantity (measured or simulated) and its true value. It is generally assumed that each error whose sign and magnitude are known has been removed by correction (e.g., calibration). Therefore, any remaining error is of unknown sign and magnitude. The uncertainty  $u$  is estimated with the idea that  $\pm u$  characterizes the range containing  $\delta$ . Stated differently, the interval  $\pm u$  is an estimate of a range within which the actual value of an error of unknown sign and magnitude is believed to reside. For example, a seepage rate stated as  $1.0 \pm 0.1$  mm d<sup>-1</sup> suggests that, with 95% confidence, the true seepage rate resides within 0.9 and 1.1 mm d<sup>-1</sup>.

Consider a variable  $X$  with constant and true value  $X_{true}$ . Even under highly controlled laboratory conditions, measurements of  $X$  are influenced by elemental error sources (e.g., due to errors in the standard used for calibration, variations in ambient temperature and humidity, vibrations, electromagnetic influences, etc.). It is important to recognize that  $X_{true}$  is unknown and that its measurement represents the sum of  $X_{true}$  plus all elemental errors. These include errors that do not vary during the measurement period ( $\beta_1, \beta_2, \beta_3, \dots$ ) and errors that do vary during the measurement period ( $\epsilon_1, \epsilon_2, \epsilon_3, \dots$ ). The analyst

---

<sup>7</sup> Other confidence intervals can be chosen (e.g., 90% or 99% confidence intervals).

---

cannot distinguish between  $\beta_1, \beta_2,$  and  $\beta_3$  or between  $\varepsilon_1, \varepsilon_2, \varepsilon_3$ . Therefore, the difference between the measured value  $X_I$  (i.e., the first measurement) and  $X_{true}$  is  $\delta_{X_I}$ , which is the sum of the systematic error  $\beta$  (i.e., the combination of all the errors from the systematic elemental error sources) and the random error  $\varepsilon_I$  (i.e., the combination at the time  $X_I$  is measured of all the errors from the elemental error sources that vary).

The objective is then to specify a range ( $X_{best} \pm u_X$ ) within one thinks  $X_{true}$  resides.  $X_{best}$  is typically estimated as the average value of N measurements. The uncertainty  $u_X$  is an estimate of the interval  $\pm u_X$  that likely contains the magnitude of the combination of all of the errors affecting the measured value  $X$ . To associate an uncertainty with a measured value  $X$ , elemental uncertainty estimates for all of the elemental error sources are needed. Therefore,  $u_X$  is found from the combination of all the elemental standard uncertainties as

**eq. 4-1**

$$u_X = (u_1^2 + u_2^2 + u_3^2 + \dots + u_N^2)^{\frac{1}{2}}$$

The elemental standard uncertainties contained in eq. 4-1 may originate from elemental error sources that vary during the measurement period and those which do not vary during the measurement period.

There is no probability associated with the standard uncertainty  $u_X$  (eq. 4-1). In the following sections, the concept of the standard uncertainty is further developed to an expanded uncertainty estimate  $U_X$ , such that one is  $C$  percent confident that  $X_{true}$  resides within the interval  $X_{best} \pm U_X$ . For this purpose, basic statistical concepts are first applied to estimate the effects of random errors on the uncertainty of a measured variable. These concepts are then extended to the estimation of systematic error effects and the overall uncertainty for a measured variable.

#### **4.1.1 Random Error**

The earlier example of a variable  $X$  with constant and true value  $X_{true}$  is again considered. Repeated measurements of  $X$  would result in scatter about a central value, with some measurements higher and some lower. The statistical distribution of measurements defined, if an infinite number of measurements could be obtained, is called the population or parent distribution. Since an infinite number of measurements cannot be obtained, parent distributions are unknown. Populations are approximated with sample distributions composed of a finite number of measurements taken from the population. For purely random errors, the resulting infinite distribution will approach a Gaussian distribution.

In practice, the distribution of elemental errors is often unknown. However, if  $X$  is not dominated by a single error source but instead is affected by a combination of multiple, independent error sources (as is typically the case), then the resulting distribution for  $X$  will be approximately Gaussian (normal). This phenomenon is explained by the central limit theorem. The tendency toward a normal distribution is strong. For example, if  $X$  has two independent errors coming from rectangular (uniform) distributions, the resulting distribution for  $X$  will be approximately normal.

The applicability of the Gaussian distribution to uncertainty analysis is critical. The equation for the Gaussian distribution is

---

eq. 4-2

$$f(X) = \frac{1}{\sigma\sqrt{2\pi}} e^{-\frac{(X-\mu)^2}{2\sigma^2}}$$

where  $\mu$  is the population mean defined as

eq. 4-3

$$\mu = \lim_{N \rightarrow \infty} \frac{1}{N} \sum_{i=1}^N X_i$$

and  $\sigma$  is the population standard deviation defined as

eq. 4-4

$$\sigma = \lim_{N \rightarrow \infty} \left[ \frac{1}{N} \sum_{i=1}^N (X_i - \mu)^2 \right]^{\frac{1}{2}}$$

The sample distribution approximates the population. For  $N$  measurements of  $X$ , the sample mean is calculated as

eq. 4-5

$$\bar{X} = \frac{1}{N} \sum_{i=1}^N X_i$$

And the sample standard deviation  $s_X$  is calculated as

eq. 4-6

$$s_X = \left[ \frac{1}{N-1} \sum_{i=1}^N (X_i - \bar{X})^2 \right]^{\frac{1}{2}}$$

By definition, the standard uncertainty  $u$  (eq. 4-1) is an estimate of the standard deviation of the population from which a particular elemental error originates. Therefore,  $u$  is computed using eq. 4-6. The influences of all elemental error sources that vary during the measurement period (whether one knows the number of them or not) are included in  $s_X$ . In contrast, elemental error sources that do not vary during the measurement period (i.e., systematic error sources) do not influence  $s_X$ . Therefore, they are not included in  $s_X$ . The systematic standard uncertainty  $b_i$  is an estimate of the standard deviation of the distribution of the population from which a particular systematic error  $\beta_i$  originates (this is discussed in the following section).

Of particular interest to uncertainty analysis is the probability that a single measurement from a Gaussian parent population will fall within a specified range,  $\pm \Delta X$ , about the mean value. This is expressed as

eq. 4-7

$$Prob(\Delta X) = \int_{\mu-\Delta X}^{\mu+\Delta X} \left( f(X) = \frac{1}{\sigma\sqrt{2\pi}} e^{-\frac{(X-\mu)^2}{2\sigma^2}} \right) dX$$

---

This integral cannot be evaluated in closed form, and if its value were tabulated for a range of  $\Delta X$ , there would have to be a table for every pair of  $(\mu, \sigma)$  values. To address this issue, a normalized deviation from the mean value is defined as

**eq. 4-8**

$$\tau = \frac{X - \mu}{\sigma}$$

and eq. 4-7 can be rewritten as

**eq. 4-9**

$$Prob(\tau_1) = \frac{1}{\sqrt{2\pi}} \int_{-\tau_1}^{\tau_1} e^{-\frac{\tau^2}{2}} d\tau$$

where  $\tau_1 = \Delta X / \sigma$ .

$Prob(\tau_1)$  is referred to as a two-tailed probability since both the negative and positive tails of the distribution are included in the integration. Values of  $Prob(\tau)$  for  $\tau$  can be obtained from a statistical table showing two-tailed Gaussian probabilities. For example, for a Gaussian distribution, 68.27% of measurements are within  $\pm 1.00\sigma$ , 95.00% are within  $\pm 1.96\sigma$ , and 99.73% are within  $\pm 3.00\sigma$ . Therefore, knowing that 95% of the population lies within  $\pm 1.96\sigma$  of the mean  $\mu$ , one can be 95% confident that any particular measurement will fall within this  $\pm 1.96\sigma$  of interval about the mean. This probability is expressed as

**eq. 4-10**

$$Prob\left(-1.96 \leq \frac{X_i - \mu}{\sigma} \leq 1.96\right) = 0.95$$

After multiplying the terms in the parentheses by  $\sigma$  and then adding  $\mu$  to each term yields

**eq. 4-11**

$$Prob(\mu - 1.96\sigma \leq X_i \leq \mu + 1.96\sigma) = 0.95$$

Differently stated,  $+1.96\sigma$  and  $-1.96\sigma$  are the upper and lower bounds on the 95% confidence interval for the measurement of  $X$ . This concept of a confidence interval is fundamental to uncertainty analysis.

The next equation expresses within what interval about a particular measurement of  $X_i$  the mean value of the distribution would reside at a confidence level of 95%

**eq. 4-12**

$$Prob(X_i - 1.96\sigma \leq \mu \leq X_i + 1.96\sigma) = 0.95$$

Therefore, one can be 95% confident that the mean  $\mu$  of the population will fall within  $\pm 1.96\sigma$  of a single measurement of  $X_i$ . Since  $\mu$  is typically not known, the concept of 95% confidence interval is applied in uncertainty analysis to estimate the range that should contain  $\mu$ . To extend the concept of confidence intervals in Gaussian distribution to sample distribution, the standard deviation associated with the sample mean  $\bar{X}$  is also of interest. The sample mean  $\bar{X}$  itself is normally distributed with mean  $\mu$  and standard deviation

---

**eq. 4-13**

$$\sigma_{\bar{x}} = \frac{\sigma}{\sqrt{N}}$$

In practice, the parent population standard deviation  $\sigma$  is not known, and the sample standard deviation of the mean is defined as

**eq. 4-14**

$$s_{\bar{x}} = \frac{s_x}{\sqrt{N}}$$

As stated previously, the standard uncertainty  $u$  (eq. 4-1) is an estimate of the standard deviation of the population from which a particular elemental error originates. Eq. 4-14 presents an alternative to eq. 4-6 to compute  $u$ .

Therefore, eq. 4-12 can be rewritten as

**eq. 4-15**

$$Prob\left(\bar{X} - 1.96 \frac{\sigma}{\sqrt{N}} \leq \mu \leq \bar{X} + 1.96 \frac{\sigma}{\sqrt{N}}\right) = 0.95$$

Consequently, one can also be 95% confident that the mean  $\mu$  of the population will fall within  $\pm 1.96\sigma/N^{0.5}$  of the sample mean  $\bar{X}$  computed from  $N$  measurements. The width of the 95% confidence interval in eq. 4-15 is narrower than the one in eq. 4-11 by a factor of  $1/N^{0.5}$ .

Since the actual value of  $\sigma$  is not known, the sample standard deviation  $s_x$  is employed. Working with a 95% confidence interval and following the same approach as in eq. 4-10, the value of  $t$  is sought that satisfies

**eq. 4-16**

$$Prob\left(-t_{95} \leq \frac{X_i - \mu}{s_x} \leq t_{95}\right) = 0.95$$

and

**eq. 4-17**

$$Prob\left(-t_{95} \leq \frac{\bar{X} - \mu}{s_x/\sqrt{N}} \leq t_{95}\right) = 0.95$$

where  $t_{95}$  is no longer equal to 1.96, because  $s_x$  is only an estimate of  $\sigma$  based on a finite number of measurements  $N$ . The fractional terms in eqs. 4-16 and 4-17 follow the  $t$ -distribution with  $N-1$  degrees of freedom  $\nu$ . Values of  $t$  are obtained from a statistical table of the  $t$ -distribution for a specified  $\nu$  and confidence level  $C$ . For a given  $C$ ,  $t$  is a function of the sample size  $N$ . For small  $N$ , confidence intervals are wider. As  $N$  approaches infinity,  $t$  approaches the Gaussian value of 1.96 for a 95% level of confidence.

Rearranging terms to isolate  $\mu$ , the confidence interval expression becomes

---

eq. 4-18

$$Prob(X_i - t_{95}s_X \leq \mu \leq X_i + t_{95}s_X) = 0.95$$

Therefore, one can be 95% confident that the mean  $\mu$  of the population will fall within  $\pm t_{95}s_X$  of a single measurement of  $X_i$ .

Using the sample mean  $\bar{X}$  to approximate the population mean  $\mu$ ,

eq. 4-19

$$Prob\left(\bar{X} - t_{95} \frac{s_X}{\sqrt{N}} \leq \mu \leq \bar{X} + t_{95} \frac{s_X}{\sqrt{N}}\right) = 0.95$$

Therefore, one can be 95% confident that the mean  $\mu$  of the population will fall within  $\pm t_{95}s_X/N^{0.5}$  of the sample mean  $\bar{X}$ .

### 4.1.2 Systematic Error

As stated previously, the standard uncertainty  $u$  is defined as an estimate of the standard deviation  $s_X$  of the population from which a particular elemental error originates. In the preceding section, it is shown that the standard uncertainty due to random errors in the measurements of a variable can be achieved by using  $s_X$ , where  $s_X$  is the standard deviation of a sample of  $N$  measurements of variable  $X$ . However, systematic errors are not detectable by taking multiple measurements<sup>8</sup>. Therefore, the influence of systematic errors is not included in  $s_X$ .

The systematic standard uncertainty  $b_i$  is an estimate of the standard deviation of the distribution of the parent population from which a particular systematic error  $\beta_i$  originates. The fixed error  $\beta$  that remains after calibration corrections, is the sum of all the significant systematic errors. However, its magnitude and sign are unknown. Systematic standard uncertainties are needed that quantify the effects of each systematic elemental error.

To estimate the magnitude of a systematic error it is assumed that, for a given case,  $\beta_i$  is a single realization drawn from some statistical parent population of possible systematic errors. In practice, manufacturers' calibration information can be used to do this. For example, a manufacturer may specify that instrumentation output resides within limits  $\pm A$ . Based on specific knowledge or experience, one has to assume some distribution within these limits (e.g., Gaussian, rectangular (uniform), or triangular). A standard deviation estimate must be made for the distributions for each systematic error source identified as being significant in the measurement of a variable. The analyst is charged with using the best information and judgment possible to make the estimate.

### 4.1.3 Overall Uncertainty of a Measured Variable

The overall uncertainty of a measured variable  $X$  is the interval around the best value of  $X$  within which the true value  $X_{true}$  is expected to reside with a given confidence level. To obtain the overall uncertainty, random and systematic standard uncertainty estimates are combined by adding the variances (i.e., the squares of the standard deviations) for these estimates. The standard deviation estimate for the systematic uncertainty for error source  $k$  is  $b_k$ , or the best estimate of the standard deviation of the possible parent

---

<sup>8</sup> For example, within the specified error range of calibrated instrumentation, an instrument may produce output that is systematically higher or lower than the true value of the measured variable.

population for the systematic error  $\beta_k$ . The standard deviation estimate for the random uncertainty is  $s_X$  from either eq. 4-5 or 4-14, depending on whether the uncertainty interval is centered on  $X$  or  $\bar{X}$ . The  $b_k$ 's have the same values regardless of whether  $X$  is a single reading or a mean value because the averaging process does not affect the systematic uncertainties. From eq. 4-1, the combined standard uncertainty  $u_c$ , for variable  $X$  is expressed as

**eq. 4-20**

$$u_c^2 = s_X^2 + \sum_{k=1}^M b_k^2$$

where  $M$  is the number of significant elemental systematic error sources.

To associate a level of confidence with the uncertainty of the variable, a coverage factor is used such that

**eq. 4-21**

$$U_{\%} = k_{\%} u_c$$

where  $U_{\%}$  is the overall or expanded uncertainty at a given percent level of confidence. Since the central limit theorem indicates that the distribution for the total errors  $\delta$  for the variable will usually approach Gaussian, where the factor  $u_c$  is an estimate of the standard deviation of this overall error distribution, values from the  $t$ -distribution are used to obtain  $k_{\%}$ , such that

**eq. 4-22**

$$U_{\%} = t_{\%} u_c$$

The  $\pm U_{\%}$  interval around the variable ( $X$  or  $\bar{X}$ ) will contain the true value of the variable with the given percent level of confidence. A number of degrees of freedom is needed to select the  $t$ -value from a statistical table of the  $t$ -distribution. As discussed earlier,

**eq. 4-23**

$$v_{s_X} = N - 1$$

To estimate the degrees of freedom for the systematic component,

**eq. 4-24**

$$v_{b_k} \approx \frac{1}{2} \left( \frac{\Delta b_k}{b_k} \right)^{-2}$$

where the quantity in parenthesis is the relative uncertainty of  $b_k$ .

For most engineering and scientific experiments including the water balance test, the degrees of freedom are large enough to consider the  $t$  value equal to a constant, which will be approximately equal to the Gaussian value for a given level of confidence (e.g., 2 for 95% or 2.6 for 99%). Therefore, from eqs. 4-20 and 4-22, the overall uncertainty for a 95% level of confidence is

---

eq. 4-25

$$U_{95} = 2 \left( s_X^2 + \sum_{k=1}^M b_k^2 \right)^{\frac{1}{2}}$$

Where the first term represents the random error contribution and the second term represents the contribution from systematic error sources. The true value of the variable will then be within the limits

eq. 4-26

$$X - U_{95} \leq X_{true} \leq X + U_{95}$$

with a 95% confidence, where  $X$  is either  $X$  or  $\bar{X}$ .

## 4.2 Uncertainty Analysis Applied to the Water Balance Test

In this section, concepts of uncertainty analysis are applied to the water balance. Eq. 4-4 suggests that the uncertainty surrounding  $S$  (i.e.,  $US$ ) depends on errors inherent in the depth measurements, precipitation, time, and the results of the evaporation model. Inaccuracies in time measurements were found to not constitute a significant error source and were, therefore, not addressed in the uncertainty analysis<sup>9</sup>. Further, since all testing was done during times of no precipitation, only the uncertainty of depth measurements and the results of the evaporation model contribute to  $US$  (mm). This combined uncertainty is calculated with a root-sum-square formula

eq. 4-27

$$US = \frac{1}{t_f - t_0} [(UD_{t_f})^2 + (UD_{t_0})^2 + (U\Sigma E)^2]^{\frac{1}{2}}$$

where

$UD_{t_f}$  = uncertainty of the depth measurement at the end of the test [mm]

$UD_{t_0}$  = uncertainty of the depth measurement at the beginning of the test [mm]

$U\Sigma E$  = uncertainty of the cumulative evaporation [mm]

The uncertainties surrounding the depth measurements at the beginning and the end of the test are calculated with eq. 4-25. To solve eq. 4-25, estimates of the random standard uncertainty and the systematic standard uncertainty are made.

- The random standard uncertainty is estimated as the sample standard deviation calculated from a given data aggregation interval using eq. 4-6.
- The systematic standard uncertainty is estimated using manufacturers' information on the instruments' accuracy (**Table 1**). Instruments that do not perform within the given accuracies fail the manufacturers' quality control. Stated differently, 100% of measurements (instead of just 95

---

<sup>9</sup> The internal clocks of the electronic logging equipment were found to deviate only a few seconds between loggers over the duration of a water balance test. Deviations between the internal clocks of the electronic logging equipment and the laptop computer that was used to reset the loggers between individual water balance tests were similarly small. The overall uncertainty introduced by these inaccuracies is several orders of magnitude smaller than the resolution given for calculated seepage rates.

% of measurements that reside within two standard deviations) reside within the given accuracy ranges. By using one half of the manufacturer-supplied accuracy range as a standard deviation estimate, a conservative estimate is obtained for the systematic standard uncertainty. For example, the systematic standard uncertainty estimate for water surface temperature is  $0.2\text{ }^{\circ}\text{C} / 2 = 0.1\text{ }^{\circ}\text{C}$ .

Some of the accuracies shown in **Table 1** are not constants but variables that change over the range of measurements. In these cases, the largest inaccuracy expected over the range of environmental conditions encountered in the field was used for the estimation of the systematic standard uncertainties. Estimates of the systematic standard uncertainties of the variables needed for the water balance calculations are shown in **Table 2**.

**Table 1: Manufacturers' Instrumentation Technical Specifications**

Variable	Model	Range	Accuracy (a)	Resolution	Threshold
Air Temperature	HMP 155A	-80 to +60 °C	$\pm (0.055 - 0.0057 \times \text{temperature})\text{ }^{\circ}\text{C}$ (b)	0.01 °C	na
	HMP 155A	-80 to +20 °C	$\pm (0.226 - 0.0028 \times \text{temperature})\text{ }^{\circ}\text{C}$ (c)	0.01 °C	na
Water Surface Temperature	SI-111	-40 to +70 °C	$\pm 0.2\text{ }^{\circ}\text{C}$ (-10 to 65 °C)	0.01 °C	na
Relative Humidity	HMP 155A	0.8 to 100 % RH	$\pm (1.0 + 0.008 \times \text{reading})\text{ } \% \text{ RH}$ (-20 to +40 °C) (d)	0.01 % RH	na
Wind Speed	F 460	0 to 60 m/s	$\pm 0.07\text{ m/s}$ or $\pm 1.0\text{ } \%$ (whichever is greater)	0.001 m/s	0.22 m/s
Wind Direction	F 460	360 degrees	$\pm 2\text{ degrees}$	0.1 degree	0.22 m/s
Precipitation	TE525MM	0 to 50 °C	$\pm 1\%$ (up to 10 mm/h)	1 tip = 0.1 mm	na
Waste Depth	PT2X	0 to 1 psi	$\pm 0.1\text{ } \%$ full range (i.e., 0.7 mm)	16 bit	na

- (a) Instruments that do not perform within the given accuracies fail the manufacturers' quality control.
- (b) The maximum error calculated over the range of temperatures encountered in the field (i.e., 0 to 35 °C) is  $\pm 0.145\text{ }^{\circ}\text{C}$  (at 35 °C).
- (c) The maximum error calculated over the range of temperatures encountered in the field (i.e., 0 to 35 °C) is  $\pm 0.226\text{ }^{\circ}\text{C}$  (at 0 °C).
- (d) The maximum error occurs at 100 % RH and is  $\pm 1.8\text{ } \%$  RH.

**Table 2: Estimates of Systematic Standard Uncertainties (a)**

Variable	Symbol	Units	Systematic Standard Uncertainty
Air Temperature	$T_a$	[°C]	0.113
Water Surface Temperature	$T_s$	[°C]	0.1
Relative Humidity	RH	[%]	0.9
Wind Speed	U	[m/s]	0.035
Waste Depth	D	[mm]	0.35
Bulk Transfer Coefficient	$C_e$	[dimensionless]	0.00015

- (a) Systematic standard uncertainties are one half of manufacturers' accuracy specifications. See Ham (2002 b) for systematic standard uncertainty for  $C_e$ .

#### 4.2.1 Uncertainty Surrounding Depth Calculations

The standard uncertainty of the random error component was estimated as the standard deviation of depth measurements calculated from the first and last data aggregation intervals, respectively

---

$$s_{t0} = 0.14 \text{ mm}$$

$$s_{tf} = 0.05 \text{ mm}$$

and the associated systematic standard uncertainty is taken from **Table 2**

$$b = 0.35 \text{ mm}$$

Using eq. 4-25,

$$UD_{t0} = U_{95} = 2 \left( s_X^2 + \sum_{k=1}^M b_k^2 \right)^{\frac{1}{2}} = 2\sqrt{0.14^2 + 0.35^2} = 0.75 \text{ mm}$$

$$UD_{tf} = U_{95} = 2 \left( s_X^2 + \sum_{k=1}^M b_k^2 \right)^{\frac{1}{2}} = 2\sqrt{0.05^2 + 0.35^2} = 0.71 \text{ mm}$$

The inaccuracy in the change-in-depth measurement ( $D_{tf} - D_{t0}$ ) can be determined using eq. 4-27 excluding the  $U_{\Sigma E}$  term. Therefore, the overall uncertainty associated with depth measurements in this particular example is  $\pm 1.03 \text{ mm}$  (i.e.,  $\sqrt{0.75^2 + 0.71^2}$ ).

This example provides notable insight. Firstly,  $UD_{t0}$  and  $UD_{tf}$  were dominated by the uncertainty inherent in the measurement of the pressure transducer itself despite the use of highly accurate instrumentation. Random variability of measurements contributed only a minor amount of uncertainty. The random variability is caused mainly by wave action which is related to wind speed. Wind speeds were smaller than  $2 \text{ m s}^{-1}$  during the depth measurements. This highlights the tremendous importance of depth measurements in the overall accuracy of seepage estimates. It is critical to use highest quality instrumentation and begin and end water balance tests during times of low wind speeds.

Secondly, the above overall uncertainty estimate applies to the entire water balance test regardless of its duration. Therefore, increasing the test duration achieves a relative decrease of the uncertainty component from depth measurements. For example, the above uncertainty of  $\pm 1.03 \text{ mm}$  in a 10 d water balance test would contribute an uncertainty of only  $\pm 0.1 \text{ mm d}^{-1}$  to the estimated seepage result. In contrast, in an overnight test with a 12 h duration, the same  $\pm 1.03 \text{ mm}$  uncertainty would contribute an uncertainty of  $\pm 2.0 \text{ mm d}^{-1}$ . In comparison to typical seepage rates reported in the literature, ranging from less than 1 to approximately  $5 \text{ mm d}^{-1}$ , this is a very large uncertainty that can significantly diminish the usefulness of the test results. This highlights a critical limitation of short-duration (e.g., overnight) water balance tests. Confidence in overnight water balance tests is not achieved by applying uncertainty analysis – it is achieved by repetition during consecutive or near-consecutive nights, thereby reducing uncertainty.

## 4.2.2 Uncertainty Surrounding Evaporation

The estimation of the uncertainty surrounding the evaporative losses calculated with the BT model is more complex than the uncertainty surrounding the depth measurements. The BT model is a data reduction equation (DRE) and necessitates measurements of ambient air temperature, relative humidity, and wind speed; and water surface temperature. In addition, the model includes an empirically determined bulk transfer coefficient  $C_e$ . The uncertainties of all measured values of the variables and  $C_e$

---

have to be propagated into the end result of the model to estimate the overall uncertainty surrounding the end results. This process is repeated for each data aggregation interval before the results can be summed over the duration of the test.

There are two methods available to propagate uncertainties through a DRE: the Monte Carlo Method (MCM) and the Taylor Series Method (TSM). Both methods yield the same results and are described below. The analyst's choice will be largely one of preference.

#### 4.2.2.1. Monte Carlo Method

The MCM is an iterative statistical method based on the concepts developed in *Section 4.1*. In the following, a step-by-step description of the MCM is given.

##### Step 1

###### Estimation of $X_{best}$

For each measured variable (i.e.,  $T_a$ ,  $T_s$ ,  $RH$ , and  $W$ ), an assumed true value  $X_{best}$  is estimated. These are the sample means  $\bar{X}$  calculated from the high-frequency measurements in a given data aggregation interval (e.g., 15-second measurements aggregated over 15 minute intervals) (eq. 4-5).  $X_{best}$  for  $C_e$  is  $2.5 \times 10^{-3}$ .

##### Step 2

###### Estimation of Standard Uncertainties

For each measured variable, estimates of the random standard uncertainties are made. These are the sample standard deviations  $s_X$  calculated from a given data aggregation interval (eq. 4-6).  $C_e$  is assumed to not have random error attached to its value. Estimates of the systematic standard uncertainties are taken from **Table 2**.

##### Step 3

###### Random Number Generator

For each variable, including  $C_e$ , random values ( $i=1$  to  $M$  iterations) for the random errors and the systematic errors are found using a random number generator (in this case a Gaussian random number generator).

##### Step 4

###### Calculation of Possible Values for Variables

For each variable, including  $C_e$ , a pair of random and systematic errors ( $\epsilon_i$ ,  $\beta_i$ ) is found. A possible value  $X(i)$  is calculated by summing  $X_{true}$  with these errors. For example, for ambient air temperature

eq. 4-28

$$T_a(i) = X_{true} + \epsilon_1(i) + \beta_1(i)$$

##### Step 5

###### Calculation of Possible Results with Evaporation Model

Using  $T_a(i)$ ,  $T_s(i)$ ,  $RH(i)$ ,  $W(i)$ , and  $C_e(i)$ ,  $E$  is calculated with eq. 2-6b.

*Steps 3 to 5* are repeated  $M$  times to obtain a distribution for the possible evaporation results values. The primary goal of the MCM propagation technique is to estimate a converged value for the standard deviation  $s_{MCM}$  for this distribution. The appropriate value for  $M$  is determined by periodically calculating  $s_{MCM}$  (eq. 4-6) during the MCM process. The converged  $s_{MCM}$  is the estimate of the combined standard

uncertainty  $u_r$  of the result. Once a converged value of  $u_r$  is determined, the overall uncertainty for the result at a 95% level of confidence is (using eq. 4-21 and rounding 1.96 to 2)

eq. 4-29

$$U_{r,95} = 2u_r$$

Once the overall uncertainty for the first time step  $t=1$  (i.e., the first data aggregation interval) is determined, Steps 1 to 5 are repeated for  $t=2, t=3$ , etc. The total uncertainty surrounding  $E$  for a given water balance test  $U\sum E$  is calculated by summing the overall uncertainties that were calculated for each data aggregation interval. Finally,  $\Delta S$  is calculated using eq. 4-27.

The quality of the MCM results depends on the quality of the random number generator used in the computations. Most programs for statistical data analysis contain a function for generating uniform random numbers. To ensure adequate performance, the employed random number generator should pass the Diehard Battery of Tests of Randomness (McCullough, 1998; McCullough, 1999).

Although large quantities of random numbers (i.e., many thousands) can be generated essentially instantaneously, automation of the process for many time steps may require more advanced computer coding.

#### 4.2.2.2. Taylor Series Method

The TSM works directly with the partial derivatives of the random and systematic components of the combined standard uncertainty. For a function of several variables (like the BT model)

eq. 4-30

$$r = r(X_1, X_2, \dots, X_j)$$

where  $r$  symbolizes the BT model, the TSM propagation equation is given by

eq. 4-31

$$u_r^2 = \sum_{i=1}^j \left( \frac{\partial r}{\partial X_i} \right)^2 s_{X_i}^2 + \sum_{i=1}^j \left( \frac{\partial r}{\partial X_i} \right)^2 b_{X_i}^2$$

where  $u_r$  is the combined standard uncertainty. It is assumed that there are no correlated random or systematic errors. The  $s_{X_i}$  values are the standard deviations calculated from a given data aggregation interval (eq. 4-6).  $C_e$  is assumed to not have random error attached to its value. The  $b_{X_i}$  values are derived from manufacturers' instrumentation specifications (see **Table 2**). The  $X_i$ 's are the  $X_{best}$  (i.e., for each variable in the BT model ( $T_a$ ,  $T_s$ ,  $RH$ , and  $W$ )). The first group of terms on the right hand side of eq. 4-31 is the random standard uncertainty of the result

eq. 4-32

$$s_r^2 = \sum_{i=1}^j \left( \frac{\partial r}{\partial X_i} \right)^2 s_{X_i}^2$$

The second group of terms on the right hand side of eq. 4-31 is the systematic standard uncertainty of the result

**eq. 4-33**

$$b_r^2 = \sum_{i=1}^j \left( \frac{\partial r}{\partial X_i} \right)^2 b_{X_i}^2$$

The combined standard uncertainty of the result is defined as

**eq. 4-34**

$$u_r = (s_r^2 + b_r^2)^{\frac{1}{2}}$$

And, following the concepts discussed in *Section 4.1.3*, the overall uncertainty for a 95% level of confidence is

**eq. 4-35**

$$U_{r95} = 2(s_r^2 + b_r^2)^{\frac{1}{2}}$$

and substituting  $s_r$  and  $b_r$  from eqs. 4-32 and 4-33 yields

**eq. 4-36**

$$U_{r95} = 2 \left[ \sum_{i=1}^j \left( \frac{\partial r}{\partial X_i} \right)^2 (s_{X_i}^2 + b_{X_i}^2) \right]^{\frac{1}{2}}$$

Taking the coverage factor inside the summation yields

**eq. 4-37**

$$U_{r95} = \left[ \sum_{i=1}^j \left( \frac{\partial r}{\partial X_i} \right)^2 (2^2 u_i^2) \right]^{\frac{1}{2}}$$

or

**eq. 4-38**

$$U_{r95} = \left[ \sum_{i=1}^j \left( \frac{\partial r}{\partial X_i} \right)^2 U_i^2 \right]^{\frac{1}{2}}$$

The partial derivatives in eq. 4-31 and 4-38 can be numerically approximated using, for example, a forward-differencing finite difference approach or the central difference approach. The central difference approach was found to converge faster. Using the central difference approach, the partial derivatives are approximated separately for each data aggregation interval with

eq. 4-39

$$\frac{\partial r}{\partial X_i} \cong \frac{r_{X_i+\Delta X_i} - r_{X_i-\Delta X_i}}{2\Delta X_i}$$

A good initial estimate of  $\Delta X_i$  is  $0.01X_i$ . The numerical derivative is calculated with this first perturbation and then with a perturbation of one-half that first perturbation. These two derivative values are compared for convergence, and the process is repeated if necessary. Once converged derivative values are obtained for all variables at each time step, they are used in eq. 4-31 or 4-38. Eq. 4-38 directly yields the overall uncertainty for a 95% level of confidence. Using eq. 4-31, the result must be multiplied by the coverage factor of 2 to obtain the overall uncertainty for a 95% level of confidence. This process is then repeated for the next data aggregation interval until an overall uncertainty estimate is computed for each interval. These estimates are then summed to yield  $U\Sigma E$ , which is input into eq. 4-27.

Using the central-difference finite differencing approach, convergence is typically achieved with 5 or less iterations. This characteristic helps implement the TSM with a spreadsheet application and makes it fairly user friendly even for water balance tests with many hundred data aggregation intervals.

### 4.2.3 Other Sources of Uncertainty

The uncertainty analysis discussed herein considers measurement error (i.e., relating to the quality of instrumentation) and ambient conditions during testing. However, there are other sources of potential error that are not considered; and therefore, the uncertainty analysis yields a lower bound on the total uncertainty. For example:

- ❑ If the IRT is incorrectly positioned, such that it senses radiation emitted by objects other than the target water surface (e.g., barns, the bank, or the sky), measurements will misrepresent the water surface temperature.
- ❑ If unaccounted inflows and outflows occur, testing results will be incorrect.
- ❑ There may be situations when the evaporation is affected by factors not included in the BT model, for example, if nearby buildings, vegetation, or topography affect wind flow and change the characteristics of the surface boundary layer and the associated bulk transfer coefficient  $C_e$ .
- ❑ In some cases, water balance testing conducted as part of this work effort demonstrated that suspect hydraulic isolation of the tested lagoon can invalidate results (*Appendix 3*).

Two potential sources of error that will not necessarily be identifiable by inspection of collected data are discussed below.

#### 4.2.3.1. Sky Radiant Energy

Sky radiant energy is influenced by clouds. Specifically, it increases with increasing cloud cover and decreasing cloud altitude. Therefore, the lowest radiant energy occurs under clear skies and the greatest radiant energy occurs during conditions of low-altitude complete overcast. The difference between these extremes over a range of conditions is up to approximately  $120 \text{ W/m}^2$ .

Direct measurements of sky radiant energy were obtained during one night with mostly clear skies and high relative humidity (averaging 94%)<sup>10</sup>. For this purpose, the IRT is positioned vertically toward the sky (this is not a preferable setup, as it leaves the instrument's lens vulnerable to precipitation, deposition

---

<sup>10</sup> The IRTs used in this work effort do not function when solar radiation is incident to the lens.

---

of dust, dew, and bird feces). Results showed that direct radiant energy measurements were consistently approximately 120 W/m<sup>2</sup> lower than those obtained with the Brutsaert formula (Brutsaert, 1975).

There are parameterization schemes available that account for degree of cloud cover and cloud altitude. However, these schemes are not practical for this work effort because they require constant cloud monitoring and ultimately necessitate substantial approximations.

The sensitivity of the bulk aerodynamic transfer model to background radiant energy was evaluated by carrying out computations over a duration of 9 days, and re-running the same computations with background sky radiant energy increased and decreased by 120 W/m<sup>2</sup>, respectively. The resulting calculated cumulative evaporative losses differed less than ±0.01 mm after 9 days. At no time during the 9-day experiment was the difference greater than ±0.01 mm.

There are two reasons that explain why the background radiant energy has little effect on the results of the bulk aerodynamic transfer model. Eq. 2-12 shows the small influence of the background radiant energy on the IRT measurement. This apparent small influence is further reduced, because background sky radiant energy is typically much smaller than energy emitted from a lagoon surface. Specifically, typical lagoon surface temperatures encountered during the testing ranged from 0 to 25 °C, whereas sky temperatures directly measured with the IRT ranged from -40 to -50 °C.

#### **4.2.3.2. Lagoon Water Density**

Corresponding to the density of (pure) water at 4 °C, the factory setting of electronic pressure transducers used in the water resources industry typically specifies the density of water as 1 g cm<sup>-3</sup> to convert the sensed pressure to a water column height. In practice, this is an approximation because the density of water is temperature-dependent. Fortunately, temperature-induced density fluctuations are very small over the range of practically encountered water temperatures in this application compared to the (also very small) random error inherent in the pressure transducer measurements. In practical terms, temperature-induced density fluctuations are much too small to be quantified with the available instrumentation, and such fluctuations do not affect seepage estimates.

Dissolved salts and other constituents have the potential to increase the density of the lagoon content above that of pure water. A cursory investigation was conducted and lagoon water was collected at several lagoons from the upper 10 cm of the liquid. Samples were stored on ice and density measurements were made without delay at room temperature using a 1,000 mL Pyrex No. 5640 volumetric flask (calibrated to ±0.3 mL) and a Mettler Toledo High-Capacity Scale *Model PM34-K Delta Range* (readability and reproducibility = 0.1 g; linearity = ±0.2 g; result deviation in inclined position [1:1,000] = 0.3 g). The dry flask was weighed on the scale, and the scale was set to zero. The flask was then carefully filled with lagoon water to its calibration mark<sup>11</sup>. This procedure was repeated three times for every sample (using the same cleaned and dried volumetric flask). Results indicated a range of densities from 1.002 to 1.005 g cm<sup>-3</sup>, which corresponds to a deviation of 0.2 to 0.5% from the density of pure water at 4 °C. If unaccounted, this deviation will result in an overestimation of the actual lagoon water level decline (i.e., introduce systematic error or bias). For example, a unit drop of 1.000 mm will appear in the transducer output as a drop of 1.005 mm (i.e., 0.5% bias). In most cases this bias will not

---

<sup>11</sup> The bottled lagoon water sample was turned upside down/right side up several times to obtain a uniformly mixed sample before filling the flask.

---

propagate into seepage results because seepage results are reported only to a tenth of a millimeter. However, in some instances, an overestimation of the seepage rate of 0.1 mm is possible due to rounding.

---

## 5 PRACTICAL GUIDANCE

### 5.1 Instrumentation and Deployment

The following instrumentation and software was used in the course of this demonstration project. The instrument specifications are included in this document as an example of the type of equipment necessary for carrying out the water balance testing. Western United Dairymen, NRCS, and the project team do not endorse the following companies or equipment nor guarantee their performance. There is no warranty for this equipment made, express or implied, by the project team. There may be other equipment providers and sources available that meet the need for accuracy and precision as required for the water balance testing.

Engineers, technicians and consultants interested in employing the water balance method are encouraged to independently research any equipment, instrumentation or software and the qualifications of the manufacturers of such prior to purchase and use.

The following instrumentation and software were used:

- ❑ HMP 155A Temperature and Relative Humidity Probe by *Vaisala, Inc.* ([www.vaisala.com](http://www.vaisala.com))
- ❑ 14-Plate Gill Solar Radiation Heat Shield for HMP 155A by *R.M. Young Company* ([www.youngusa.com](http://www.youngusa.com))
- ❑ F460 Wind Speed Sensor by *Climatronics Corporation* ([www.climatronics.com](http://www.climatronics.com))
- ❑ F460 Wind Direction Sensor by *Climatronics Corporation* ([www.climatronics.com](http://www.climatronics.com))
- ❑ Two SI-111 Precision Infrared Radiation Transducers with 22.0° half-angle by *Apogee Instruments, Inc.* ([www.apogeeinstruments.com](http://www.apogeeinstruments.com))
- ❑ TE525MM tipping bucket rain gauge by *Texas Electronics, Inc.* ([www.texaselectronics.com](http://www.texaselectronics.com))
- ❑ Two PT2X (1 psi) vented Submersible Pressure/Temperature Smart Sensor with internal data logger and Aqua4Plus support software by *Instrumentation Northwest, Inc.* ([www.inwusa.com](http://www.inwusa.com))
- ❑ CR1000 PTO Measurement and Control System with ENC 12/14 Weather-Resistant Enclosure and PC400 data logger support software by *Campbell Scientific, Inc.* ([www.campbellsci.com](http://www.campbellsci.com))
- ❑ BPALK 12V Alkaline Battery Pack and SC115 PTO 2G CS I/O USB Port Flash Drive by *Campbell Scientific, Inc.* ([www.campbellsci.com](http://www.campbellsci.com))
- ❑ CM 10 10-ft Tripod with CM10 Tripod Guy Kit by *Campbell Scientific, Inc.* ([www.campbellsci.com](http://www.campbellsci.com))
- ❑ mounting hardware, crossbars, cables, and connectors
- ❑ Excel spreadsheet application by *Microsoft* ([www.microsoft.com](http://www.microsoft.com))
- ❑ Statistica by *StatSoft* ([www.statsoft.com](http://www.statsoft.com))

#### 5.1.1 Meteorological Measurements

All sensors and the data acquisition system were, at the time of purchase, state-of-the-art research-grade equipment characterized by excellent workmanship and calibration, and high accuracy and precision. All instrumentation performed satisfactorily. Manufacturers' specification sheets are provided in *Appendix 1*. User manuals and additional product specific information can be downloaded from the manufacturers' websites. Technical specifications should be carefully researched prior to purchase.

---

To carry out the water balance testing, five variables must be measured (i) air temperature, (ii) relative humidity, (iii) wind speed, (iv) water surface temperature, and (v) lagoon water depth. However, it is recommended to also deploy a sensitive tipping bucket rain gauge and a wind vane. The tipping bucket rain gauge is used to verify the absence of precipitation during the testing. This instrument also gives the analyst the option to estimate a seepage rate despite precipitation during testing. If precipitation is small compared to the seepage losses, seepage rates may still be estimated with a reasonable degree of confidence. Knowledge of the prevailing wind direction (as measured with the wind vane) can affect the positioning of the weather station and the evaluation of water depth changes.

Sensors for wind speed and direction are mounted on the weather station at reference height of 2 m above ground surface. Sensors for air temperature and relative humidity are mounted on the weather station at reference height between 1.5 to 2 m above ground surface. The tipping bucket rain gauge can be deployed at a distance from the tripod on level ground. The CR1000 data logger is housed in a weather resistant enclosure mounted to the mast of the weather station. The weather station itself should be deployed on the bank of the lagoon, or, if there is no bank, directly next to the lagoon. The position of the weather station with respect to the prevailing wind is not critical in most cases because evaporation across small agricultural water bodies is relatively independent of fetch, as increases in humidity above the water surface are offset by increases in wind speed (Condie and Webster, 1997). However, deploying the weather station on the leeward side of the lagoon would likely provide a more representative measure of the aerielly averaged conditions above the lagoon surface, especially at larger lagoons in arid conditions (Ham and Baum, 2009) (**Figure 13**). A photograph of the deployed weather station is shown in **Figure 14**.

IRT surface temperature measurements are non-contact and integrated over a relatively large area. The non-contact nature of the measurement provides for easy deployment. The spatial integration provides for a more representative average temperature measurement. These properties were found to be of advantage in this application compared to instrumentation that employs contact, point measurements. However, despite spatial averaging, data collected in this work effort showed that significant water surface temperature differences sometimes exist. Therefore, two IRTs should be deployed such that each IRT senses a different part of the lagoon surface to obtain representative average temperature measurements for the computation of evaporative losses.

IRTs should be deployed 1 to 2 m over the lagoon surface and oriented toward the center of the lagoon surface to capture a large oval. For mounting, a 35° to 45° angle from horizontal was chosen in most cases. If IRTs with a smaller half angle are selected (e.g., 11°), a smaller mounting angle should be chosen to increase the captured target surface. *Apogee Instruments, Inc.* provides a spreadsheet for viewing field calculations. For sensor mounting, an ordinary 2-inch diameter, galvanized steel fence post is installed near the water with a fence post digger. A crossbar, reaching over the lagoon surface, is installed, and the IRT is mounted to the end of the crossbar using the appropriate hardware (see cover photographs). Care must be taken to ensure that the instrumentation views only the water surface. If any other objects are within the view field (e.g., bank, sky, or the end of the crossbar), measurements will not be representative of the water surface temperature. A large cardboard template of the view angle, or a self-made compass-type device can be used to properly position the IRTs.

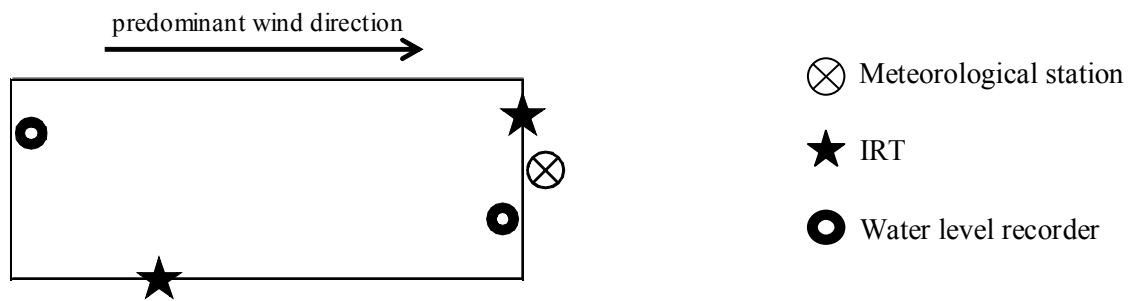


**Figure 13:** Example of lagoon layout and instrumentation deployment with respect to predominant wind direction (not to scale).



**Figure 14:** Meteorological station featuring tripod; lightning rod (top) and ground rod (left of tripod); cross arm with wind vane and anemometer; 14-plate radiation shield housing the temperature and relative humidity probe; fiberglass-reinforced, reflective enclosure housing the power source and data logger; and tipping bucket rain gauge. The rain gauge was deployed in a pea gravel filled container with perforated bottom, such that the instrument was firmly supported by gravel on all sides. This arrangement allows swift, accurate (level) deployment. The photograph also shows wires leading away from the station to the IRTs.

### 5.1.2 Depth Measurements

Accurate depth measurements are critical for the water balance testing. In this work effort, vented pressure transducers were successfully employed. These transducers are open to the atmosphere. Thus atmospheric pressure fluctuations do not affect their pressure readings. For comparison, absolute pressure

---

measurements from non-vented pressure transducers would need to be corrected for atmospheric pressure fluctuations based on barometric measurements. This would potentially introduce very large uncertainty. Following the manufacturer's instructions, the calibration of the pressure transducers should be frequently checked to avoid undetected systematic error in the measurements, which can lead to large error in the seepage estimates. Regardless of the type of instrumentation, it is important to always deploy two depth recorders in the same lagoon but on opposite ends (one windward and one leeward). This is particularly important in large lagoons where wind push can tilt the water surface and introduce large bias in the seepage estimates (here, knowledge of the predominant wind direction can be useful). This practice can also help assess atypical signals in the measurements that may otherwise be difficult to interpret.

For pressure transducer deployment, a secure reference point needs to be created in the lagoon. This was achieved by firmly driving a 7-foot heavy duty T-fence post into the ground a few steps into the water<sup>12</sup> (see cover photograph). The post can be driven with a fence post driver. In most cases, the fence post cannot be retrieved after testing unless the water level is lowered to obtain better access. Prior to deployment, a hole is drilled through the fence post near its top (leaving about 20 cm space). An S-hook is placed in the hole after the post is driven into the ground. The transducer is then suspended by attaching a stainless steel fiber optic grip to its vented cable and hooking the grip to the S-hook (i.e., it is freely hanging into the lagoon water). This suspension system minimizes vertical movement via stretch during the testing. Installation of a stilling well was not found to increase data quality. The transducer should be deployed in the upper portion of the supernatant (i.e., near the water surface) to avoid potential error due to water density changes with depth. However, the stainless steel body of the transducer must be fully submerged in the water to avoid inaccuracies caused by solar heating of the sensor's body. To allow data downloading during testing, several meters of extra vented cable are useful. The cable can be passed to the bank and its end piece (connector and air intake with desiccant) placed in a container (with lid) to protect it from precipitation, dust, mud, animal activity, etc. When this is done, the cable should be fastened to the T-fence post above the S-hook to avoid jiggling of the S-hook during data downloads and kinking. This can be done with electrical tape or a zip-tie.

## 5.2 Site Selection

The water balance methodology has been applied to over 150 lagoons on a variety of confined animal facilities in Kansas, including cattle feed lots, dairy farms, and hog farms (Ham and Baum, 2009). Investigated lagoons (including this work effort) have ranged in size from 0.1 to 5.1 ha. The methodology is applicable to lagoons regardless of their shape and liquid depth.

The seepage rate of lagoons that are in direct subsurface hydraulic communication with shallow groundwater (i.e., the groundwater table intersects the lagoon) cannot be reliably computed with the water balance method. Under such conditions, the seepage rate would be a function of ambient groundwater levels (other variables constant), and subject to potentially large temporal changes. In addition, subsurface inflows and outflows could occur simultaneously in different portions of the lagoon and, thus, mask actual seepage losses.

Large buildings or other structures (e.g., barns, warehouses, hay stacks, silage piles, rows of trees) in the immediate vicinity of a lagoon can have site-specific effects on the bulk transfer coefficient by

---

<sup>12</sup> This type of installation does not work when a plastic liner is present. Alternatively, the pressure transducer can be suspended from a discharge pipe extending over the waste surface or any other existing structure providing a secure reference point (no vertical movement).

---

introducing turbulence. Conducting water balance testing during times of low winds and overall low evaporation minimizes these effects.

Particulate matter on the lagoon surface changes the evaporation. The BT model produces accurate results only when the lagoon surface is free of floating particulate matter.

### **5.3 Hydraulic Isolation**

Most of the questions that need to be resolved prior to testing revolve around the ability to isolate the lagoon from inflow and outflow components. There may be many operational inflow components – some are more controllable than others; some are less than obvious. Below are several examples of inflow components:

1. Wash water from flush lanes
2. Wash water from milking parlors, facility yards, heifer pens, and other management units
3. Water from animal hospital
4. Miscellaneous stormwater runoff which can last for many hours or days after precipitation ceases (e.g., from facility yards, silage areas, roadways, banks, and adjacent forage fields)
5. Back flow through faulty check valves or leaking hoses
6. Back flow from irrigation pipes
7. Underground bank drainage

Examples of outflow components are:

1. Removal via floating pumps
2. Gravity flow or pumped flow to forage fields
3. Incidental syphonage

In the best of all cases, an air gap exists below pipes that discharge to the lagoon. These pipes need to be capped. Thin plastic sheeting fastened to the outfall with large zip-ties or elastic rubber ties suffices. The purpose of such capping is not to hold back potential inflow but to be an indicator that such inflow occurred (e.g., blown out plastic sheeting), in which case the test would need to be repeated. Therefore, frequent visual inspection of the caps is important.

Any potential inflow and outflow that occurs below the water surface needs special attention. It cannot be assumed that a valve is performing to the standard necessary for water balance testing, or that all pertinent dairy staff members are aware of the implications of the testing on dairy operations. Therefore, electrical connections to pumps should be disconnected or panels/switches clearly labeled to avoid incidental inflows or outflows. Bypass valves should be opened well in advance of actual testing to decrease pressure on check valves and allow for stabilization of water levels in pipes and the lagoon.

### **5.4 Communication with Facility Operator**

Clear communication with somebody who fully understands lagoon operations prior to instrumentation deployment is critical. It is also critical that the owner/operator of the dairy is directly involved in the communication between the analyst and any other dairy facility staff charged with explaining lagoon operations and understanding the scope of the testing. During an initial site visit, face-to-face

---

communication is imperative, preferably between the analyst and at least two dairy facility staff (including operator/owner).

## 5.5 Weather Conditions

The uncertainty in the computed seepage estimates is proportional to the evaporation rate. If evaporative losses account for a large portion of the change in storage, this uncertainty can negate the seepage estimates. To avoid this problem, testing should be conducted during times of low evaporative demand (i.e., during times of low air temperature, high relative humidity, low wind speed, and low solar radiation).

1. Testing for this work effort was conducted in temperatures above freezing and all water surfaces were free of ice. Testing is theoretically possible on lagoons with a frozen water surface, and this was described as an option with the advantage of very low evaporation/sublimation rates (Ham and DeSutter 2003). However, it also introduces significant sources of uncertainty in the water depth measurements. This uncertainty can, for example, be caused by pressure changes under the ice caused by (i) density and volumetric changes water experiences during the liquid-solid phase change, and (ii) uneven settling of the ice cover over a declining water surface.
2. When the relative humidity approaches 100%, the analyst must be alert to the possible formation of small water droplets suspended in the air that can adhere to the water surface and constitute an unmeasured inflow.
3. The start and end of an overnight water balance test should coincide with periods of low wind speed (i.e., less than  $3 \text{ m s}^{-1}$ ) to support accurate depth measurements.
4. Short term testing is preferably conducted during the night when solar radiation is absent.

Precipitation, even in small amounts, can introduce substantial uncertainty in the seepage estimates. One contributor is the relative low resolution of the precipitation measurements (e.g., 0.1 mm) in relation to the other measurements. However, the main contributor is the spatial heterogeneity of precipitation, which is not addressed by the uncertainty analysis discussed herein. Therefore, seepage estimates should preferably be computed during times of no precipitation. The bucket of the tipping bucket rain gauge should always be checked for traces of precipitation that were not large enough to tip the bucket. Ultimately, the analyst needs to make a decision as to the appropriateness of environmental conditions based on testing results. For example, in cases where seepage rates are found to be high, acceptable confidence in seepage estimates may still be achievable with small precipitation depths (e.g., less than 5% of the total measured depth change).

## 5.6 Test Duration

Random error inherent in the seepage estimates is attenuated with time. In most cases, several days are needed before the water balance generates stable results, and an additional several days to confirm stabilization. Based on the pertinent literature and the experience gathered during this work effort, expecting a testing duration of a minimum of 5 days is realistic.

In cases where uninterrupted longer term testing is not possible, overnight testing presents an alternative. Overnight testing takes advantage of lower evaporative losses and generally more favorable environmental conditions. However, despite this, overnight testing presents other challenges. The shorter testing duration is not always sufficient for the water balance to generate stable results. Also, the shorter

---

duration places proportionally greater significance on the depth measurements and increases both its absolute and relative contribution of uncertainty to the end result. Overnight testing should occur during consecutive or near-consecutive nights. The number of repetitions will depend on the variability of the results. Based on the pertinent literature and the experience gathered during this work effort, expecting a minimum of 5 overnight tests is realistic.

Regardless of whether longer term testing or overnight testing is performed, testing progress can be assessed on an ongoing basis during the test. Ultimately, given the framework and objectives of any specific water balance testing project, the analyst will determine when it is appropriate to terminate testing.

At sites where longer term testing is performed, seepage estimates should also be computed using only the night time data to complement data analysis and strengthen interpretation.

## 5.7 Data Processing and Computations

The CR1000 was programmed using PC400 support software to retrieve meteorological measurements every 15 seconds and aggregate data over 15 minute intervals, including means, standard deviations, maxima, and minima. The CR1000 was also programmed to convert the energy flux [ $\text{W m}^2$ ] sensed by the IRTs to a temperature [ $^{\circ}\text{C}$ ]. The computer code is included in the PC400 software. The PT2X was programmed using Aqua4Plus support software to retrieve depth measurements every minute. These data were aggregated in a spreadsheet over 15 minute intervals, including means, standard deviations, maxima, and minima. If more than one instrument is used for depth measurements, average depth measurements should be used for the water balance.

Data were compiled in a spreadsheet and eq. 2-5 was solved to calculate seepage losses over 15-minute time steps. Wind speed measurements obtained on the bank of the lagoon should be reduced by 25% to approximate conditions at the water surface (Ham and Baum, 2009). To solve eq. 2-5, evaporative losses (eq. 2-6b) need to be computed. Components of eq. 2-6b are obtained by solving eqs. 2-8, 2-13, 2-14, and 2-15.

The overall uncertainty in the depth measurements at the beginning and end of the tests was computed using eq. 4-25. The random component was estimated for the sample standard deviation calculated from a given data aggregation interval using eq. 4-6. The systematic standard uncertainty was estimated as one half of the manufacturer's information on the instrument's accuracy range (100% of measurements fall within the accuracy range to pass quality control). Using a spreadsheet application, the overall uncertainty in the results of the evaporation model was computed with the TSM and the central-differencing finite difference approach outlined in *Section 4.2.2.2*. The overall uncertainty surrounding the computed seepage rate was then computed using eq. 4-27.

## 5.8 Summary

Key items for carrying out water balance testing are summarized below.

1. Key items to consider during site selection:

- 
- a. The seepage rate of lagoons that are in direct subsurface hydraulic communication with shallow groundwater (i.e., the groundwater table intersects the lagoon) cannot be reliably computed with the water balance method.
  - b. Large buildings or other structures (e.g., barns, warehouses, hay stacks, silage piles, rows of trees) in the immediate vicinity of a lagoon can have site-specific effects on the bulk transfer coefficient by introducing turbulence. Conducting water balance testing during times of low winds and overall low evaporation minimizes these effects.
  - c. Floating scum and debris changes evaporation off the water surface. The BT model produces accurate results only when the water surface is free of floating scum and debris.
  - d. The operator must be able to fully and reliably stop all inflows and outflows to and from the lagoon for the duration of the testing.
2. Clear communication with somebody who fully understands lagoon operations prior to instrumentation deployment is critical.
  3. The analyst carrying out the water balance testing should make no assumptions about lagoon operation, regardless of how obvious they might seem.
  4. Key items to consider during instrumentation deployment:
    - a. Deploy the weather station on the bank of the lagoon or, if there is no bank, directly next to the lagoon. Leeward deployment is preferred.
    - b. Sensors for wind speed and direction are mounted on the weather station at reference height of 2 m above ground surface. Sensors for air temperature and relative humidity are mounted on the weather station at reference height between 1.5 to 2 m above ground surface. The tipping bucket rain gauge can be deployed at a distance from the tripod on level ground.
    - c. Two IRTs should be deployed at different locations on the lagoon 1 to 2 m over the lagoon surface and oriented toward the center of the lagoon surface to capture a large oval.
    - d. To improve data quality, at least two depth recorders should be deployed at on opposite ends of the lagoon (one windward and one leeward). Installation must minimize vertical movement of the recorders. If vented pressure transducers are used, deploy in the upper portion of the supernatant. The body of the transducer must be fully submerged in the water.
  5. Water balance testing should be conducted during times of no precipitation and low evaporative demand (i.e., during times of low air temperature, high relative humidity, low wind speed, and low solar radiation).
  6. The start and end of an overnight water balance test should coincide with periods of low wind speed (i.e., less than  $3 \text{ m s}^{-1}$ ) to support accurate depth measurements.
  7. To improve data quality, short term testing is preferably conducted during the night when solar radiation is absent and evaporative losses are relatively small.
  8. Best results are obtained when in- and outflows can be halted for several days. This testing can be complemented with formal uncertainty analysis. Multi-day testing results can also be compared to results obtained from overnight testing. When conducting multi-day testing, a duration of 5 days should be expected to obtain sufficient confidence in results.
  9. Overnight testing should occur during consecutive or near-consecutive nights. The number of repetitions will depend on the variability of the results. A minimum of 5 repetitions should be expected to obtain sufficient confidence in results.
  10. Meteorological measurements and water level measurements should be retrieved at high frequency (e.g., every 15 seconds) and aggregated over a longer period (e.g., 15 minute intervals) to moderate random error.
  11. Wind speed measurements obtained on the bank of the lagoon should be reduced by 25% to approximate conditions at the water surface.

---

## 6 REFERENCES

- Bowen, I. S. (1926). "The ratio of heat losses by conduction and by evaporation from any water surface." Physics Review **27**: 779-787.
- Brutsaert, W. (1975). "On a Derivable Formula for Long-Wave Radiation from Clear Skies." Water Resources Research **11**(5): 742-744.
- Coleman, H. W. and W. G. Steele (2009). Experimentation, Validation, and Uncertainty Analysis for Engineers, Wiley.
- Condie, S. A. and I. T. Webster (1997). "The influence of wind stress, temperature, and humidity gradients on evaporation from reservoirs." Water Resources Research **33**(12): 2813-2822.
- DeBruin, H. A. R. (1978). "A Simple Model for Shallow Lake Evaporation." Journal of Applied Meteorology **17**: 1132-1134.
- Ham, J. M. (1999). "Measuring evaporation and seepage losses from lagoons used to contain animal waste." Transactions of the ASAE **42**(5): 1303-1312.
- Ham, J. M. (2002a). "Seepage losses from animal waste lagoons: A summary of a four-year investigation in Kansas." Transactions of the ASAE **45**(4): 983-992.
- Ham, J. M. (2002b). "Uncertainty analysis of the water balance technique for measuring seepage from animal waste lagoons." Journal of Environmental Quality **31**(4): 1370-1379.
- Ham, J. M. (2007). Measuring the Seepage Rate from Lagoons Using an Overnight Water Balance Test. International Symposium on Air Quality and Waste Management for Agriculture. Broomfield, Colorado.
- Ham, J. M. and K. A. Baum (2009). "Measuring Seepage from Waste Lagoons and Earthen Basins With an Overnight Water Balance Test." Transactions of the ASABE **52**(3): 835-844.
- Ham, J. M. and T. M. DeSutter (1999). "Seepage losses and nitrogen export from swine-waste lagoons: A water balance study." Journal of Environmental Quality **28**(4): 1090-1099.
- Ham, J. M. and T. M. DeSutter (2000). "Toward site-specific design standards for animal-waste lagoons: Protecting ground water quality." Journal of Environmental Quality **29**(6): 1721-1732.
- Ham, J. M. and T. M. DeSutter (2003). Standards for Measuring Seepage from Anaerobic Lagoons and Manure Storages. 2003 ASAE Annual International Meeting. Las Vegas, Nevada.
- Ham, J. M. and R. S. Senock (1992). "On the Measurement of Soil Surface-Temperature." Soil Science Society of America Journal **56**(2): 370-377.
- McCullough, B. D. (1998). "Assessing the reliability of statistical software: Part I." The American Statistician **52**: 358-366.
- McCullough, B. D. (1999). "Assessing the reliability of statistical software: Part II." The American Statistician **53**: 149-159.
- Murray, F. W. (1967). "On the Computation of Saturation Vapor Pressure." Journal of Applied Meteorology **6**: 203-204.
- Penman, H. L. (1948). "Evaporation from open water, bare soil, and grass." Proceedings of the Royal Society London **A193**: 120-146.
- Priestley, C. H. B. and R. J. Taylor (1972). "On the assessment of surface heat flux and evaporation using large-scale parameters." Monthly Weather Review **100**: 81-92.



## APPENDIX

---



# Appendix 1

## Instrumentation Specifications

---

### **Disclaimer**

The following instrumentation and software was used in the course of this demonstration project. The instrument specifications are included in this document as an example of the type of equipment necessary for carrying out the water balance testing. Western United Dairymen, NRCS, and the project team do not endorse the following companies or equipment nor guarantee their performance. There is no warranty for this equipment made, express or implied, by the project team. There may be other equipment providers and sources available that meet the need for accuracy and precision as required for the water balance testing.

Engineers, technicians and consultants interested in employing the water balance method are encouraged to independently research any equipment, instrumentation or software and the qualifications of the manufacturers of such prior to purchase and use



# HMP155A

## Vaisala Temperature and Relative Humidity Probe



The HMP155A provides reliable relative humidity (RH) and temperature measurements for a wide range of applications. It uses a HUMICAP®180R capacitive thin film polymer sensor to measure RH over the 0 to 100% RH range. A PRT measures temperature over the -80° to +60°C range. This rugged, accurate temperature/RH probe is manufactured by Vaisala.

To reduce the current drain, power can be supplied to the HMP155A only during measurement when the sensor is connected to the datalogger's switched 12 V terminal. Dataloggers that do not have a switched 12 V terminal, such as the CR510 or CR7, can use the SW12V switched 12 V device to switch power to the sensor only during measurement.

### Sensor Mounts

The 41005-5 14-plate Gill Radiation Shield should be used when the HMP155A is exposed to sunlight. The 41005-5 can attach directly to a mast or tower leg or to a CM202, CM204, or CM206 crossarm.

### Ordering Information

#### Air Temperature and Relative Humidity Probe

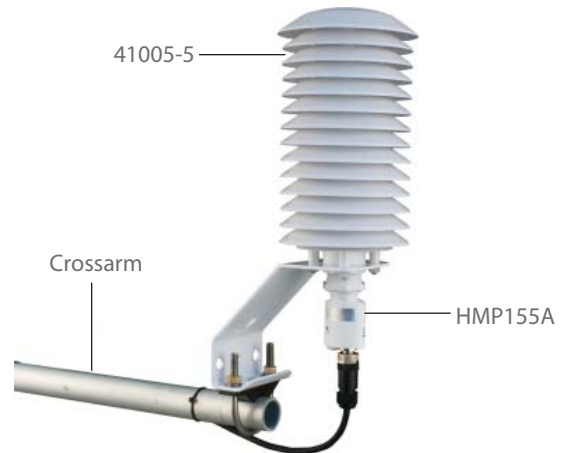
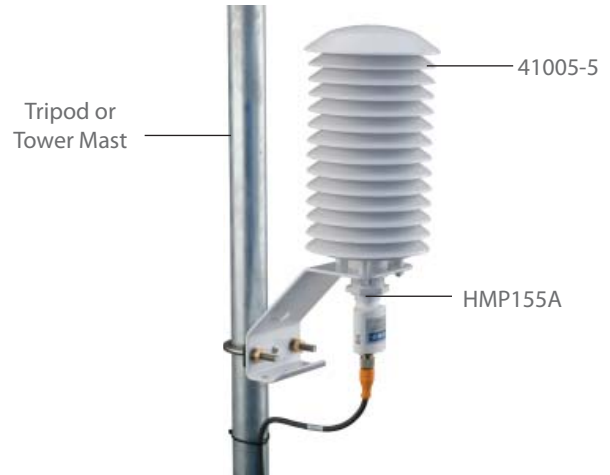
**HMP155A-L** Vaisala Temperature/RH Probe with user-specified cable length. Enter cable length, in feet, after the -L. Must choose a cable termination option (see below).

#### Cable Termination Options (choose one)

- PT** Cable terminates in stripped and tinned leads for direct connection to a datalogger's terminals.
- PW** Cable terminates in connector for attachment to a prewired enclosure.

#### Accessories

- SW12V** Switched 12 V device that uses a control port and a 12 V channel to switch power to the HMP155A instead of a switched 12 V terminal.
- 41005-5** 14-Plate Gill Radiation Shield to house the HMP155A



### Recommended Cable Lengths

2 m Height		Atop a tripod or tower via a 2 ft crossarm such as the CM202							
Mast/Leg	CM202	CM6	CM10	CM110	CM115	CM120	UT10	UT20	UT30
9 ft	11 ft	11 ft	14 ft	14 ft	19 ft	24 ft	14 ft	24 ft	37 ft

*Note: Add two feet to the cable length if you are mounting the enclosure on the leg base of a light-weight tripod.*

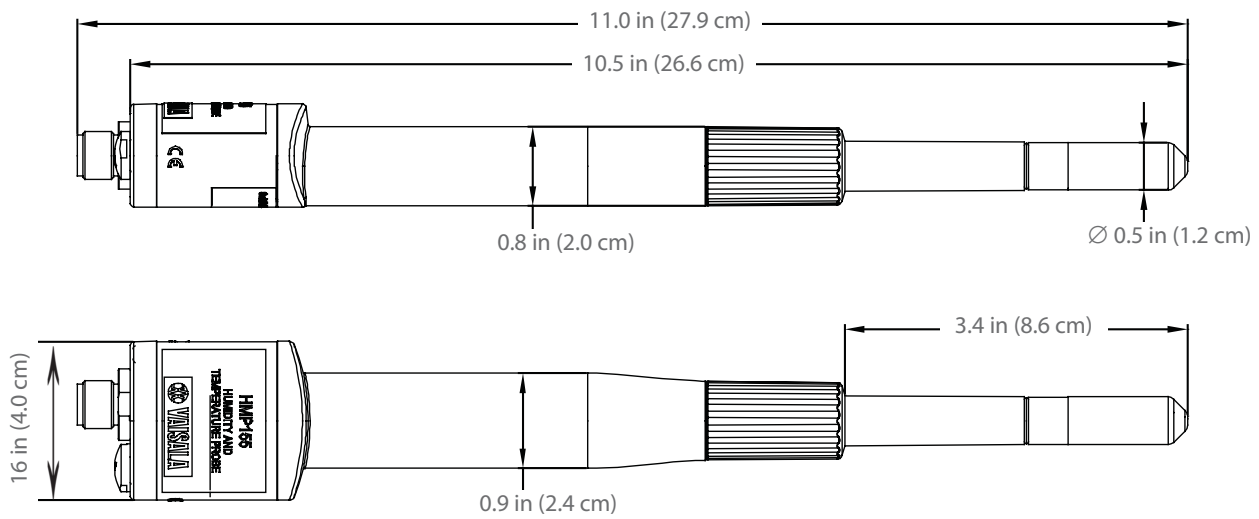
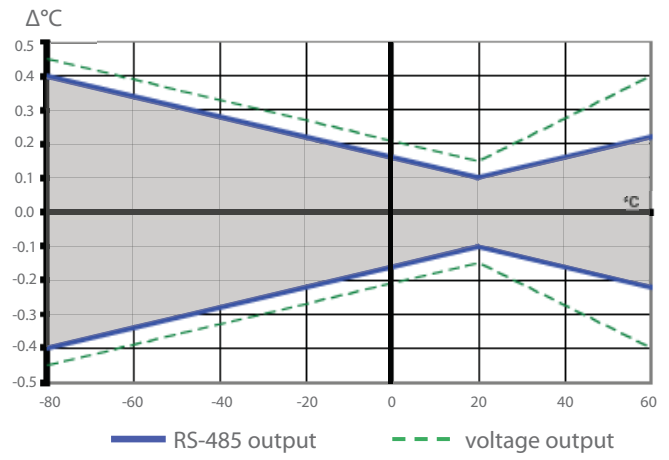
# Specifications

<b>Temperature Range</b>	
Operating:	-80° to +60°C
Storage:	-80° to +60°C
<b>Electromagnetic Compatibility:</b>	Complies with EMC standard EN61326-1
<b>Filter:</b>	Sintered PTFE
<b>Housing</b>	
Material:	PC
Classification:	IP66
<b>Weight:</b>	3 oz (86 g)
<b>Voltage Output:</b>	0 to 1 Vdc
<b>Average Current Consumption:</b>	≤3 mA (analog output mode)
<b>Operating Voltage:</b>	7 to 28 VDC
<b>Settling Time at Power Up:</b>	2 seconds

<b>Relative Humidity (RH)</b>	
<b>Sensor:</b>	HUMICAP®180R
<b>Measurement Range:</b>	0.8 to 100% RH, non-condensing
<b>Response Time*:</b>	20 s (63% RH), 60 s (90% RH)
<b>Factory Calibration Uncertainty (+20°C)**</b>	
0 to 40% RH:	±0.6% RH
40 to 97% RH:	±1.0% RH

<b>Accuracy (including non-linearity, hysteresis &amp; repeatability)</b>	
<b>+15° to +25°C:</b>	±1% RH (0 to 90% RH) ±1.7% RH (90 to 100% RH)
<b>-60° to -40°C:</b>	±(1.4 + 0.032 × reading) % RH
<b>-40° to -20°C:</b>	±(1.2 + 0.012 × reading) % RH
<b>-20° to +40°C:</b>	±(1.0 + 0.008 × reading) % RH
<b>+40° to +60°C:</b>	±(1.2 + 0.012 × reading) % RH

<b>Air Temperature</b>	
<b>Temperature Sensor:</b>	Pt 100 RTD 1/3 class B IEC 751
<b>Measurement Range:</b>	-80° to +60°C
<b>Accuracy with Voltage Output</b>	
<b>-80° to +20°C:</b>	±(0.226 - 0.0028 × temperature)°C
<b>-80° to +60°C:</b>	±(0.055 - 0.0057 × temperature)°C
<b>Entire Temperature Range:</b>	see graph below



\*The response time for the RH specification is for the HUMICAP®180R© at 20°C in still air with sintered PTFE filter.  
 \*\*The factory calibration uncertainty is defined as ±2 standard deviation limits. Small variations possible; see also calibration certificate.

# F460 WIND SENSORS

## FEATURES

- **High Survivability**
- **Excellent Dynamic Response**
- **Low Threshold**
- **Low Power CMOS Design**
- **Optional External Heaters**

Climatronics' F460 Wind Sensors are capable of operation in virtually all weather conditions. Designed to meet the requirements of Specification No. F460-SP001 for the National Weather Service, the durability of these sensors makes them ideal for multi-level tower installations. Although moderately priced, the F460 wind sensors offer the combination of low starting threshold, quick response, and high accuracy with excellent reliability over a wide range of operating conditions.

The F460 Wind Speed Sensor P/N 100075 monitors the wind speed with a three-cup anemometer. An LED photo chopper device provides a frequency output directly proportional to the wind speed. NIST traceability is optionally available for each anemometer cup assembly by comparison testing against a NIST transfer standard in our wind tunnel test facility.

The F460 Wind Direction Sensor, P/N 100076, consists of a counter-balanced, lightweight vane and a precision, low torque, highly reliable potentiometer that yields a voltage output proportional to the wind direction. Once properly oriented on the keyed cross-arm, the wind direction sensor may be removed or replaced without requiring reorientation.

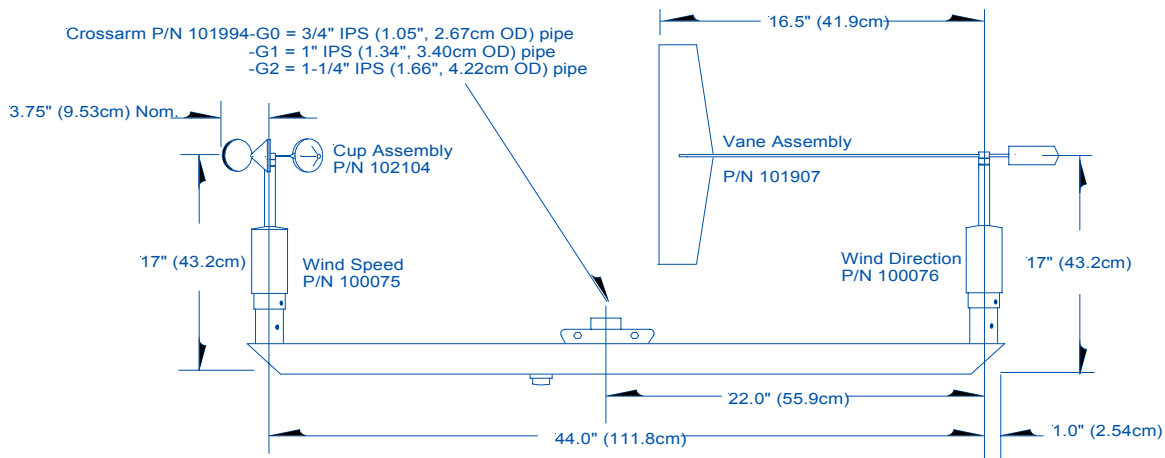
Installation is a simple matter of fastening each sensor to the crossarm, P/N 101994, which fits a  $\frac{3}{4}$ , 1, or 1- $\frac{1}{4}$  inch IPS pipe. Optional, thermostatically controlled external heaters are also available. Our single-board signal conditioner, the Universal Interface Module (UIM), can be used with the F460 sensors. Please consult the Universal Interface Module (UIM) data sheet for more details. The sensors can also be directly interfaced to Climatronics' IMP-800 series of data loggers or other commonly available data acquisition units.

The Component Anemometer, P/N 102236, can be used in conjunction with the F460 System to measure the vertical component of the wind. Consult the Vertical Component Anemometer data sheet for additional details.



# SPECIFICATIONS

	<b>F460 Wind Speed P/N 100075</b>	<b>F460 Wind Direction P/N 100076</b>
<b>PERFORMANCE</b>		
Accuracy	0.15 mph ( $\pm 0.07$ m/s) or $\pm 1.0\%$ of true air speed (whichever is greater)	$\pm 2$ degrees
Threshold	0.5 mph (0.22 m/s)	0.5 mph (0.22 m/s)
Distance Constant	102104 LEXAN <1.5 m (4.9 ft) 101287 HD Aluminum <4.0 m (13.1 ft) 100057 Stainless Steel <2.4 m (7.9 ft)	101907 Standard <1.0 m (3.0 ft) 101288 Heavy Duty <2.5m (8.2 ft)
Damping Ratio	N/A	>0.4 at 10° initial angle of attack
Operating Range	0 to 125 mph (0 to 60 m/s)	0 to 360 degrees - mechanical
<b>ELECTRICAL SPECIFICATIONS</b>		
Signal Output	Nominal 2.0 Vpp into 2.0 Kohm, frequency proportional to wind speed, amplitude dependant on supply voltage	Variable DC voltage, magnitude proportional to wind direction
Power Requirements	5 to 15 VDC @ 1 mA nominal	Max 1 mA through 10 Kohms
<b>PHYSICAL SPECIFICATIONS</b>		
Size	2.25 in (5.7 cm) max diameter 11.5 in (29.2 cm) high	2.25 in (5.7 cm) max diameter 11.5 in (29.2 cm) high
Weight	Less than 2 lbs (0.9 kg)	Less than 2 lbs (0.9 kg)
Turning Radius	3.75 in (9.5 cm)	16.5 in (41.9 cm)
Operating Temperature	-40° to 140° F (-40° to 60° C)	-40° to 140° F (-40° to 60° C)
<b>CROSSARM SPECIFICATIONS</b>		
Length	45 in (114.3 cm)	
Weight	7 lbs (3.2 kg)	
Mounting	1.66 in (4.2 cm) - O.D. 1-1/4 in IPS pipe (3/4 in & 1.0 in IPS also available)	
<b>SENSOR HEATER SPECIFICATIONS</b>		
Internal (P/N 101263)	12 VDC, 2 Watts per sensor	
External (P/N 101235)	115 VAC/60Hz 20 Watts per sensor, thermostatically controlled	



**Climatronics Corporation**  
140 Wilbur Place  
Bohemia, NY 11716-2404

TEL: 631-567-7300  
FAX: 631-567-7585  
E-Mail: sales@climatronics.com

Rev. 2/13/01

### MEASURES THE TEMPERATURES OF ROAD SURFACES, PLANT CANOPIES, AND SOIL, SNOW, AND WATER SURFACES.

#### DESCRIPTION

Measures the temperatures of road surfaces, plant canopies, and soil, snow and water surfaces.

Measurement of surface temperature is a crucial component of energy transfer. Accurate measurement of the leaf-to-air temperature gradient is essential to the determination of transpiration rate and stomatal conductance in both single leaves and plant canopies.

This gradient is often less than 1 degree Celsius, which means that leaf temperature should be measured to within 0.2 C. To achieve this accuracy, the Infrared Radiometers correct for changes in the sensor body temperature with a subroutine designed for Campbell Scientific dataloggers.

Field of View (FOV) is reported as the half-angle of the apex of the cone formed by the target (cone base) and the detector (cone apex). The target is a circle from which 98% of the radiation being viewed by the detector is being emitted.



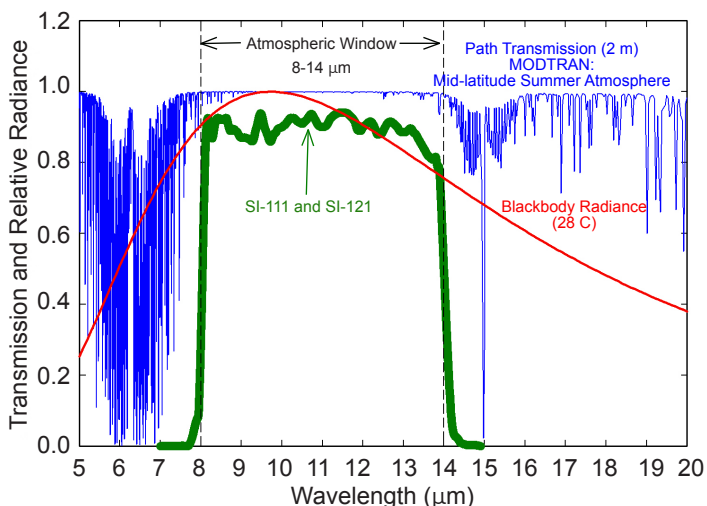
Model SI-111 half-angle = 22.0°

Model SI-121 half-angle = 18.0°

#### ORDERING

All products can be ordered at [www.apogeeinstruments.com](http://www.apogeeinstruments.com)

For technical information contact [techsupport@apogee-inst.com](mailto:techsupport@apogee-inst.com)



The 8-14 µm window of the IRR models corresponds to the atmospheric window. This minimizes the effects of water bands below 8 µm and above 14 µm.

# SPECIFICATIONS

## FIELD OF VIEW

- Standard: 22° half angle
- Narrow: 18° half angle

## WAVELENGTH RANGE

- 8 - 14  $\mu\text{m}$  (corresponds to atmospheric window)

## RESPONSE TIME

- < 1 second to changes in target temperature

## ACCURACY -10 TO 65 C

- $\pm 0.2$  C absolute accuracy
- $\pm 0.1$  C uniformity
- $\pm 0.05$  C repeatability

## ACCURACY -40 TO 70 C

- $\pm 0.5^\circ$  C absolute accuracy
- $\pm 0.3^\circ$  C uniformity
- $\pm 0.1^\circ$  C repeatability and uniformity

## OUTPUT TARGET TEMP

- Standard: 60  $\mu\text{V}$  per  $^\circ\text{C}$  difference from sensor body
- Narrow: 40  $\mu\text{V}$  per  $^\circ\text{C}$  difference from sensor body

## CABLE

- 5 meters twisted-pair 4-conductor wire
- Foil shield
- Santoprene jacket
- Ending in pigtail leads
- Additional cable is available in multiples of 5 meters

## OUTPUT SENSOR BODY TEMP

- Standard: 0 - 2500 mV
- Precision Narrow: 0 - 2500 mV

## MASS

- 190 g

## INPUT POWER

- 2.5 V excitation
- Additional cable \$2.95/meter

## DATALOGGER CHANNELS

- 1 differential (detector)
- 1 single-ended (thermistor)

## OPTICS

- Germanium lens

## OPERATING ENVIRONMENT

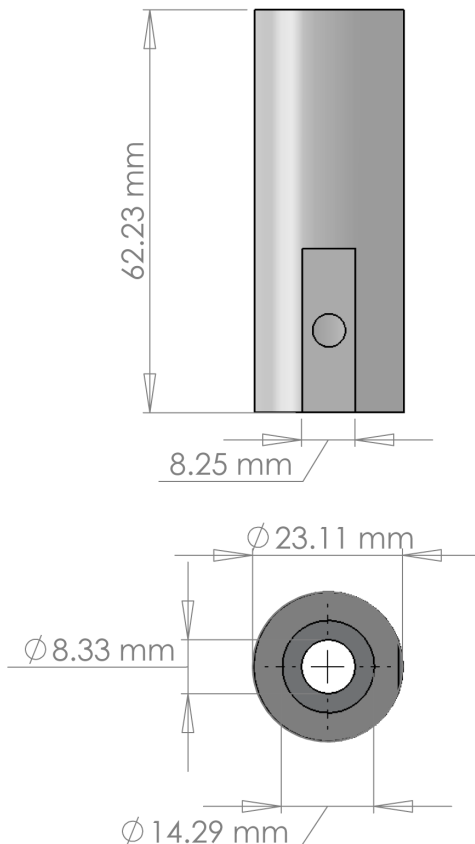
- -55 to 80° C
- 0 to 100% non-condensing relative humidity
- Water resistant
- Designed for continuous outdoor use

## WARRANTY

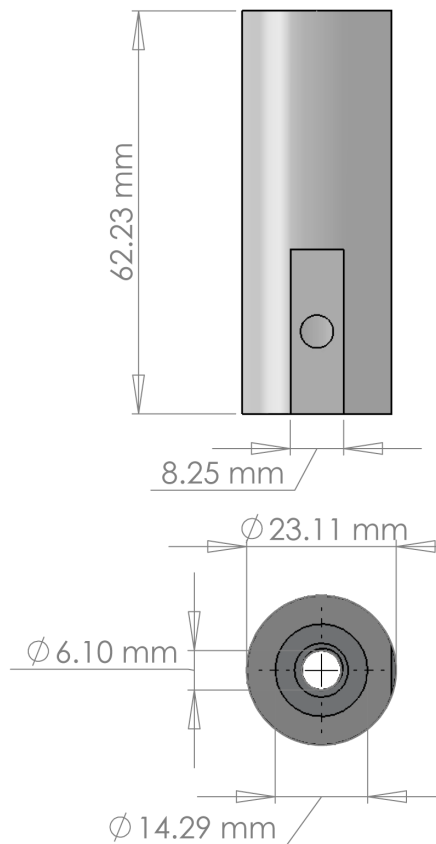
- 1 year against defects in materials and workmanship

# MEASUREMENTS

SI-111



SI-121



# TE525-Series

## Texas Electronics Tipping Bucket Rain Gages



The TE525-series tipping bucket rain gages are manufactured by Texas Electronics. They funnel precipitation into a bucket mechanism that tips when filled to a calibrated level. A magnet attached to the tipping mechanism actuates a switch as the bucket tips. The momentary switch closure is counted by the pulse-counting circuitry of Campbell Scientific dataloggers.

Three models are available:

- TE525WS—provides an 8-inch diameter orifice, and measures in 0.01-inch increments
- TE525—provides a 6-inch diameter orifice, and measures in 0.01-inch increments
- TE525MM—provides a 9.6-inch orifice, and measures in 0.1-mm increments

### Mounting

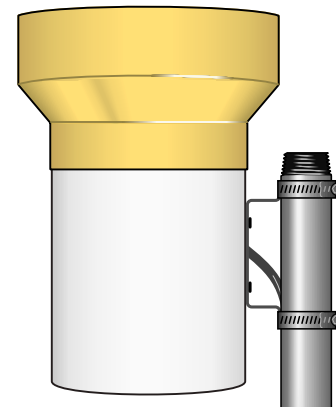
The TE525-series rain gages mount to a CM300-series Mounting Pole or a user-supplied 1.5" IPS pole. Several pedestal options are available to secure a CM300-series pole to the ground (see Ordering Information on page 2). Accurate measurements require the gage to be level.

### Snowfall Adapter

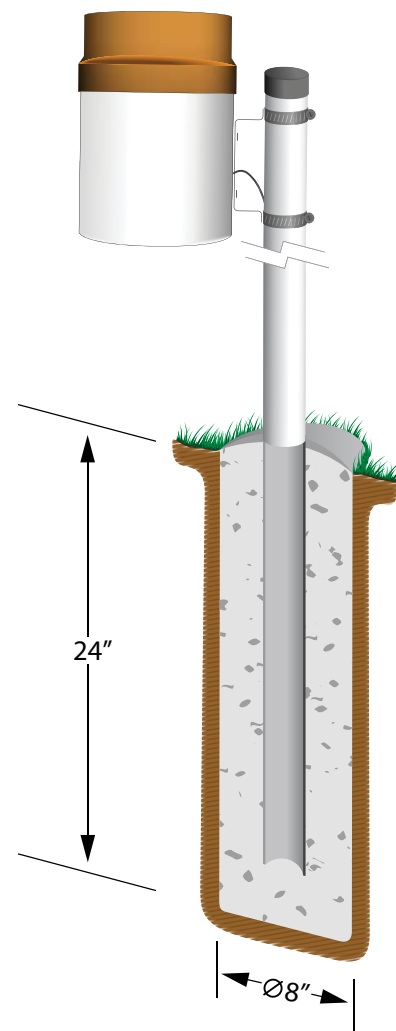
Campbell Scientific's CS705 Snowfall Conversion Adapter uses antifreeze to melt snow, allowing the TE525WS to measure the water content of snow. The CS705 cannot be directly used with either the TE525 or TE525MM. However, both the TE525 and TE525MM can be converted to a TE525WS by returning them to Campbell Scientific. For more information about the CS705, refer to the CS705 brochure.

### Wind Screen

Campbell Scientific offers the 260-953 Wind Screen to help minimize the affect of wind on the rain measurements. This wind screen consists of 32 leaves that hang freely and swing as the wind moves past them.



The TE525WS conforms to the National Weather Service recommendation for an 8-inch funnel orifice.



A TE525 mounted onto a CM310 pole is embedded directly in a concrete pad (-NP no pedestal base option).

## Ordering Information

### Tipping Bucket Raingages

*Recommended cable length is 25 feet, but many customers will order a 50-ft cable to place the gage away from the tower or tripod.*

<b>TE525WS-L</b>	Tipping bucket with 8-inch diameter orifice and 0.01-inch tips. Enter cable length (in feet) after the -L. Must choose a cable termination option (see below).
<b>TE525-L</b>	Tipping bucket with 6-inch diameter orifice and 0.01-inch tips. Enter cable length (in feet) after the -L. Must choose a cable termination option (see below).
<b>TE525MM-L</b>	Tipping bucket with 24.5 cm diameter orifice and 0.1-mm tips. Enter cable length (in feet) after the -L. Must choose a cable termination option (see below).

### Cable Termination Options (choose one)

<b>-PT</b>	Cable terminates in stripped and tinned leads for direct connection to a datalogger's terminals.
<b>-PW</b>	Cable terminates in connector for attachment to a prewired enclosure.

### Mounting Poles

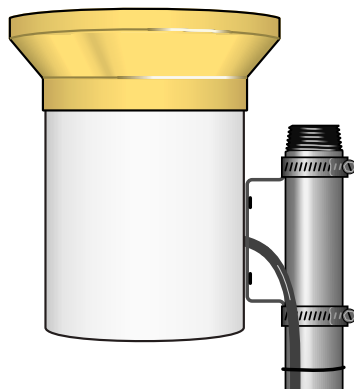
<b>CM300</b>	23-inch Mounting Pole with Cap
<b>CM305</b>	47-inch Mounting Pole with Cap
<b>CM310</b>	56-inch Mounting Pole with Cap

### Pedestal Options for Mounting Poles (choose one)

<b>-NP</b>	No Pedestal Base
<b>-PJ</b>	CM340 Pedestal J-Bolt Kit
<b>-PS</b>	CM350 Pedestal Short Legs (23-in. legs)
<b>-PL</b>	CM355 Pedestal Long Legs (39-in. legs)

### Common Accessories

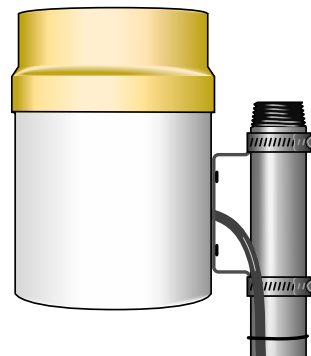
<b>CS705</b>	Snowfall adapter for the TE525WS
<b>10869</b>	Four one-gallon containers of 50:50 PG:E Antifreeze; only US ground shipments
<b>260-953</b>	Novalynx Alter-type Rain Gage Wind Screen



The TE525MM measures rainfall in metric rather than US units.

## Specifications

<b>Sensor Type:</b>	Tipping bucket/magnetic reed switch
<b>Material:</b>	Anodized aluminum
<b>Temperature:</b>	0° to +50°C
<b>Resolution:</b>	1 tip
<b>Volume per Tip:</b>	0.16 fl. oz./tip (4.73 ml/tip)
<b>Rainfall per Tip</b>	
<b>TE525WS, TE525:</b>	0.01 in. (0.254 mm)
<b>TE525MM:</b>	0.004 in. (0.1 mm)
<b>Accuracy</b>	
<b>TE525WS:</b>	±1% (up to 1 in./hr) +0, -2.5% (1 to 2 in./hr) +0, -3.5% (2 to 3 in./hr)
<b>TE525:</b>	±1% (up to 1 in./hr) +0, -3% (1 to 2 in./hr) +0, -5% (2 to 3 in./hr)
<b>TE525MM:</b>	±1% (up to 10 mm/hr) +0, -3% (10 to 20 mm/hr) +0, -5% (20 to 30 mm/hr)
<b>Funnel Collector Diameter</b>	
<b>TE525WS:</b>	8 in. (20.3 cm)
<b>TE525:</b>	6.06 in. (15.4 cm)
<b>TE525MM:</b>	9.66 in. (24.5 cm)
<b>Height</b>	
<b>TE525WS:</b>	10.5 inches (26.7 cm)
<b>TE525:</b>	9.5 inches (24.1 cm)
<b>TE525MM:</b>	11.5 inches (29.21 cm)
<b>Tipping Bucket Weight</b>	
<b>TE525WS:</b>	2.2 lb. (1.0 kg)
<b>TE525:</b>	2.0 lb. (0.9 kg)
<b>TE525MM:</b>	2.4 lb. (1.1 kg)
<b>Cable:</b>	2-conductor shielded cable
<b>Cable Weight:</b>	0.2 lb. (0.1 kg) per 10-ft length



The TE525 is widely used in environmental monitoring applications.





## PT2X SUBMERSIBLE

# PRESSURE/TEMPERATURE SMART SENSOR

## WITH DATALOGGING

### Measure AND Record

#### Pressure AND Temperature

with this easy-to-use

yet powerful and accurate

#### AquiStar® PT2X Smart Sensor!

Great almost anywhere you need to measure level and temperature – whether it be in a lake, in a tank, or in a well.

## FEATURES

### SENSOR

- Pressure, temperature, time
- Absolute, gauge, or sealed gauge
- Thermally compensated – *great where water temperatures vary, such as in streams or in industrial tank applications*
- $\pm 0.06\%$  FSO typical accuracy
- Low power – *2 internal AA batteries*
- External power options (12 VDC) with AA's acting as backup
- 316 SS, Viton®, Teflon® construction (titanium optional)
- Small diameter – 0.75" (1.9 cm)
- Modbus® and SDI-12 interface for greater flexibility

### DATALOGGER

- 130,000 record, 260,000 record, and 520,000 record versions
- Non-volatile memory – *data will not be lost in the event of a power failure*
- Flexible, multi-phase logging sequences – *save sequences to disk to reuse in the future*
- Pause logging feature – *temporarily pause the logging while repositioning or transporting sensor*
- Delayed start feature – *state a specific future start time, making it easy to set several sensors to start at the same time*

### CABLING AND NETWORKING

- Wireless connectivity – *radios and/or cellular*
- RS485 network – *allows several sensors to be networked together and allows much longer cable leads than does RS232*
- Field serviceable connectors – *easily remove the connector, route cable through well seals, walls, or conduit, and then replace connector*
- Available cableless or with a variety of cable options – *polyethylene, polyurethane, or FEP Teflon®*

### SOFTWARE - FREE, EASY-TO-USE

- Real time viewing
- Easy export to spreadsheets and databases
- Barometric compensation utility for use with absolute sensors
- Ability to update sensor via firmware while in the field – *great for future updates or custom development*

## APPLICATIONS

- Pump and slug tests
- Stormwater runoff monitoring
- Well, tank, tidal levels
- River, stream, reservoir gauging
- Wetland monitoring
- Resource administration



**Instrumentation  
Northwest, Inc.**

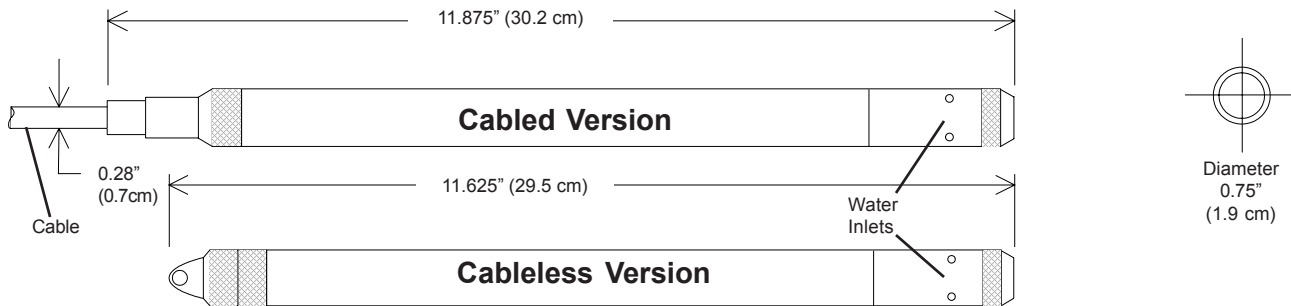
**1-800-776-9355**  
<http://www.inwusa.com>



# PT2X SUBMERSIBLE

# PRESSURE/TEMPERATURE SMART SENSOR

## DIMENSIONS, SPECIFICATIONS, and ORDERING INFORMATION



### GENERAL

<b>Length</b>	11.875" (30.2 cm)
<b>Diameter</b>	0.75" (1.9 cm)
<b>Weight</b>	0.8lb. (0.4 kg)
<b>Body Material</b>	Delrin® & 316 Stainless Steel or Titanium
<b>Wire Seal Materials</b>	Viton® and Teflon®
<b>Submersible Cable</b>	Polyurethane, Polyethylene, FEP or Tefzel® available
<b>Protection Rating</b>	IP68, NEMA 6P
<b>Desiccant</b>	1-3mm indicating silica gel ( <i>high or standard capacity</i> )
<b>Terminating Connector</b>	Available
<b>Communication</b>	RS485 Modbus SDI-12 (ver.1.3)
<b>Operating Temp. Range<sup>3</sup></b>	-15°C to 55°C
<b>Storage Temp. Range<sup>1</sup></b>	-20°C to 80°C

### LOGGING

<b>Memory</b>	1MB - 130,000 records 2MB - 260,000 records 4MB - 520,000 records
<b>Log Types</b>	Variable, User-Defined, Logarithmic, Profiled
<b>Programmable Baud Rate</b>	9600, 19200, 38400
<b>Logging Rate</b>	8x/sec
<b>Software</b>	Complimentary Aqua4Plus or Aqua4Push
<b>Networking</b>	32 available addresses per junction w/ batching capabilities (up to 255)
<b>File Formats</b>	.xls/.csv/.a4d

### POWER

<b>Internal Battery</b>	2x1.5V AA Alkaline <sup>2</sup>
<b>Auxiliary Power</b>	12VDC - Nominal 6-15 VDC - Range
<b>Exp. Battery Life</b>	18 months at 15m polling interval

### TEMPERATURE

<b>Element Type</b>	Digital IC on board
<b>Accuracy</b>	±0.5°C
<b>Resolution</b>	0.06°C
<b>Range</b>	-20°C to 80°C
<b>Units</b>	Celsius, Fahrenheit, Kelvin

### PRESSURE

<b>Transducer Type</b>	Silicon Strain Gauge
<b>Transducer Material</b>	316 Stainless or Titanium
<b>Pressure Ranges</b>	
<i>Gauge</i>	
PSIG <sup>5</sup>	1,2,5,15,30,50,100,300
mH <sub>2</sub> O <sup>5</sup>	0.7,1.75,3.5,10.5,21,35,70,210
<i>Absolute</i>	
PSIA <sup>5</sup>	20,30,50,100,300
mH <sub>2</sub> O <sup>5</sup>	14,21,35,70,210
<b>Units</b>	PSI, FtH <sub>2</sub> O, inH <sub>2</sub> O, cmH <sub>2</sub> O, mmH <sub>2</sub> O, mH <sub>2</sub> O, inHg, cmHg, mmHg, Bars, mBars, kPa
<b>Static Accuracy</b>	±0.06% FSO <i>typical</i> ±0.1% FSO <i>maximum</i> (B.F.S.L. 25°C)
<b>Resolution</b>	16 bit
<b>Maximum Zero Offset</b>	±0.25% FSO (@ 25°C)
<b>Maximum Operating Pressure</b>	1.1 x FS
<b>Burst Pressure<sup>4</sup></b>	3.0 x FS
<b>Compensated Range</b>	0°C to 40°C

1 Storage without batteries  
2 Lithium available upon request  
3 Requires freeze protection kit if in water below freezing  
4 Burst reduced at PSI>300  
5 Higher Pressure ratings available upon request

Information in this document is subject to change without notice.

## Instrumentation Northwest, Inc.



**Sales and Service Locations**  
8902 122nd Avenue NE, Kirkland • Washington 98033 USA  
(425) 822-4434 • (425) 822-8384 FAX • info@inwusa.com  
4620 Northgate Boulevard, Suite 170 • Sacramento, California 95834  
(916) 922-2900 • (916) 648-7766 FAX • inwsw@inwusa.com



# CR1000 Specifications

Electrical specifications are valid over a -25° to +50°C range unless otherwise specified; non-condensing environment required. To maintain electrical specifications, Campbell Scientific recommends recalibrating dataloggers every two years. We recommend that the system configuration and critical specifications are confirmed with Campbell Scientific before purchase.

## PROGRAM EXECUTION RATE

10 ms to one day @ 10 ms increments

## ANALOG INPUTS (SE1-SE16 or DIFF1-DIFF8)

8 differential (DF) or 16 single-ended (SE) individually configured. Channel expansion provided by AM16/32B and AM25T multiplexers.

RANGES and RESOLUTION: Basic resolution (Basic Res) is the A/D resolution of a single conversion. Resolution of DF measurements with input reversal is half the Basic Res.

Range (mV) <sup>1</sup>	DF Res (µV) <sup>2</sup>	Basic Res (µV)
±5000	667	1333
±2500	333	667
±250	33.3	66.7
±25	3.33	6.7
±7.5	1.0	2.0
±2.5	0.33	0.67

<sup>1</sup>Range overhead of ~9% on all ranges guarantees that full-scale values will not cause over range.

<sup>2</sup>Resolution of DF measurements with input reversal.

## ACCURACY<sup>3</sup>:

±(0.06% of reading + offset), 0° to 40°C

±(0.12% of reading + offset), -25° to 50°C

±(0.18% of reading + offset), -55° to 85°C (-XT only)

<sup>3</sup>Accuracy does not include the sensor and measurement noise. The offsets are defined as:

Offset for DF w/input reversal = 1.5-Basic Res + 1.0 µV

Offset for DF w/o input reversal = 3-Basic Res + 2.0 µV

Offset for SE = 3-Basic Res + 3.0 µV

INPUT NOISE VOLTAGE: For DF measurements with input reversal on ±2.5 mV input range; digital resolution dominates for higher ranges.

250 µs Integration: 0.34 µV RMS

50/60 Hz Integration: 0.19 µV RMS

## ANALOG MEASUREMENT SPEED:

Integra- tion Type/ Code	Integra- tion Time	Settling Time	Total Time <sup>5</sup>	
			SE w/ No Rev	DF w/ Input Rev
250	250 µs	450 µs	~1 ms	~12 ms
60 Hz <sup>4</sup>	16.67 ms	3 ms	~20 ms	~40 ms
50 Hz <sup>4</sup>	20.00 ms	3 ms	~25 ms	~50 ms

<sup>4</sup>AC line noise filter.

<sup>5</sup>Includes 250 µs for conversion to engineering units.

INPUT LIMITS: ±5 V

DC COMMON MODE REJECTION: >100 dB

NORMAL MODE REJECTION: 70 dB @ 60 Hz when using 60 Hz rejection

SUSTAINED INPUT VOLTAGE W/O DAMAGE: ±16 Vdc max.

INPUT CURRENT: ±1 nA typical, ±6 nA max. @ 50°C; ±90 nA @ 85°C

INPUT RESISTANCE: 20 Gohms typical

ACCURACY OF BUILT-IN REFERENCE JUNCTION THERMISTOR (for thermocouple measurements): ±0.3°C, -25° to 50°C  
±0.8°C, -55° to 85°C (-XT only)

## ANALOG OUTPUTS (Vx1-Vx3)

3 switched voltage, active only during measurement, one at a time.

RANGE AND RESOLUTION: Voltage outputs programmable between ±2.5 V with 0.67 mV resolution.

V<sub>x</sub> ACCURACY: ±(0.06% of setting + 0.8 mV), 0° to 40°C  
±(0.12% of setting + 0.8 mV), -25° to 50°C  
±(0.18% of setting + 0.8 mV), -55° to 85°C (-XT only)

V<sub>x</sub> FREQUENCY SWEEP FUNCTION: Switched outputs provide a programmable swept frequency, 0 to 2500 mV square waves for exciting vibrating wire transducers.

CURRENT SOURCING/SINKING: ±25 mA

## RESISTANCE MEASUREMENTS

MEASUREMENT TYPES: The CR1000 provides ratiometric measurements of 4- and 6-wire full bridges, and 2-, 3-, and 4-wire half bridges. Precise, dual polarity excitation using any of the 3 switched voltage excitations eliminates dc errors.

VOLTAGE RATIO ACCURACY<sup>6</sup>: Assuming excitation voltage of at least 1000 mV, not including bridge resistor error.

±(0.04% of voltage reading + offset)/V<sub>x</sub>

<sup>6</sup>Accuracy does not include the sensor and measurement noise. The offsets are defined as:

Offset for DF w/input reversal = 1.5-Basic Res + 1.0 µV

Offset for DF w/o input reversal = 3-Basic Res + 2.0 µV

Offset for SE = 3-Basic Res + 3.0 µV

Offset values are reduced by a factor of 2 when excitation reversal is used.

## PERIOD AVERAGE

Any of the 16 SE analog inputs can be used for period averaging. Accuracy is ±(0.01% of reading + resolution), where resolution is 136 ns divided by the specified number of cycles to be measured.

## INPUT AMPLITUDE AND FREQUENCY:

Voltage Gain	Input Range (±mV)	Signal (peak to peak) <sup>7</sup>		Min Pulse Width (µV)	Max <sup>8</sup> Freq (kHz)
		Min. (mV)	Max (V)		
1	2500	500	10	2.5	200
10	250	10	2	10	50
33	25	5	2	62	8
100	2.5	2	2	100	5

<sup>7</sup>With signal centered at the datalogger ground.

<sup>8</sup>The maximum frequency = 1/(Twice Minimum Pulse Width) for 50% of duty cycle signals.

## PULSE COUNTERS (P1-P2)

(2) inputs individually selectable for switch closure, high frequency pulse, or low-level ac. Independent 24-bit counters for each input.

MAXIMUM COUNTS PER SCAN: 16.7x10<sup>6</sup>

## SWITCH CLOSURE MODE:

Minimum Switch Closed Time: 5 ms

Minimum Switch Open Time: 6 ms

Max. Bounce Time: 1 ms open w/o being counted

## HIGH-FREQUENCY PULSE MODE:

Maximum Input Frequency: 250 kHz

Maximum Input Voltage: ±20 V

Voltage Thresholds: Count upon transition from below 0.9 V to above 2.2 V after input filter with 1.2 µs time constant.

LOW-LEVEL AC MODE: Internal AC coupling removes AC offsets up to ±0.5 V.

Input Hysteresis: 12 mV @ 1 Hz

Maximum ac Input Voltage: ±20 V

Minimum ac Input Voltage:

Sine Wave (mV RMS)	Range(Hz)
20	1.0 to 20
200	0.5 to 200
2000	0.3 to 10,000
5000	0.3 to 20,000

## DIGITAL I/O PORTS (C1-C8)

8 ports software selectable, as binary inputs or control outputs. Also provide edge timing, subroutine interrupts/wake up, switch closure pulse counting, high frequency pulse counting, asynchronous communications (UART), SDI-12 communications, and SDM communications.

HIGH-FREQUENCY MAX: 400 kHz

SWITCH CLOSURE FREQUENCY MAX: 150 Hz

EDGE TIMING RESOLUTION: 540 ns

OUTPUT VOLTAGES (no load): high 5.0 V ±0.1 V; low <0.1

OUTPUT RESISTANCE: 330 ohms

INPUT STATE: high 3.8 to 16 V; low -8.0 to 1.2 V

INPUT HYSTERESIS: 1.4 V

INPUT RESISTANCE: 100 kohms

## SWITCHED 12 V (SW-12)

One independent 12 V unregulated sources switched on and off under program control. Thermal fuse hold current = 900 mA @ 20°C, 650 mA @ 50°C, 360 mA @ 85°C.

## CE COMPLIANCE

STANDARD(S) TO WHICH CONFORMITY IS DECLARED: IEC61326:2002

## COMMUNICATIONS

RS-232 PORTS:

9-pin: DCE port for battery-powered computer or non-CSI modem connection.

COM1 to COM4: Four independent Tx/Rx pairs on control ports (non-isolated); 0 to 5 VUART

Baud Rates: selectable from 300 bps to 115.2 kbps.

Default Format: 8 data bits; 1 stop bits; no parity

Optional Formats: 7 data bits; 2 stop bits; odd, even parity

CS I/O PORT: Interface with CSI peripherals

SDI-12: Digital control ports 1, 3, 5, and 7 are individually configured and meet SDI-12 Standard version 1.3 for datalogger mode. Up to ten SDI-12 sensors are supported per port.

PERIPHERAL PORT: 40-pin interface for attaching CompactFlash or Ethernet peripherals

PROTOCOLS SUPPORTED: PakBus, Modbus, DNP3, FTP, HTTP, XML, POP3, SMTP, Telnet, NTCIP, NTP, SDI-12, SDM

## CPU AND INTERFACE

PROCESSOR: Renesas H8S 2322 (16-bit CPU with 32-bit internal core)

MEMORY: 2 MB of Flash for operating system; 4 MB of battery-backed SRAM for CPU usage, program storage and data storage.

CLOCK ACCURACY: ±3 min. per year. Correction via GPS optional.

## SYSTEM POWER REQUIREMENTS

VOLTAGE: 9.6 to 16 Vdc (reverse polarity protected)

EXTERNAL BATTERIES: 12 Vdc nominal

TYPICAL CURRENT DRAIN:

Sleep Mode: ~0.6 mA

1 Hz Sample Rate (1 fast SE meas.): 1 mA

100 Hz Sample Rate (1 fast SE meas.): 16.2 mA

100 Hz Sample Rate (1 fast SE meas. w/RS-232 communication): 27.6 mA

Optional Keyboard Display On (no backlight): add 7 mA to current drain

Optional Keyboard Display On (backlight on): add 100 mA to current drain

PHYSICAL DIMENSIONS: 9.4" x 4" x 2.4" (23.9 x 10.2 x 6.1 cm); additional clearance required for serial cable and sensor leads.

## PHYSICAL

WEIGHT: 2.1 lbs (1 kg)

WARRANTY

3-years against defects in materials and workmanship.





# ENC-series

## Weather-Resistant Enclosures



Campbell Scientific offers fiberglass-reinforced polyester enclosures for housing our dataloggers and peripherals. These non-corrosive, white enclosures are UV-stabilized and reflect solar radiation—reducing temperature gradients inside the enclosure without requiring a separate radiation shield. Dataloggers and peripherals housed in an enclosure with desiccant are protected from water and most pollutants.

The NEMA 4X enclosures (modified for cable entry) include a door gasket, external grounding lug, stainless steel hinge, and a lockable hasps. The enclosures are shipped with the 7363 enclosure supply kit that consists of desiccant, a humidity indicator card, cable ties, wire tie tabs, putty, grommets, and screws. Additionally, Campbell Scientific offers a CS210 Enclosure Humidity Sensor for monitoring relative humidity inside of the enclosure.

### Backplate

Dataloggers, peripherals, and brackets are mounted to an internal plate punched with a grid of one-inch-on-center holes. This mounting scheme simplifies system configuration and facilitates addition and removal of equipment in the field.

An internal backplate is included with each ENC10/12, ENC12/14, or ENC14/16 enclosure. Two internal mounting plate options are offered for the ENC16/18. The *-SB* option provides a backplate that is similar to the one included with the other enclosures. The *-EB* option provides both a backplate and sideplate.

### Models Available

#### *ENC10/12*

Campbell Scientific's ENC10/12 enclosure has internal dimensions of 10-in x 12-in x 4.5-in (25.4-cm x 30.5-cm x 11.4-cm) and weighs 9.0 lbs (4.1 kg). It can house one CR200(X)-series datalogger, power supply, and one small peripheral. A CR800, CR850, or CR1000 can also be housed in the ENC10/12 if the #17565 stack mounting kit is used. For peripherals that are taller, an enclosure that has a raised lid is available; contact Campbell Scientific for more information.

#### *ENC12/14*

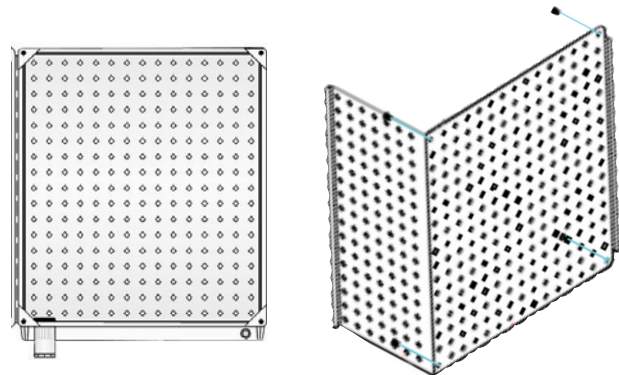
The ENC12/14 has internal dimensions of 12-in x 14-in x 5.5-in (30.5-cm x 35.6-cm x 14-cm). This enclosure can house one CR200(X)-series, CR800, CR850, CR1000, or CR3000 datalogger, power supply, and one or more peripherals (depending on the peripheral's footprint). It weighs 11.2 lbs (5 kg).

#### *ENC14/16*

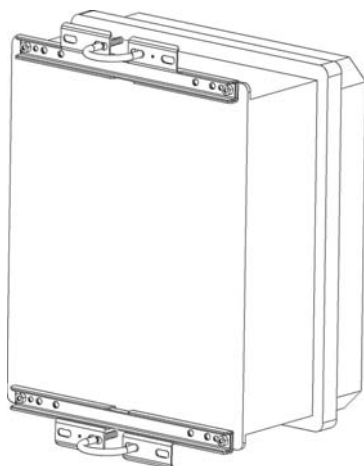
This enclosure has internal dimensions of 14-in x 16-in x 5.5-in (35.6-cm x 40.6-cm x 14-cm). It can house one CR200(X)-series, CR800, CR850, CR1000, CR3000, or CR5000 datalogger, power supply, and one or more peripherals (depending on the peripheral's footprint).

#### *ENC16/18*

Our largest enclosure provides internal dimensions of 16-in x 18-in x 9-in (40.6-cm x 45.7-cm x 22.9-cm) and weighs 17 lbs (7.7 kg). It can house one CR200(X)-series, CR800, CR850, CR1000, CR3000, or CR5000 datalogger, power supply, and two or more peripherals (depending on the peripheral's footprint).



An ENC16/18 ordered with option *-SB* comes with the backplate shown on the left. Option *-EB* provides the backplate and sideplate that is shown on the right.

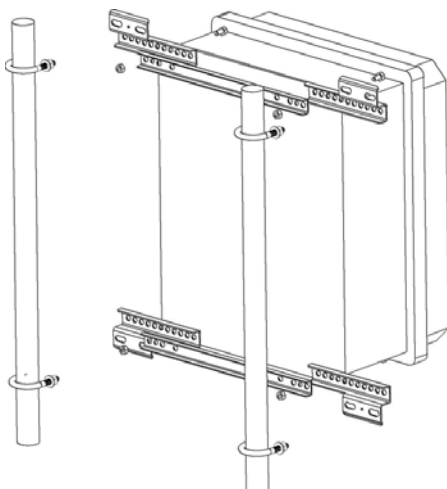


The above enclosure is configured with the *-MM* bracket option and is ready to be attached to a mast or user-supplied pole.

## Mounting Bracket Options

Order the *-MM* option if you want to mount your enclosure to the mast of one of our tripods or to a user-supplied pole with a 1.25-in to 2.1-in OD. A three-piece bracket attaches to the top of the enclosure and an identical three-piece bracket attaches to the bottom of the enclosure (see illustrations at right). Each bracket is attached to the mast or pole via a 2-in u-bolt.

Order the *-TM* option if you want to mount your enclosure to a UT10, UT20, or UT30 tower. This mounting bracket option uses the same three-piece brackets as the *-MM* option, except the pieces are rearranged so that the flanges are on the side of the bracket instead of in the middle. Four 1.5-in u-bolts attach the brackets to the tower legs.

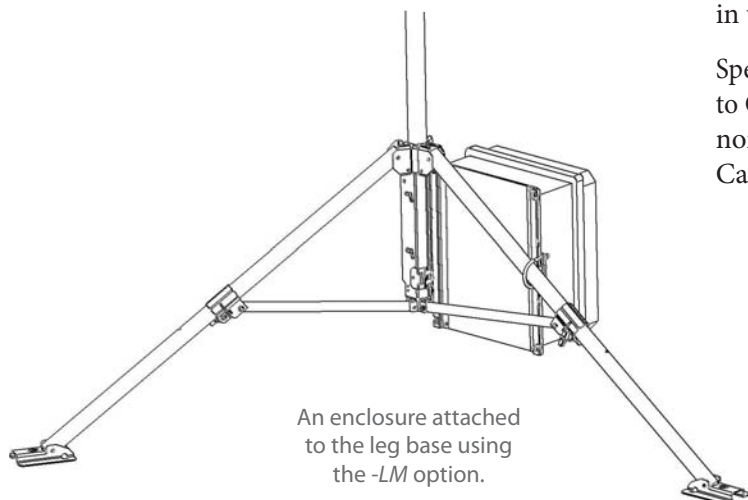


This exploded view of the *-TM* option shows the bracket components and how the enclosure attaches to a tower.

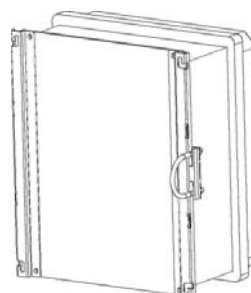
Please note that enclosures with the *-TM* option are shipped configured for the UT10 tower. UT20 and UT30 customers will need to: (1) remove the bolts attaching the bracket to the enclosure, (2) slide out the flange sections so that the distance between the center of each flange is 17 inches, and (3) reattach the bracket to the enclosure using the original bolts.

The *-LM* option allows the enclosure to be attached to the leg base of a CM110, CM115, or CM120 light-weight tripod. This option includes a metal flange, two brackets, and a 2.5-in u-bolt. The brackets attach to the right and left side of the enclosure, and the flange attaches to the tripod near the mast. The flange fits into a notch in one of the brackets, and the other bracket connects to a tripod leg via the u-bolt. Please note that the *-LM* option is not offered for our ENC16/18 enclosures. Two enclosures may be mounted back-to-back in this configuration.

Special brackets are also available for attaching enclosures to CTS Towers, Rohn Towers, Aluma Towers, or other non-Campbell Scientific instrument mounts. Contact Campbell Scientific for more information.



An enclosure attached to the leg base using the *-LM* option.



At left is an enclosure with the *-LM* bracket option.

## Cable-Entry Options

### *Conduit(s)*

Multiple cables can be routed through one conduit. The -SC option provides one 1.5-in diameter conduit; the -DC option provides two horizontally-arranged 1.5-in diameter conduits; and the -VC option (ENC16/18 only) provides two vertically-arranged 1.5-in diameter conduits. A removable plug is included to reduce the internal diameter to 0.5 inches (1.3 cm). The 7363 enclosure supply kit contains putty for sealing each conduit.

### *Entry Seals (individual compression fittings)*

Choose the -ES entry seals option for a more water-tight seal than provided by the conduits. With this option, each entry seal is compressed around one cable. A small vent is included to equalize pressure with the atmosphere. Please note that the entry seal option is not offered for the ENC14/16. The number and size of seals provided for our enclosures are as follows:

**ENC10/12:** (1) **Medium** (fits 0.231-in to 0.394-in cables)

(2) **Small** (fits 0.118-in to 0.275-in cables)

**ENC12/14:** (2) **Medium** (fits 0.231-in to 0.394-in cables)

(2) **Small** (fits 0.118-in to 0.275-in cables)

**ENC16/18:** (2) **Large** (fits 0.236-in to 0.512-in cables)

(2) **Medium** (fits 0.231-in to 0.394-in cables)

(2) **Small** (fits 0.118-in to 0.275-in cables)

## Accessory Installations

### *Antenna Cable/Bulkhead*

These accessories are offered for enclosures that will house a cellular phone, satellite transmitter, or radio. When ordered, Campbell Scientific will punch a special bulkhead hole in the enclosure and install a 17-in antenna cable. Available antenna cable/bulkhead accessories are:

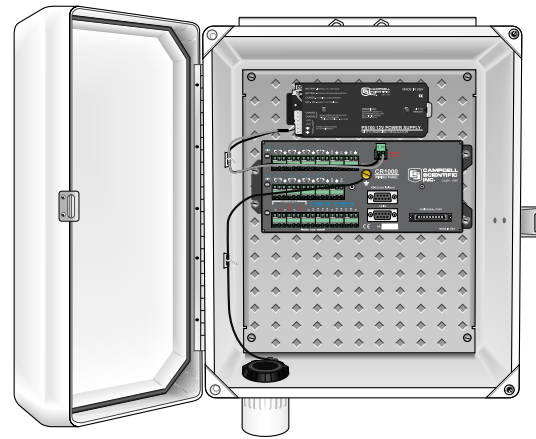
**19335:** Type N-to-RPSMA Antenna Cable for our RF400-series spread spectrum radios or CR200-series dataloggers

**19334:** Type N-to-SMA Antenna Cable for the RF450 radio or RavenXT-series cellular modems

**19332:** Type N-to-Type N Antenna Cable for the RF310-series radios, TX312 GOES satellite transmitter, or FGR-115 radios

**19336:** Type SMA-to-SMA Antenna Cable for the GPS device used with satellite transmitters

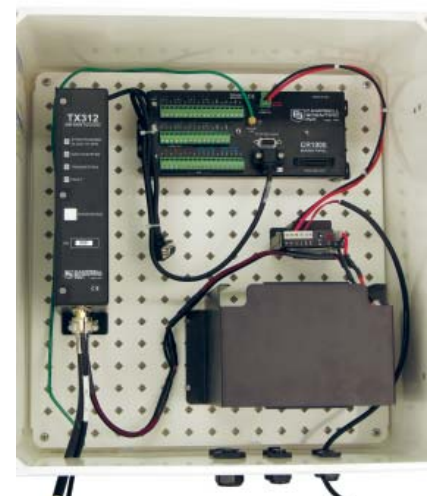
**19333:** Type N-to-TNC Antenna Cable for our Raven100-series or Redwing100-series digital cellular modems



An enclosure with the -SC option includes one 1.5-in diameter port for cable entry. Shown is an ENC12/14 housing a CR1000 datalogger and PS100 power supply.



An enclosure with the -DC option includes two horizontally-arranged 1.5-in diameter ports for cable entry (shown above).



This ENC16/18 with the -ES cable entry option and 19332 Antenna Cable/Bulkhead accessory houses the equipment commonly used in a GOES satellite system.

### *CD294 Data View Display*

Specify #16737 to have Campbell Scientific install a CD294 Data View Display in the enclosure door. The CD294 is a two-line, 32-character LCD that is used with mixed-array dataloggers (e.g., CR510, CR10X). When the CD294 is installed in an enclosure door, you can view real-time data on-site without opening the enclosure. A stainless steel cover is provided to help protect the display from the effects of ultraviolet radiation.

### *CD295 Data View II Display*

Specify #18132 to have Campbell Scientific install a CD295 Data View II Display in the enclosure door. The CD295 is a two-line, 32-character LCD that is used with PakBus® dataloggers (i.e., CR200, CR800, CR850, CR1000, CR3000). When the CD295 is installed in an enclosure door, you can view real-time data on-site without opening the enclosure. A stainless steel cover is provided to help protect the display from the effects of ultraviolet radiation.

### *Enclosure Door Switch Indicator*

Specify #18166 to have Campbell Scientific install an enclosure door switch indicator or specify #18165 to have the customer install the indicator. This small accessory monitors when the door of the enclosure is open. It consists of an actuator and a magnetic switch—one is located on the case side, the other on the door side of the enclosure. The switch is monitored with a control port on the datalogger.



When a CD295 DataView II is installed in an enclosure door, you can view real-time data in the field without opening the enclosure.

### *SC-IRDA Infrared Interface*

Campbell Scientific will install an SC-IRDA Infrared Interface in the enclosure's case when you specify #17206. The SC-IRDA provides an infrared interface that facilitates communication between the datalogger and an infrared-equipped PDA. This device allows you to interrogate the datalogger on-site without opening the enclosure. PConnect or PConnectCE software is required. The SC-IRDA is secured and sealed in the enclosure with a compression fitting.



On the ENC10/12 and ENC12/14, the actuator (above left) for the door switch indicator is attached to the enclosure case and the switch (above right) is attached to the enclosure door. For the other enclosures, the actuator is attached to the door and the switch is attached to the case.



# ENCLOSURE SUPPLY KIT (Part #7363)

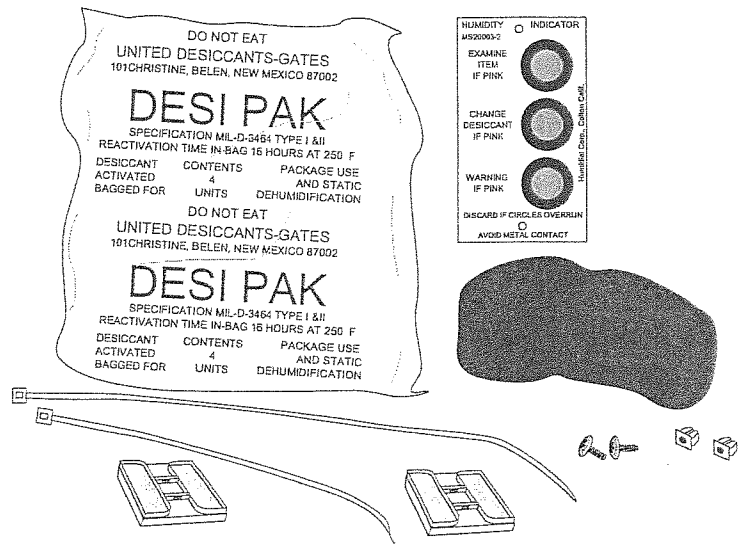
The contents of this bag are for use with Campbell Scientific's field enclosures. Please note that some of the enclosed items should be saved for future use.

1. Use the #6 screws and plastic grommets to mount additional peripherals to the enclosure backplate. Dataloggers, power supplies, and most peripherals are usually attached to the backplate prior to shipment from the factory or are supplied with additional screws and grommets. To insert the grommet, push the points of the flanges into the center of any square hole. To remove a grommet without damage, remove the enclosure backplate and use pliers to pinch the grommet flanges together.
2. If desired, insert the 25745 PVC coupling to reduce the conduit's diameter to 0.5". Route the sensor leads through the enclosure conduit to the datalogger or peripheral terminal strips.
3. Use the cable tie tabs and 8" cable ties to strain relief the cables to the side of the enclosure as shown.

**NOTE:** The adhesive of the cable tie tab may not stick during extremely cold temperatures or extremely high humidity. In these situations, fasten the cable tie tab to the backplate using a #6 screw and grommet.

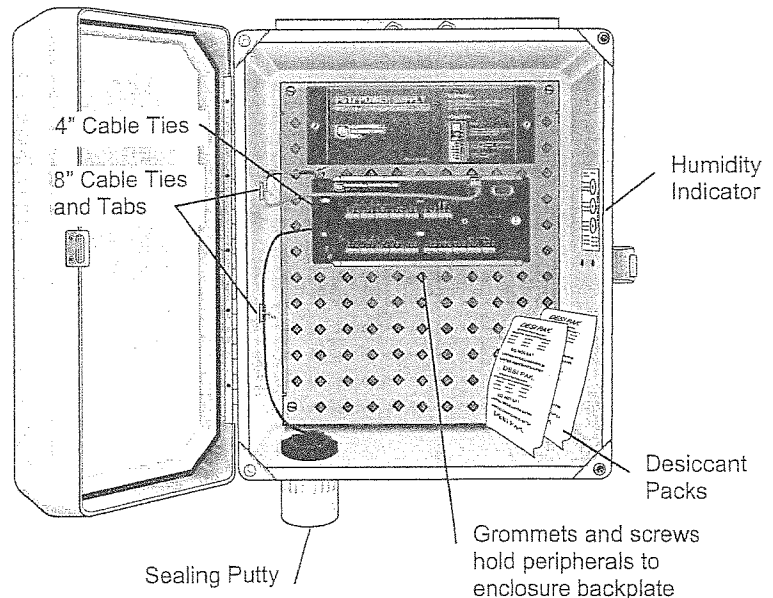
4. Strain relief the sensor leads to the datalogger's strain relief flanges with the 4" cable ties.
5. Remove the backing tape from the humidity indicator and attach to the side of the enclosure as shown.
6. Seal the gap between the sensor leads and the enclosure conduit with sealing putty.
7. Place two desiccant packs inside the enclosure; reseal the other two inside the plastic bag. Store the extra packs in a dry area and use them to replace the two in the enclosure during a site visit or when the 40% ring on the humidity indicator turns pink.

**CAUTION:** To prevent bursting, reactivation of the desiccant packs requires a slow initial temperature increase and precise temperature control. Therefore, we recommend purchasing new desiccant instead of oven drying.



The contents of the enclosure supply kit are the following.

Qty.	Part #	Description
8	505	#6 x 32 x .375" screws
8	6044	grommets
4	2376	3 cm cable tie tabs
6	2207	4" cable ties
6	4005	8" cable ties
1	6571	humidity indicator card
2	6596	4 oz container of sealing putty
4	4905	4-unit desiccant packs
1	6290	Phillips screwdriver
1	25745	PVC coupling





# BPALK and PS100

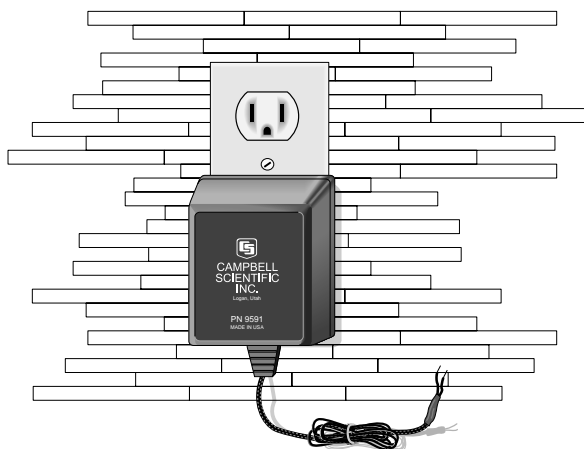
Power Supplies for CR800, CR850, and CR1000



The BPALK Alkaline Battery Pack includes eight “D” cell batteries for powering a CR800, CR850, or CR1000 datalogger.



The PS100 is used with our CR800, CR850, or CR1000 dataloggers. It includes a rechargeable battery and a regulator.



One end of the #9591 transformer plugs into a wall ac outlet while the other end connects to the PS100 Power Supply.

The BPALK and PS100 are 12 Vdc power supplies for our CR800, CR850, CR1000, CR10X, CR510, or CR500 dataloggers, and peripherals. They can also be used as a separate auxiliary 12-V power supply to power remotely located sensors or peripherals, such as a multiplexer located at a distance from the datalogger enclosure. However, to avoid errors in analog measurements and ground loops, the power supplies must share a common ground.

## BPALK Alkaline Power Supply

The BPALK is an alkaline 12-Vdc, 7.5-Ahr power supply that consists of eight replaceable D-cell alkaline batteries, battery connectors, and a temporary 12-V AA battery pack [#8862] used during D-cell replacement. The 8862 requires eight AA-cell batteries (not included).

Alkaline batteries are not rechargeable, and their Amp hour ratings decrease with temperature extremes. Alkaline batteries may leak when used outside the temperature range of -25° to +50°C, or when the battery voltage drops below 9.6 V.

## PS100 Rechargeable Power Supply

The PS100 is a 12-Vdc, 7-Ahr rechargeable power supply that consists of a sealed rechargeable battery and a voltage regulator. The regulator controls the current flowing to the battery and prevents the battery current from flowing to the charging source. The sealed rechargeable battery should be trickle-charged via ac power or solar power (see below).

### Charging Sources for PS100

Several wall chargers and solar panels are available for recharging the PS100's sealed rechargeable battery. Solar panels charge batteries by converting sunlight into direct current. Wall chargers use power from external ac power lines to recharge the batteries.

### Adapters for PS100

Campbell Scientific offers two adapters that fasten onto our PS100 power supply. The A100 allows the PS100 to power peripherals and external devices at non-datalogger sites such as repeater stations. The A105 adapter increases the number of 12 V and ground terminals available on the PS100. The A100 and A105 cannot be used at the same time.

## Ordering Information

### Power Supplies

<b>BPALK</b>	12 V, 7.5 Ahr Alkaline Battery Pack
<b>PS100</b>	12 V Power Supply with Charging Regulator and 7Ahr Sealed Rechargeable Battery

### Adapters for the PS100

<b>A100</b>	Null Modem Adapter
<b>A105</b>	12 V Terminal Expansion Adapter

### Wall Chargers for PS100

<b>9591</b>	Wall Charger 18 Vac 1.2 A Output, 110 Vac Input, 6 ft Cable
<b>22110</b>	Wall Charger 18 Vac 1.2 A Output, 110 Vac Input, 6 ft Cable for prewired enclosure.
<b>14014</b>	Wall Charger 18 Vdc Output 90 to 264 Vac 47 to 63 Hz Input. Must choose a power cable option (see below).
<b>22111</b>	Wall Charger 18 Vdc Output 90 to 264 Vac 47 to 63 Hz Input for prewired enclosure. Must choose a power cable option (see below).

### Power Cable Options for 14014 or 22111 (choose one)

<b>-NC</b>	No Power Cable
<b>-USC</b>	US Cable
<b>-EUC</b>	Continental European Cable
<b>-UKC</b>	United Kingdom/Ireland Cable
<b>-AUC</b>	Australia/New Zealand Cable
<b>-CNC</b>	China Cable

### Solar Panels for PS100

<b>SP10</b>	10 W Solar Panel with 20 ft Cable
<b>SP10-PW</b>	10 W Solar Panel with 20 ft cable for prewired enclosure
<b>SP20</b>	20 W Solar Panel with 20 ft Cable
<b>SP20-PW</b>	20 W Solar Panel with 20 ft cable for prewired enclosure

## Specifications\*

### BPALK Alkaline Battery Pack

<b>Nominal Rating:</b>	7.5 Ahrs @ 20°C
<b>Batteries:</b>	8 Alkaline D cells (not rechargeable)
<b>Output Voltage:</b>	12 Vdc
<b>Weight:</b>	1.8 kg
<b>Dimensions (including mounts and connectors):</b>	7.1" x 2.9" x 3.1" (18.1 x 7.4 x 8.0 cm)
<b>Operating Temperature:</b>	-25° to +50°C

### PS100 Rechargeable Power Supply

<b>Output Voltage:</b>	12 Vdc
<b>Nominal Capacity:</b>	7 Amp hours
<b>Input Voltage (CHG terminals):</b>	15 to 28 VDC or 18 VAC RMS
<b>Battery Connections</b>	
<b>Charging Output Voltage:</b>	Temperature compensated float charge for battery
<b>Temperature Compensation Range:</b>	-40° to +60°C
<b>Max. Charging Current:</b>	1.2 A (allows one SP20 or SP10 to be used)
<b>Power Out (+12 terminals)</b>	
<b>Voltage:</b>	Unregulated 12 V from battery
<b>Temperature Current Limited with 3 A Thermal Fuse:</b>	> 3 A @ < 20°C; 3 A @ 20°C; 2.1A @ 50°C; 1.8 A @ 60°C
<b>Weight:</b>	6.9 lbs (3.1 kg)
<b>Dimensions (including mounts and connectors)</b>	
<b>Height:</b>	4.1" (10.5 cm)
<b>Width:</b>	7.6" (19.0 cm)
<b>Depth:</b>	2.8" (7.0cm)

\*Information about calculating power usage is included in our Power Supply Overview brochure and Power Supply application note. Brochures and application notes are available from: [www.campbellsci.com](http://www.campbellsci.com)



# SC115

## CS I/O 2G Flash Memory Drive with USB Interface



The SC115 is a lightweight, portable instrument that can serve as a 2-GB storage device or as a USB-to-CSI/O synchronous device communications (SDC) adapter. When serving as a storage device, the SC115 allows you to augment your onsite data storage or to transport data between the datalogger and PC. As a USB-to CSIO adapter, the SC115 supports direct communication between a Campbell Scientific datalogger and a PC equipped with a USB port.

The SC115 is used with many of our CRBasic dataloggers, and is the only storage device compatible with the CR800 and CR850.

### Connections

You can connect the SC115 to the PC or datalogger either directly or via the supplied cables. Cables supplied with the SC115 are the SC12 CS I/O Cable (for datalogger connection) and a USB cable (for PC connection). A driver CD is also shipped with the SC115. The drivers contained on the CD are needed when using the SC115 as a USB-to-CSIO adapter.



### Features/Benefits

- Connects to the PC's USB port and/or the datalogger's CS I/O port (either directly or via the supplied cables)
- Fits in your pocket for easy transport between the datalogger and PC
- Supports USB-to-CS I/O communications
- Expands data storage for our CR1000, CR800, CR850, and CR3000 dataloggers
- Stores 2 GB of data
- Consists of electronics protected in a custom molded package
- Provides a USB 2.0 compliant device
- Allows field upgrades and configuration by using our Device Configuration utility
- Contains an on-board file system to offload datalogger CPU overhead
- Uses CRBasic's TableFile I/O instruction

### Ordering Information

#### Memory Device/USB Interface

**SC115** CS I/O 2G Flash Memory Drive with USB Interface. It includes a USB cable, an SC12 cable, and driver CD.

#### Common Accessories

- 16987** Peripheral Mounting Kit that is used when the SC115 resides with the datalogger and is connected to the datalogger via an SC12 cable. This mounting kit fastens the SC115 to an enclosure backplate.
- 193** Spacer Jack for Screw #4-40. Two 193 Spacer Jacks are needed if screws are used to secure the SC12 cable to the SC115.

# Specifications

**Storage Capacity:** 2 GB

**Power Requirements:** 12 V supplied through the PC's USB port or the datalogger's CS I/O port

**Typical Current Drain**

Active: 35 mA

Quiescent: 200  $\mu$ A

**Datalogger Operating System (OS)**

CR1000: Version OS4 or later

CR3000: All CR3000 OSs

CR800/CR850: All CR800/CR850 OSs

**Software Requirements**

LoggerNet: Version 3.1.3 or later

PC400: Version 1.2.1 or later

**Temperature Range:** -25° to +50°C

**Case:** Sealed, custom molded packaging

**Dimensions:** 4.15 x 1.7 x 0.7 in  
(10.54 x 4.32 x 1.78 cm)

**Weight:** 2.25 oz (63.79 g)

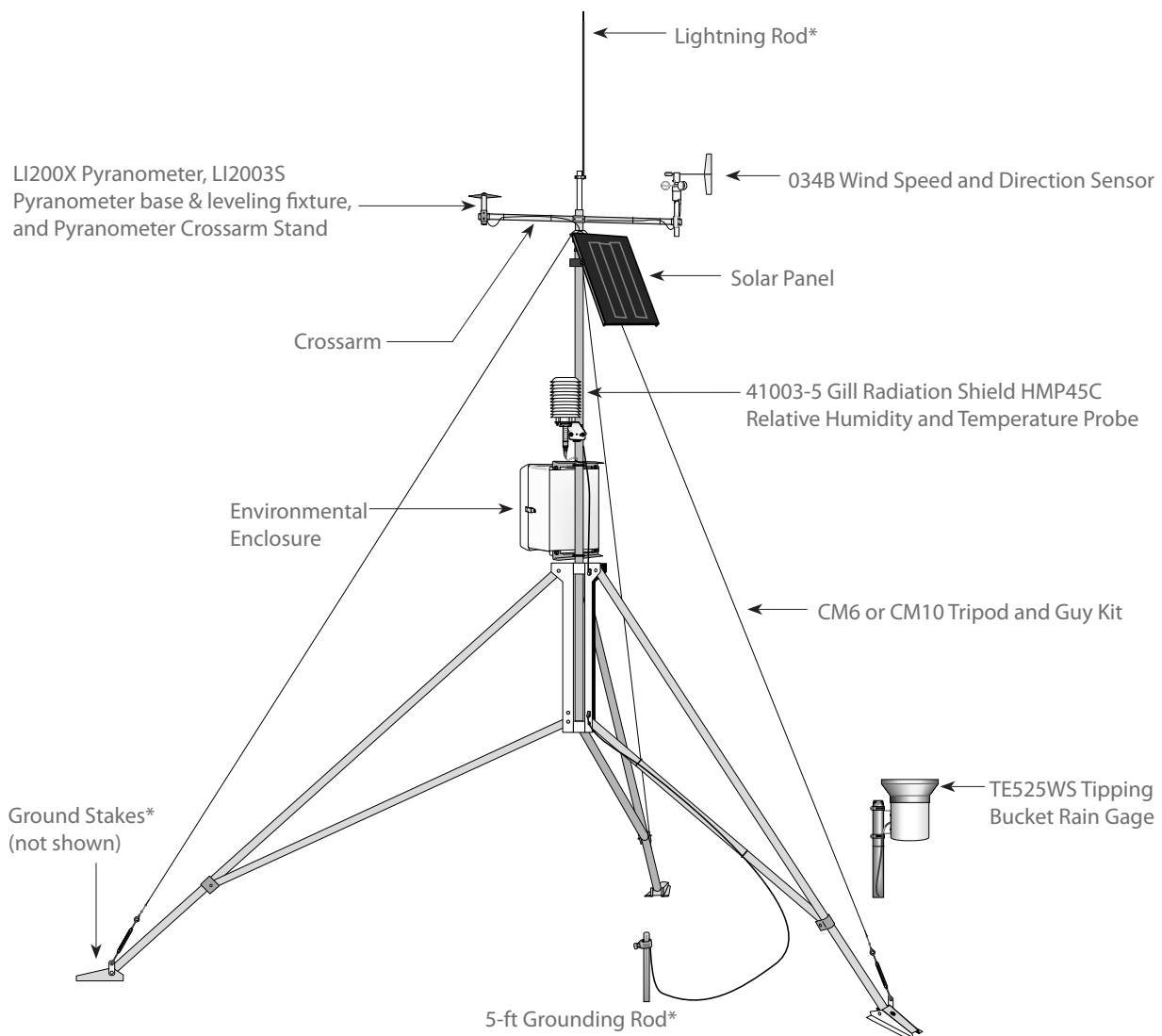


# CM6 and CM10

## Galvanized Steel Instrumentation Tripods

The CM6 and CM10 tripods are general purpose instrument mounts constructed out of corrosion-resistant galvanized steel. They support the attachment of sensors and mounts, solar panels, and environmental enclosures. The CM6 provides a 6 foot (2 m) measurement height for the wind sensors (see below), the CM10 a 10 foot (3 m) measurement height. Individually adjustable legs allow installation over uneven terrain. Both tripods include lightning and grounding rods, grounding cables, grounding cable clamps, ground stakes, and UV-resistant cable ties. An optional guy kit to improve the CM10's wind load rating (see back) is also available.

The CM6 and CM10 are used as portable instrument mounts in a variety of applications. For meteorological applications, tripods augmented with mounts (e.g., CM204 Crossarm) support the attachment of sensors such as wind sets, pyranometers, and temperature/relative humidity probes. Barometers, soil temperature and moisture probes, and rain gauges are also used with tripod-based weather stations. For non-meteorological applications, tripods can provide a portable instrument mount for enclosures and a mounting point for antennas.



\*Included with CM6/10 purchase. Other items purchased separately; alternate sensors available.

## CM10K Tripod Kit

The CM10K Tripod Kit is intended for overseas shipments. The kit contains most of the tripod's hardware. Customers must purchase threaded and unthreaded lengths of 0.75-in and 1.25-in galvanized pipe and a copper ground rod. The overseas shipping costs are significantly reduced when the galvanized pipe is purchased locally.

## Ordering Information

### Tripods and Tripod Kits

<b>CM6</b>	6 ft (1.8 m) galvanized-steel tripod with grounding kit
<b>CM10</b>	10 ft (3 m) galvanized-steel tripod with grounding kit
<b>CM10K</b>	CM6/CM10 Tripod Kit.

### Common Accessory

<b>10844</b>	Optional tripod guy kit for the CM10
--------------	--------------------------------------

## Specifications

### Measurement Height

<b>CM6:</b>	6 ft (2 m)
<b>CM10:</b>	10 ft (3 m)

**Vertical Load Limit:** 100 lbs (45 kg)

**Mast:** 1.25 in PS (1.66 in outer diameter)

### Maximum Base Diameter

<b>CM6:</b>	6 ft (2 m)
<b>CM10:</b>	10 ft (3 m)

**Leveling Adjustment:** Slide collars on each leg adjust individually

### Leg Base

<b>CM6:</b>	2 in x 4 in with 0.5-in hole for ground stake
<b>CM10:</b>	2 in x 5 in with 0.5-in hole for ground stake

### Portability

<b>CM6:</b>	Collapsible to 4-ft length by 9-in diameter
<b>CM10:</b>	Collapsible to 6-ft length by 9-in diameter

### Weight

<b>CM6:</b>	45 lbs (20 kg)
<b>CM10:</b>	70 lbs (32 kg)
<b>CM10K:</b>	14.8 lbs (6.7 kg)

### Wind Load Recommendations

#### Sustained Wind

<b>Tolerance:</b>	100 mph (unguyed CM6); 70 mph (unguyed CM10); 120 mph (guyed CM10);
<b>Gust Tolerance:</b>	130 mph (unguyed CM6); 100 mph (unguyed CM10); 150 mph (guyed CM10);







## Appendix 2

### Water Balance Testing – Plastic Lined Lagoon

---

The accuracy of the BT model and the overall water balance approach were demonstrated via systematic testing on a plastic lined lagoon (Ham, 1999). Under the assumption that the liner is intact (i.e., essentially no seepage), the change in storage should equal the evaporative losses calculated with the BT model. Similar testing was performed for purposes of this work effort. However, the only available plastic lined lagoon offered less than favorable associated circumstances. As a result, the testing on the plastic lined lagoon could not be used to definitively demonstrate the accuracy of the BT model and the overall water balance approach. However, the data indicate that the BT model does not overestimate evaporation. This is important, because systematic overestimation of the evaporative losses would result in systematic underestimation of the seepage rate.

The lagoon was relatively recently constructed with a single 60 mil HDPE liner. At the time of testing, the lagoon was filled near capacity with a surface area of 0.6 ha. The lagoon receives inflow from an adjacent lagoon (also lined with 60 mil HDPE liner) of equal size with a plastic cover. Hydraulic separation of the two lagoons was not possible. To address this issue, ample time was allowed for the water level in the lagoon system to equilibrate. During the water balance testing, the cover was floating on the lagoon with no apparent pressure build-up under the cover. Due to the hydraulic connection, the water balance testing applies to the lagoon system, i.e., the open lagoon and the covered lagoon together. This presents a complication, because evaporative losses from the cover could not be quantified. To address this complication, three alternative assumptions regarding the magnitude of evaporation from the cover were considered in the interpretation of the test results.

**No evaporation from plastic cover.** Lagoon water under the cover cannot evaporate and leave the system. If the cover had been completely dry, a zero-evaporation assumption would have been appropriate. Under this assumption, the change in storage due to evaporation, as indicated by the water level transducers, would only be one-half of the evaporation that actually occurred. This is so, because a drop of the water level in the open lagoon would cause lagoon water to flow from the covered lagoon to the open lagoon until equilibrium was attained (i.e., redistribution between lagoons of equal size).

**Evaporation from plastic cover equal to evaporation from open lagoon.** Recent precipitation had left puddles occupying approximately 10-20% of the cover. Due to the dissected pattern of long, narrow, and shallow puddles; solar heating of the black plastic cover; and lack of vertical convection exchange with cooler lagoon water from greater depths, the evaporation rate from the puddles is thought to have been significantly greater than from the surface of the open lagoon. Consequently, evaporative losses integrated over the area of the whole cover may have been identical to that of the open lagoon (i.e., a condition of unity). Under the unity assumption, the covered lagoon is treated as if it were open, and the change in storage due to evaporation losses, as indicated by the water level transducers, would be identical to the evaporation that actually occurred.

**Evaporation from plastic cover greater than evaporation from open lagoon.** If evaporation from the cover had been greater than from the open lagoon, the change in storage indicated by the water level transducers would be greater than the estimated evaporation depth. This is so, because a drop of the water level in the covered lagoon would cause lagoon water to flow from the open lagoon to the covered lagoon until equilibrium was attained.

Since recent precipitation had left puddles on the cover, the zero-evaporation assumption is not appropriate for the evaluation of the water balance results. Similarly, given the relatively small aerial coverage of the puddles and low ambient air temperature, it is highly unlikely that evaporation from the cover was greater than from the open lagoon. Rather, the actual evaporative losses from the cover were likely near unity, but below it.

## Discussion of Results

The mean cumulative evaporation over the testing period of 5 d 11.5 hrs was 9.9 mm (**Figure A2-4**). Mean night time evaporation (i.e., between shortly after sunset until shortly before sun rise; in this case from 19:30 to 7:00 h; i.e., 11.5 h testing period) ranged from 0.2 to 0.5 mm (**Figure A2-5**). Water level elevations at this lagoon were characterized by considerable short-term variability (i.e., noise) (**Figure A2-6**). However, integrated over the duration of the test, measurements indicate a linear mean water level elevation drop of 9.4 mm. **Figure A2-7** shows very good agreement between the change in storage and the BT model output, indicating that the change in storage is entirely attributable to evaporation<sup>1</sup> (i.e., no seepage). Under the unity assumption, these results are interpreted as an indication for the accurate performance of the BT model. If evaporation from the cover had been greater than from the open lagoon (i.e., a condition believed to be highly unlikely), these results would indicate that the BT model overestimates the actual evaporation from the open lagoon. Under the zero-evaporation assumption (i.e., a condition not appropriate in this context), these results would indicate that the BT model underestimates the actual evaporation from the open lagoon by a factor of 0.5. Importantly, any evaporation from the cover between zero and unity indicates that the BT model tends to underestimate evaporation.

The short-term water level elevation variability is illustrated by the overnight testing results (**Figure A2-8**). This figure also shows 0.2 mm of precipitation measured during the second night with the tipping bucked rain gauge.

The normalized seepage rate computed from the cumulative test duration stabilized on DOY 88 just over  $1.0 \text{ mm d}^{-1}$  and remained virtually invariable throughout the remaining test, resulting in a seepage rate of  $1.0 \pm 1.4 \text{ mm d}^{-1}$  (a large portion of the uncertainty stems from unstable water level readings at the beginning of the test) (**Figure A2-8**). Despite the short-term water level elevation variability, the results from the overnight testing also show quick convergence with the exception of the last night of testing, when the test duration was not sufficient to allow the apparent computed seepage rate to stabilize. Normalized seepage rates estimated from the other nights were as follows: Night 1 ( $1.1 \text{ mm d}^{-1}$ ), Night 2 ( $1.1 \text{ mm d}^{-1}$ ) (precipitation was accounted for), Night 3 ( $0.4 \text{ mm d}^{-1}$ ), Night 4 ( $0.7 \text{ mm d}^{-1}$ ), Night 5 ( $1.0 \text{ mm d}^{-1}$ ). The average of these results is  $0.9 \text{ mm d}^{-1}$ .

---

<sup>1</sup> At the conclusion of the test, the measured change in storage was actually 0.5 mm smaller than the evaporation indicated by the BT model. This is due to the noise in the depth measurements, not to systematic overestimation of evaporative losses.

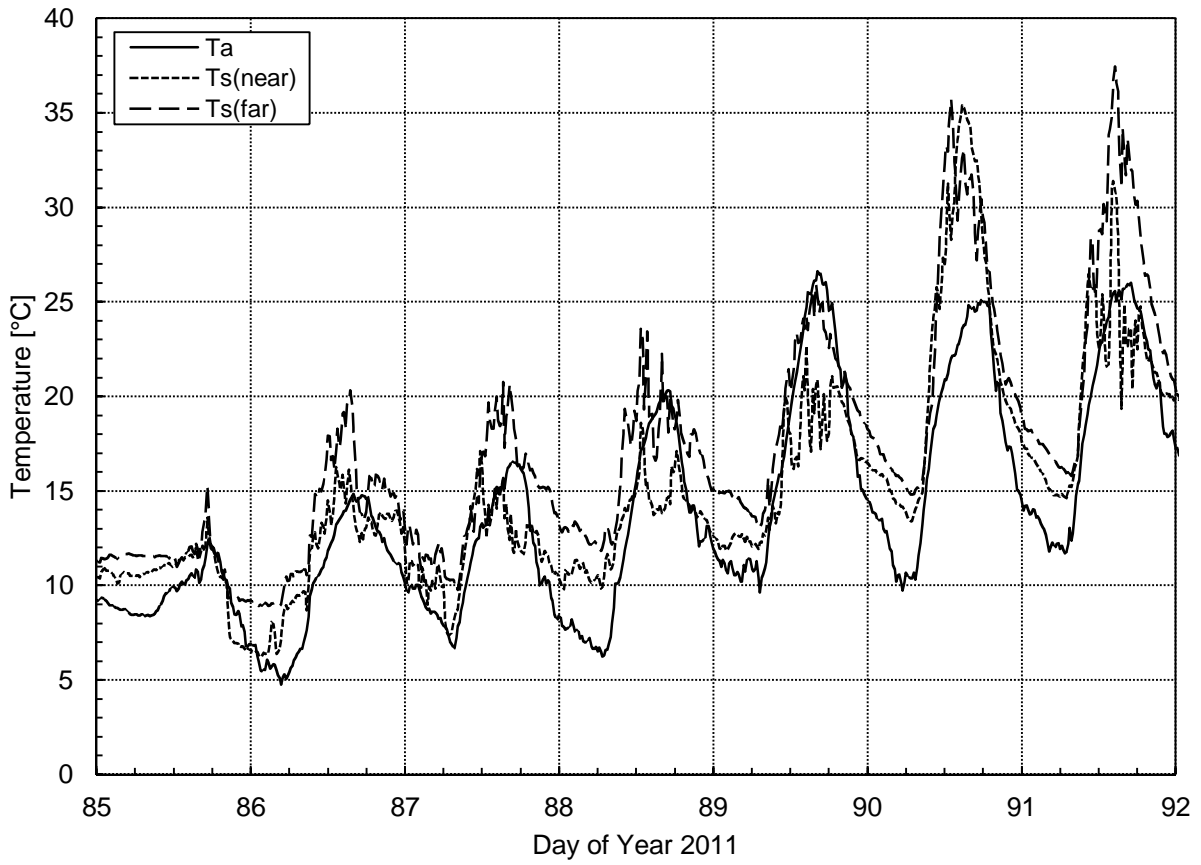


**Figure A2-1:** Air temperature,  $T_a$ ; water surface temperature  $T_s$ , sensed near the point of lagoon inflow (near) and at a distance (far); Dairy B.

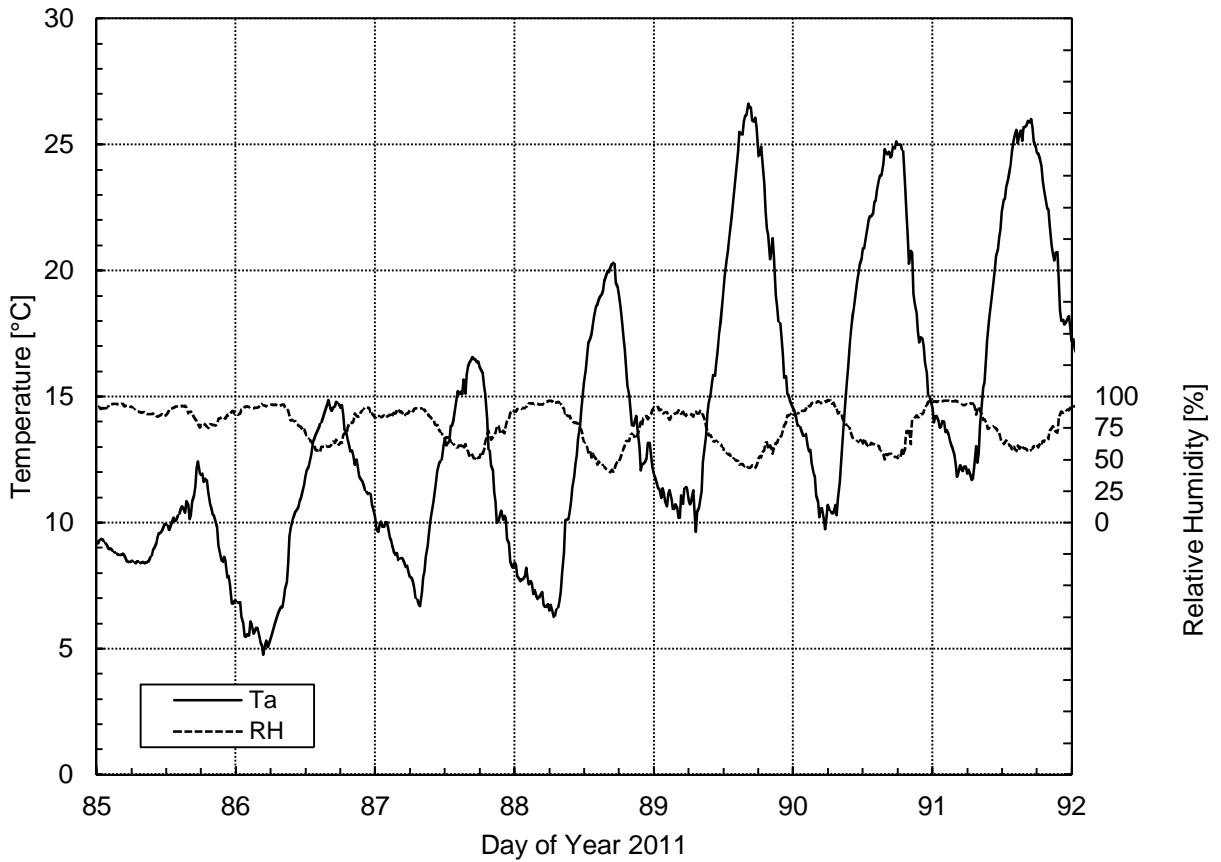


**Figure A2-2:** Air temperature,  $T_a$ , and relative humidity, RH; Dairy B.

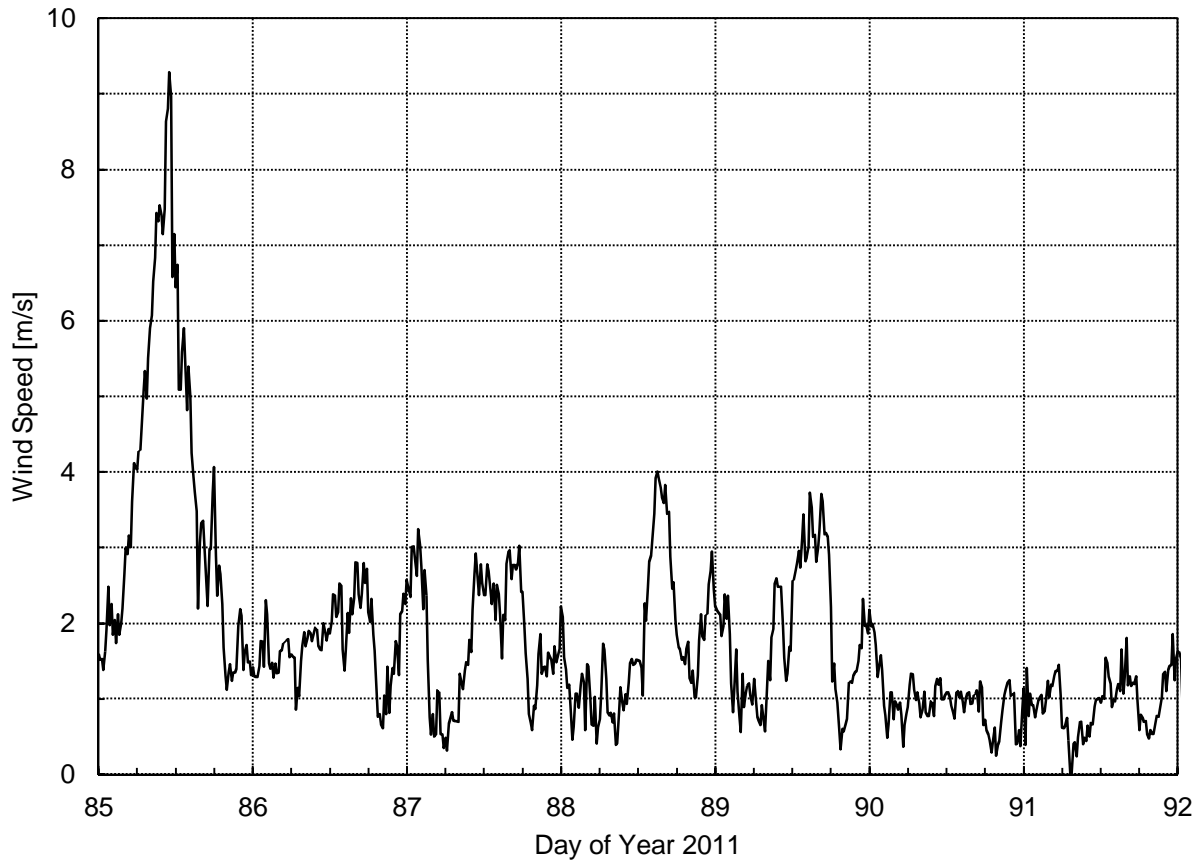


Figure A2-3: Wind speed measurements; Dairy B.

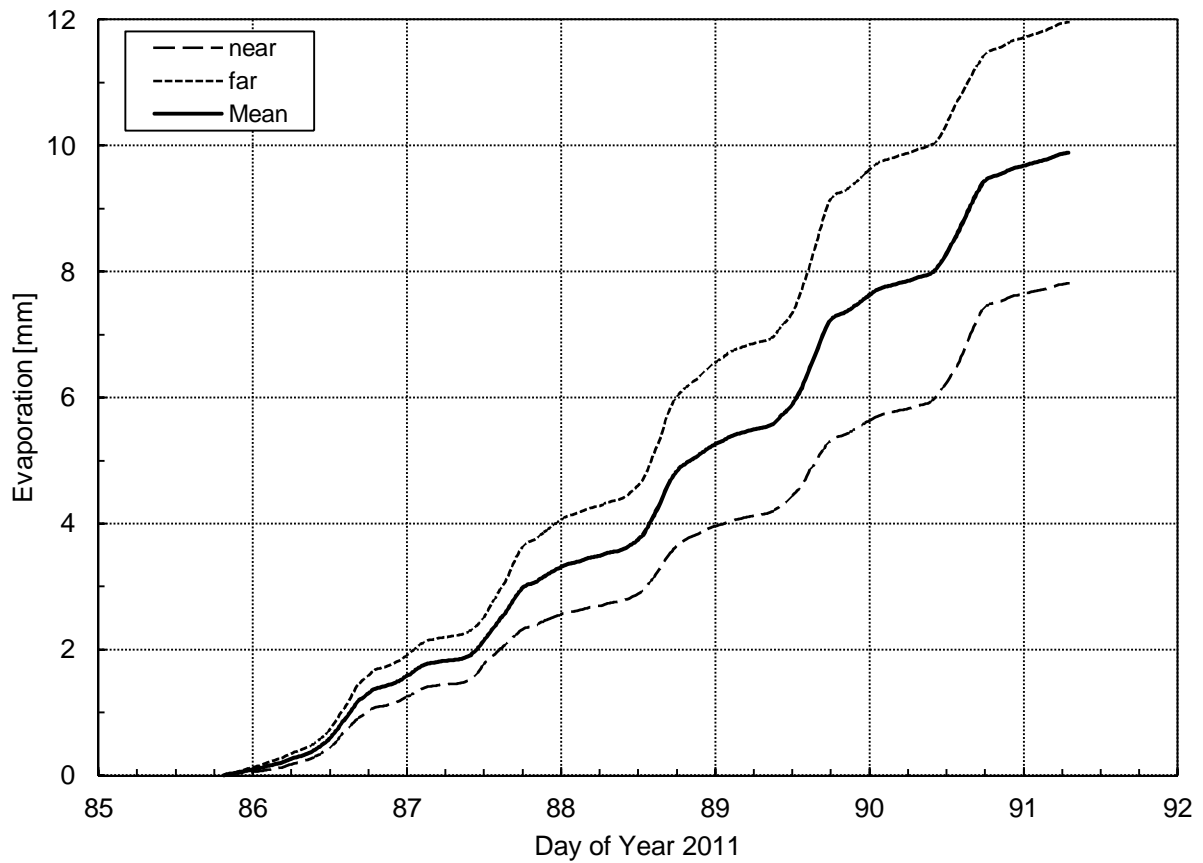
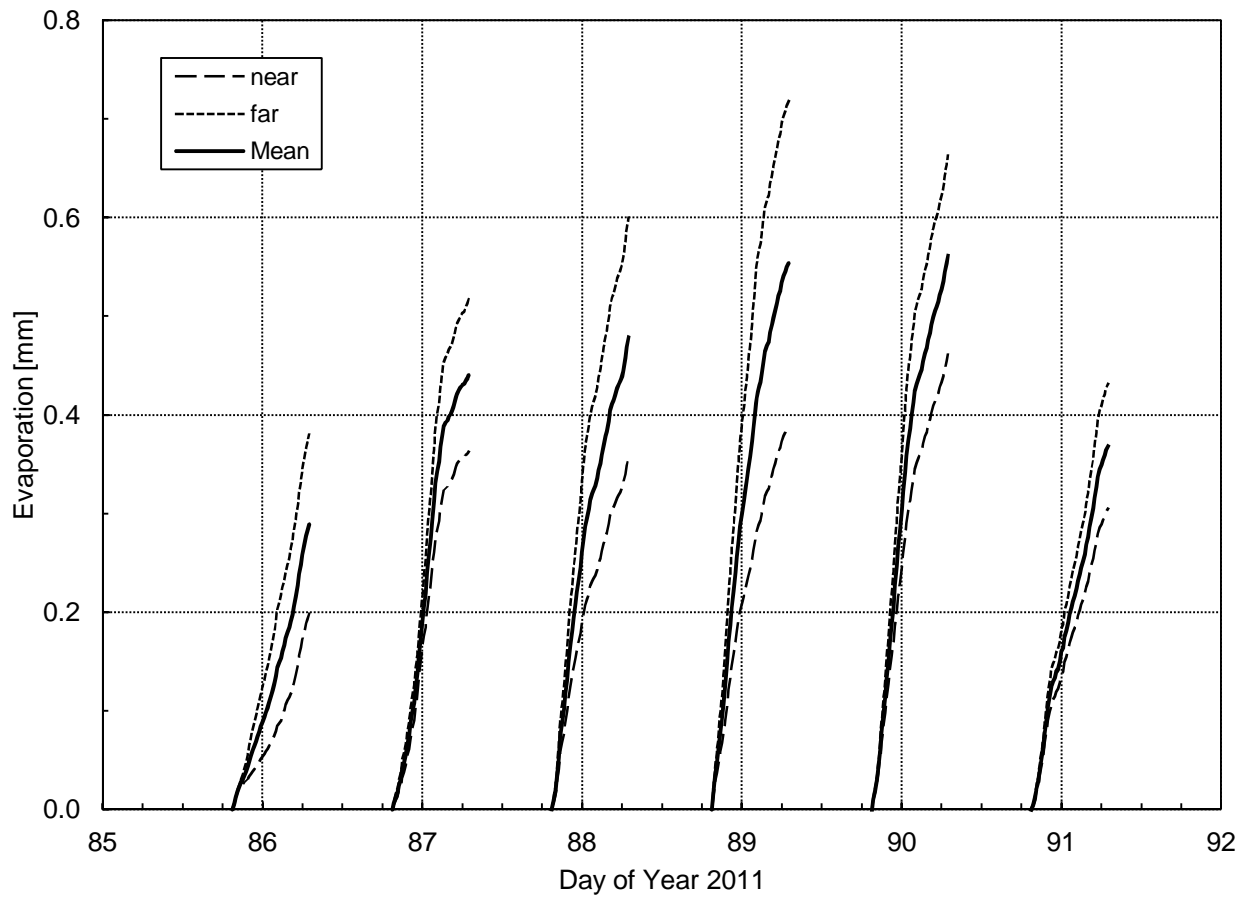
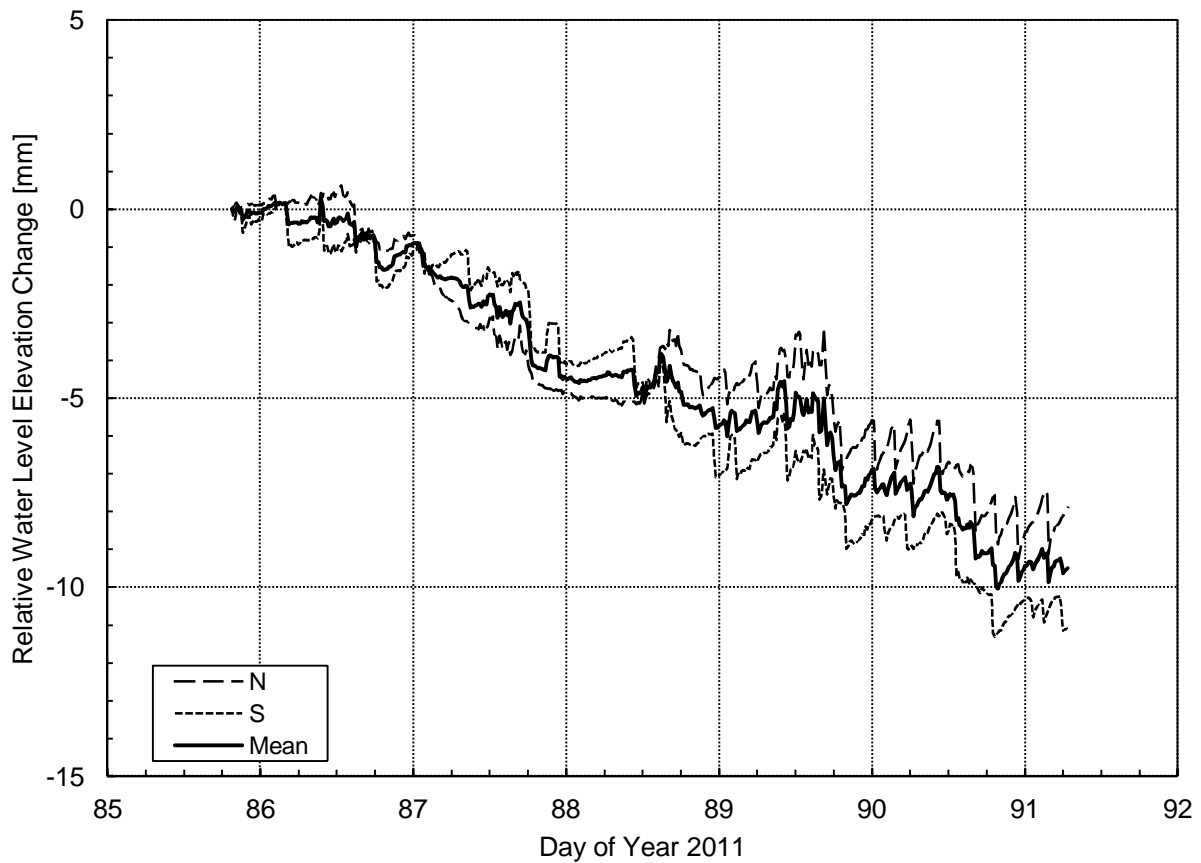


Figure A2-4: Cumulative evaporation near the point of lagoon inflow (near) and at a distance (far); Dairy B.



**Figure A2-5:** Night time evaporation near the point of lagoon inflow (near) and at a distance (far); Dairy B.



**Figure A2-6:** Water level elevation changes as measured at the north (N) and south (S) locations; Dairy B.

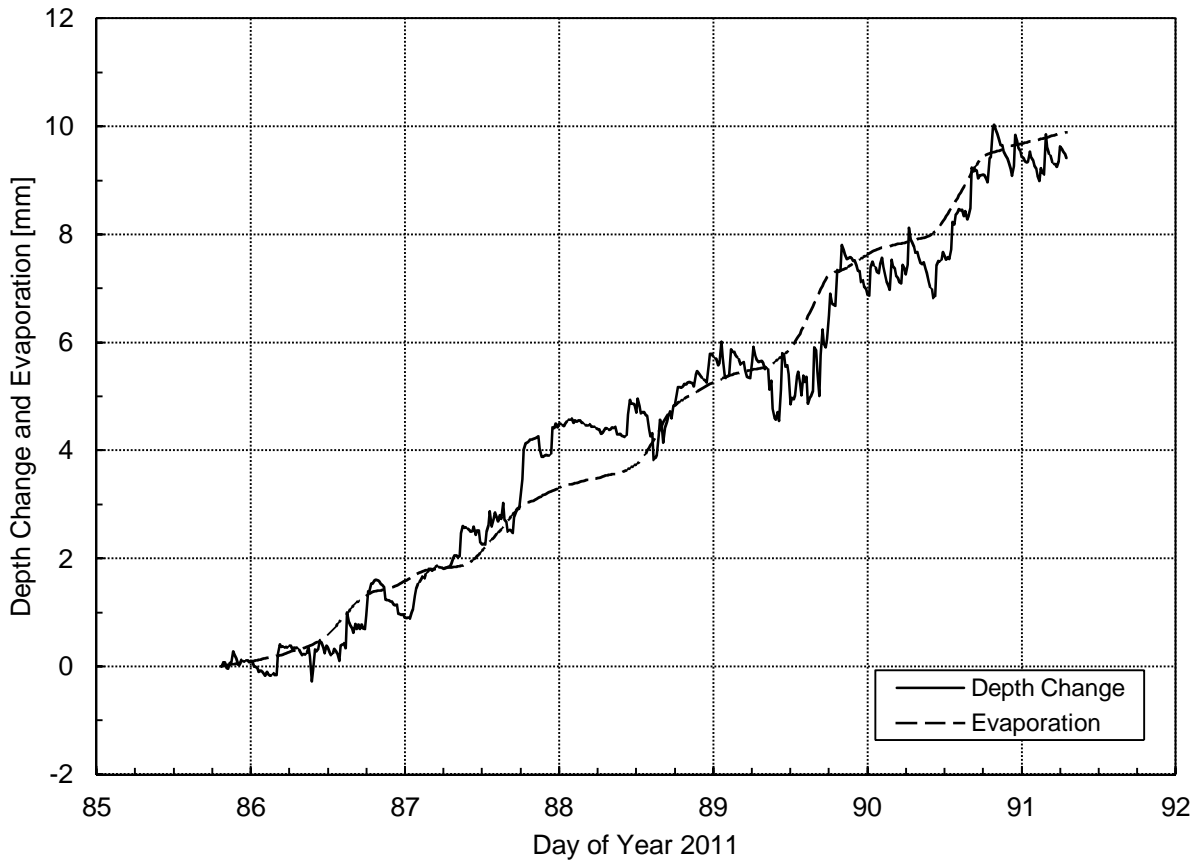


Figure A2-7: Cumulative change in depth and evaporation; Dairy B.

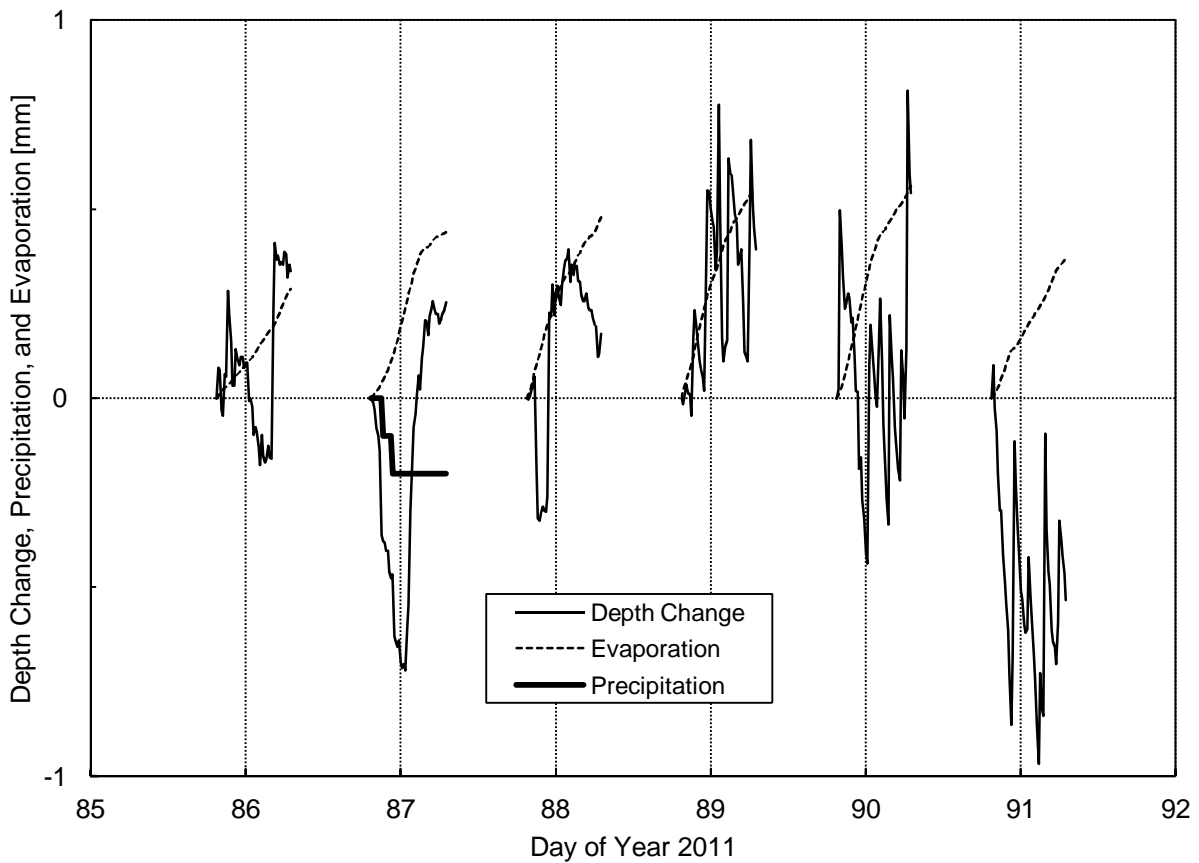
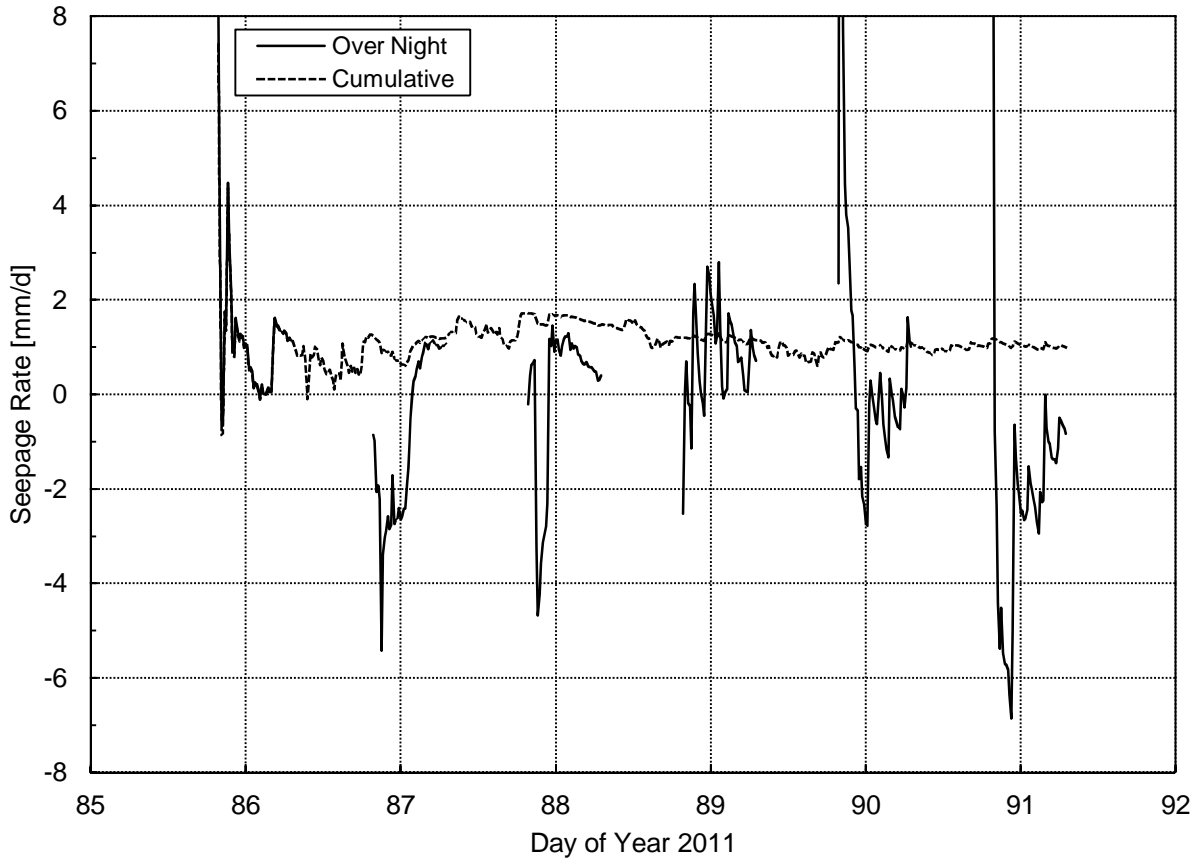


Figure A2-8: Night time (19:30 h – 07:00 h) change in depth and evaporation; Dairy B.



**Figure A2-9:** Normalized seepage rates as computed from the overnight water balance and the entire (cumulative) test duration; Dairy B.







## Appendix 3

### Water Balance Testing – Examples with Confounding Results

---

Many water balance tests will not generate data as easily interpretable as in Case 1 (Dairy A, *Section 3.1*); and most challenges will likely originate from difficult-to-interpret signals in the water level measurements. Three additional water balance tests, all carried out on unlined earthen dairy lagoons, are discussed to demonstrate difficulties that were encountered during testing. In these cases, signals in the water level measurements cast doubt on the hydraulic isolation of the tested lagoons. The discussed examples show that the computation of seepage rates alone, even if stable results are achieved over time, do not suffice to generate confidence in results. Rather, the results of these water balance tests underscore the importance of hydraulic isolation of the tested lagoons, review and evaluation of raw data, and an overall comprehensive analysis including assessment of the local hydrologic conditions.

#### Dairy C

The recorded depth change is suspect because virtually all of it occurred during the nights (**Figure A3-1**) whereas essentially none occurred during the daytime despite greater evaporation (not shown). As a result, seepage rates computed from overnight testing were much greater than from the cumulative test. While it is certain that a thick unsaturated zone exists between the bottom of the lagoon and the groundwater table, it is unclear what caused the atypical water level changes. However, it cannot be ruled out that unaccounted in- and/or outflows occurred.

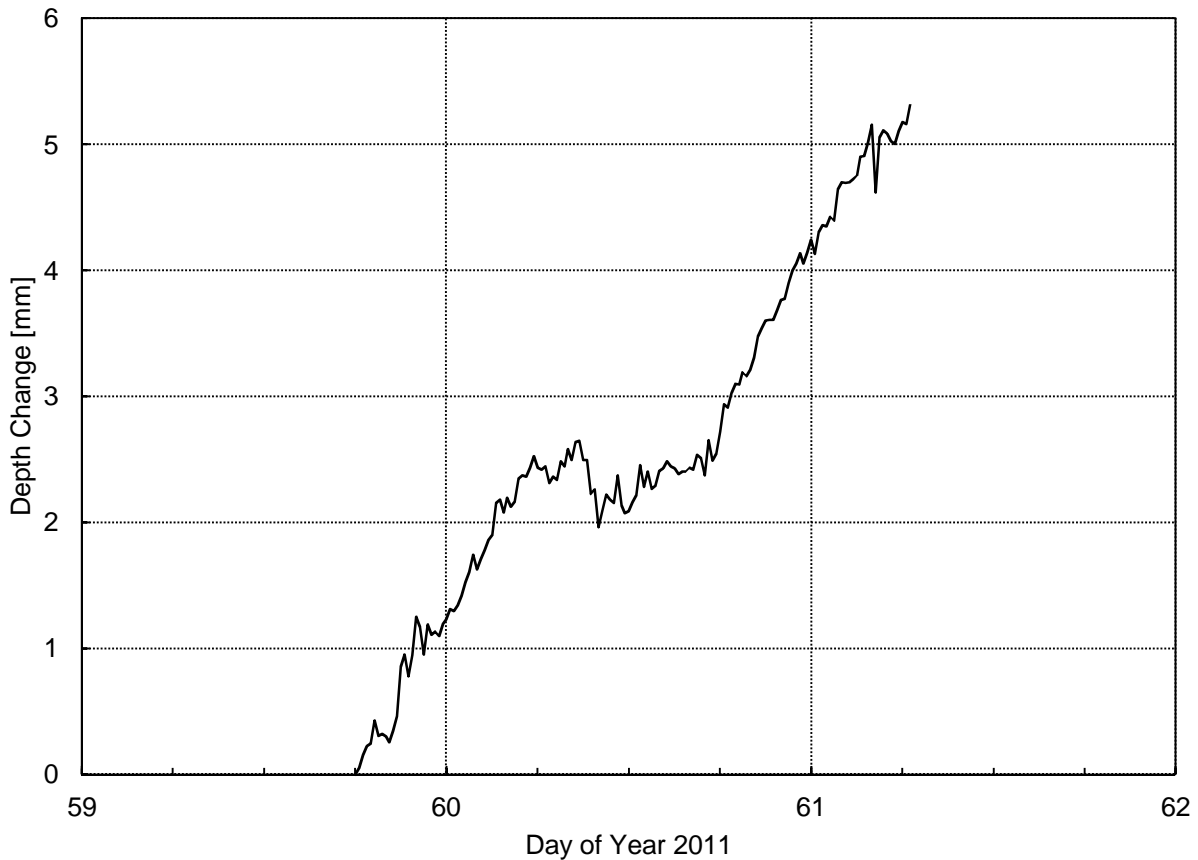


**Figure A3-1:** Cumulative change in depth; Dairy C.

### Dairy D

Water depth changes at this location were characterized by relatively large short-term fluctuations (**Figure A3-2**). Such large fluctuations are inconsistent with water level changes expected in a hydraulically isolated lagoon. It is suspected that the tested lagoon was either in hydraulic communication with an adjacent operational lagoon, which was used for daily operations during the time of testing, and/or with shallow groundwater. Due to these water level fluctuations, the water balance from the initial 2-day test and the subsequent 4-day test (the test was interrupted due to rain) produced different results (**Figure A3-3**). This figure also shows that, despite these water level fluctuations, random error was largely attenuated with time, producing relatively stable seepage rates for each of the two test runs. If the test had been run uninterrupted, it is quite likely that computations would have eventually produced a stabilized seepage rate. This demonstrates that singular focus on seepage rate results can be misleading.

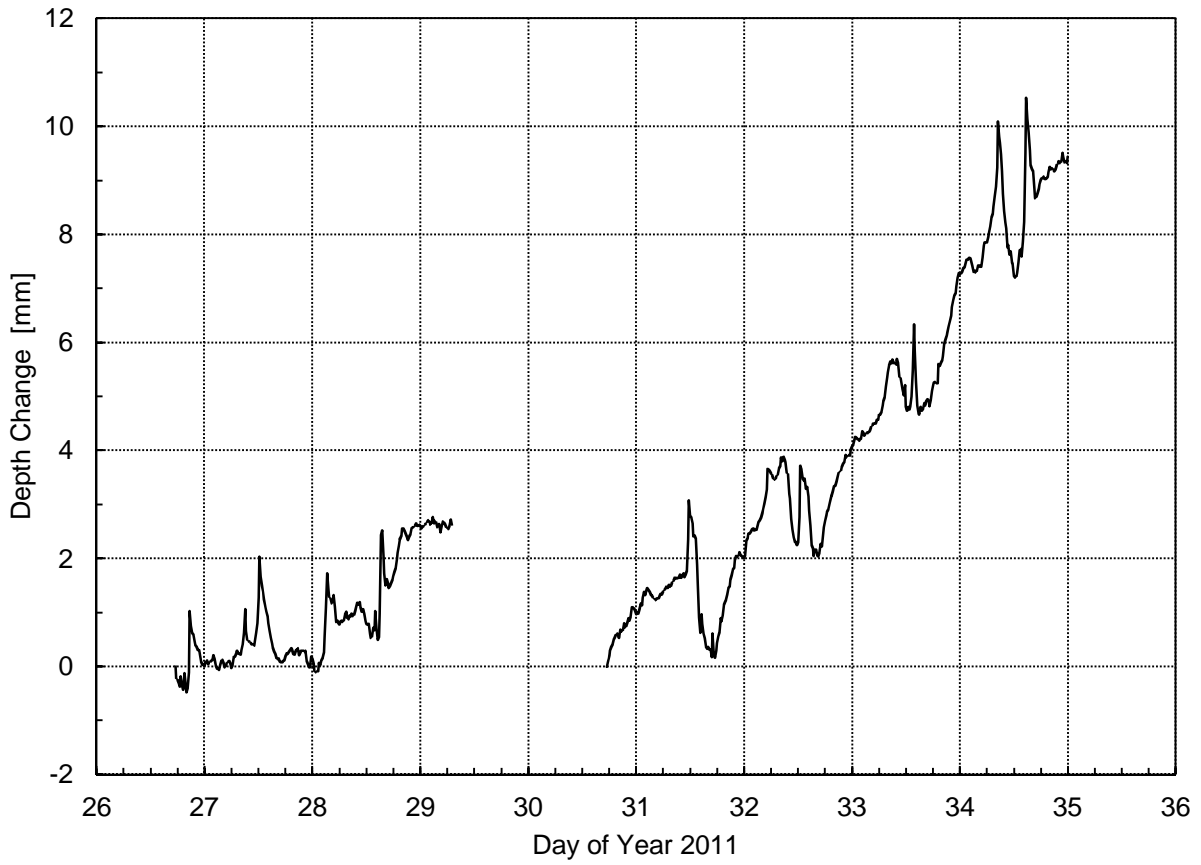


Figure A3-2: Cumulative change in depth; Dairy D.

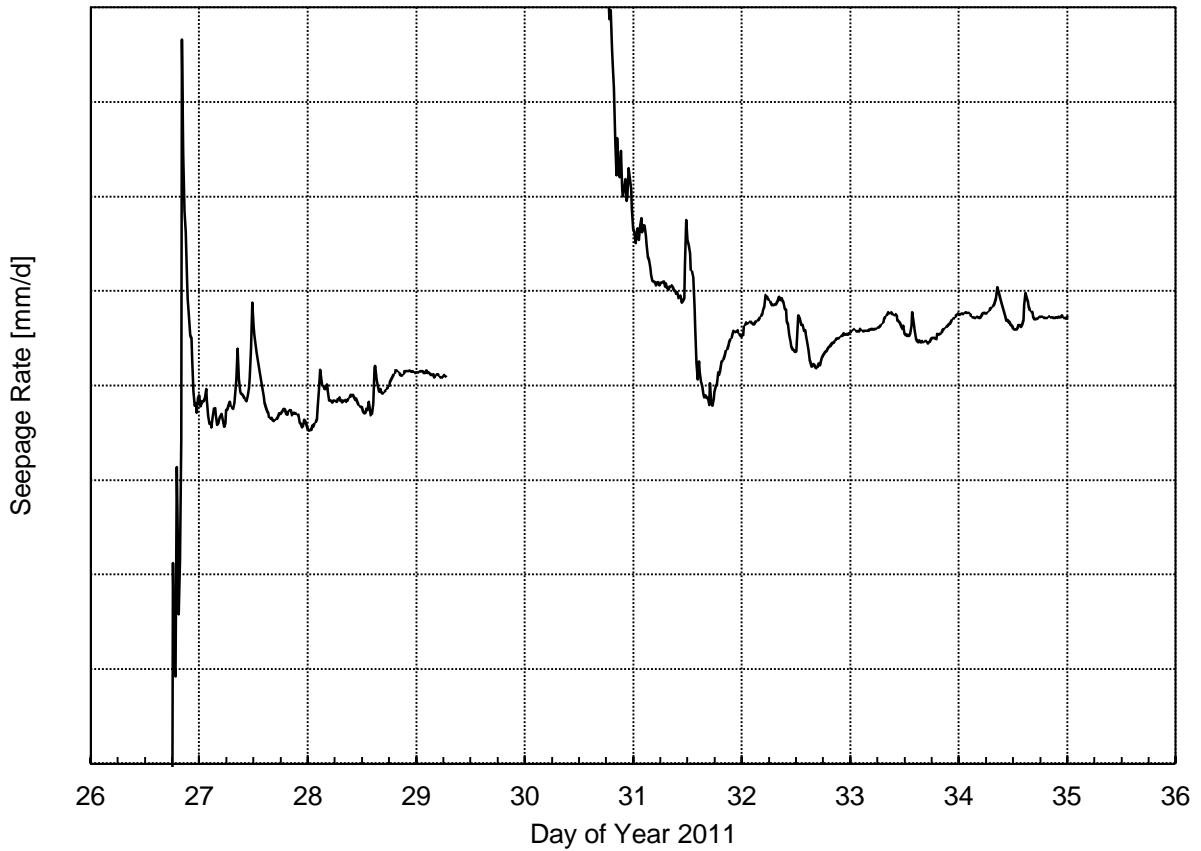
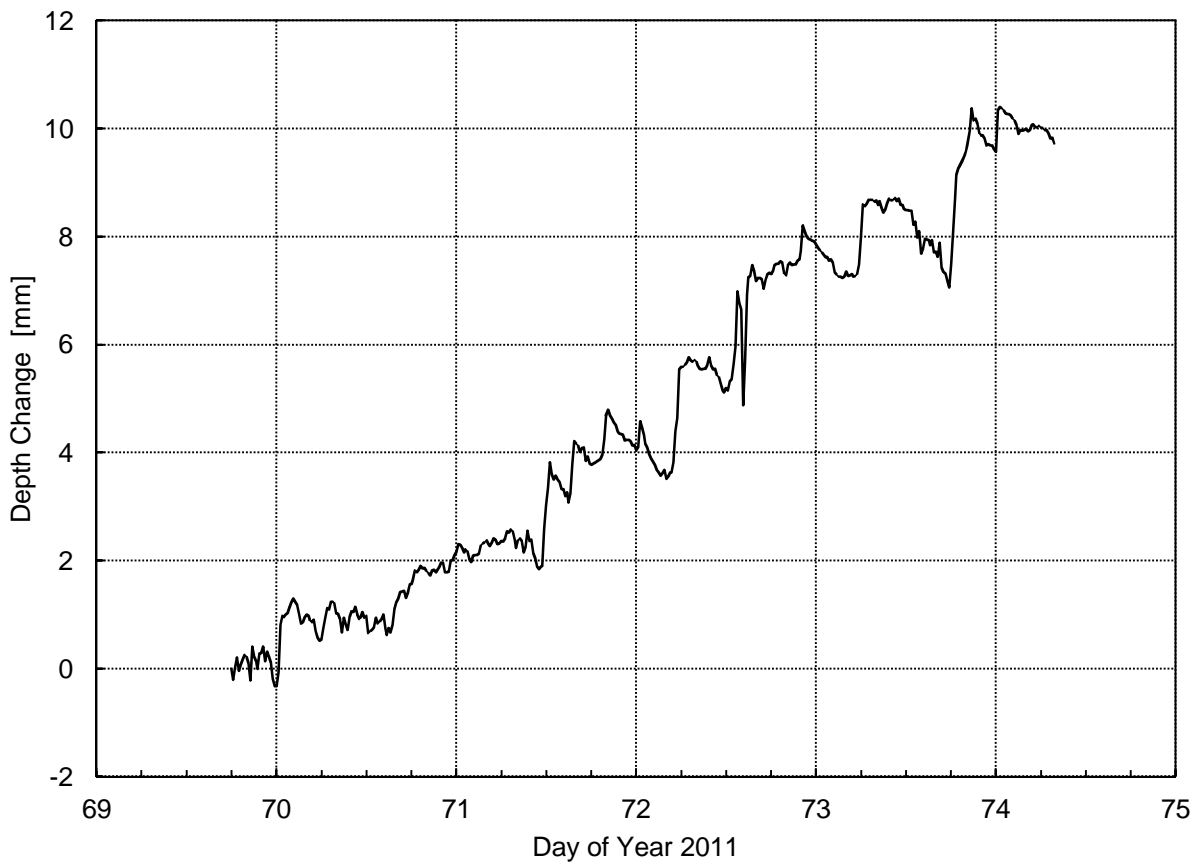


Figure A3-3: Seepage rates; Dairy D. Scale omitted to facilitate qualitative comparison without normalization.

## Dairy E

Similar to Dairy D, water depth changes at this location were characterized by relatively large short-term fluctuations (**Figure A3-4**). The tested lagoon was between two other lagoons, separated by narrow banks. These lagoons experienced large water level fluctuations during the testing, and it cannot be ruled out that the tested lagoon was in hydraulic communication with the adjacent lagoons. In addition, the tested lagoon intermittently produced large amounts of gas. This caused a lather-type layer of foam early in the morning that disappeared later in the morning. In addition to potentially affecting the evaporation rate, the substantial degassing may have affected the performance of the transducers by small gas bubbles temporarily obstructing the sensor port, thus, causing intermittent erratic measurements. Therefore, the results from this water balance test are considered questionable (**Figure A3-5**). The duration of the overnight testing was not long enough for the seepage estimates to stabilize, and large differences were observed between the results of the overnight testing and the multi-day testing. Similar to the example of Dairy D, random error was largely attenuated with time, producing a relatively stable seepage rate for the multi-day test, despite the erratic water level fluctuations.



**Figure A3-4:** Cumulative change in depth; Dairy E.

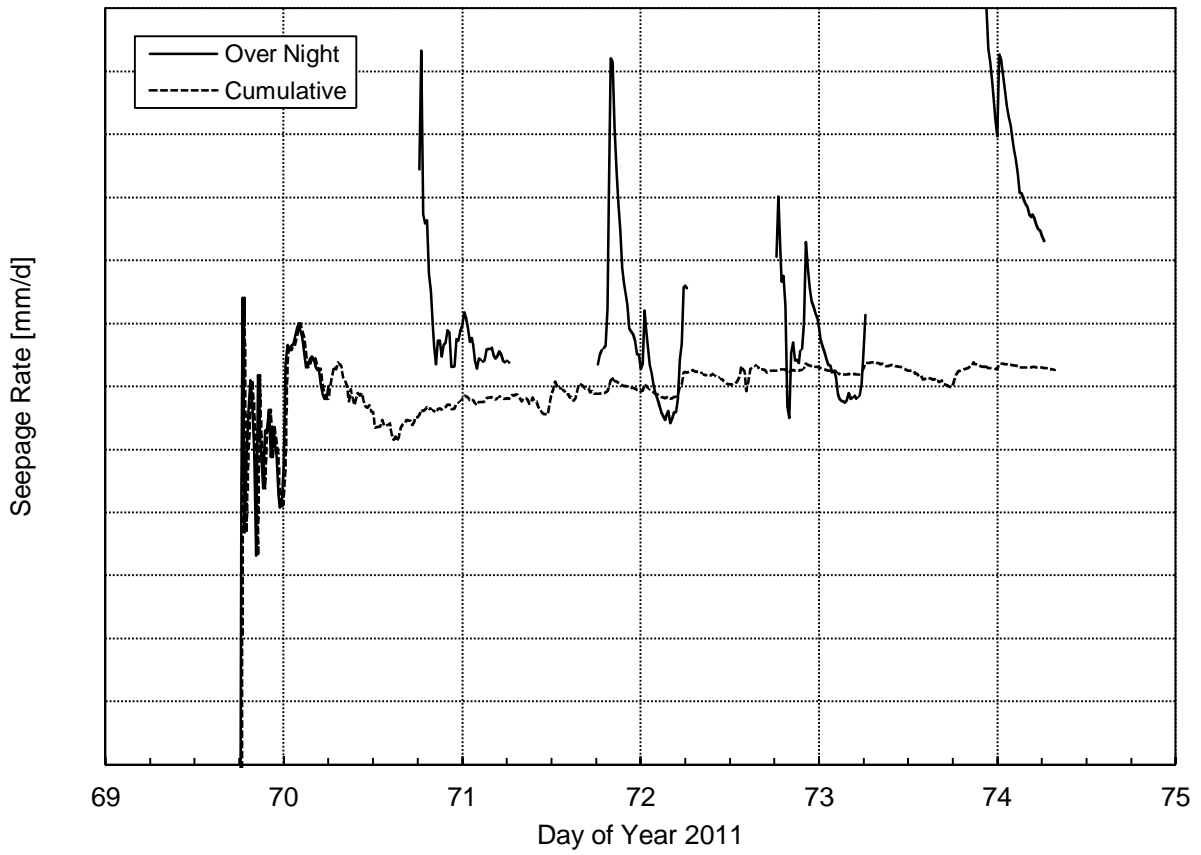


**Figure A3-5:** Seepage rates as computed from the overnight water balance and the entire (cumulative) test duration; Dairy E. Scale omitted to facilitate qualitative comparison without normalization.